January 2012

Model Estimation of Electric Power Systems by Phasor Measurement Units Data

Yasser Wehbe
University of South Florida, ywehbe@mail.usf.edu

Model Estimation of Electric Power Systems by Phasor Measurement Units Data

by

Yasser Wehbe

A dissertation submitted in partial fulfillment
of the requirements for the degree of
Doctor of Philosophy
Department of Electrical Engineering
College of Engineering
University of South Florida

Major Professor: Lingling Fan, Ph.D.
Kenneth Buckle, Ph.D.
Fangxing Li, Ph.D.
Stephen Saddow, Ph.D.
Qiong Zhang, Ph.D.

Date of Approval:
October 10, 2012

Keywords: Parameter Estimation, Synchronous Machine Model, Kalman Filter, System Identification, Sub-set Selection

TABLE OF CONTENTS

LIST OF TABLES

LIST OF FIGURES

ABSTRACT

This dissertation tackles the online estimation of synchronous machines' power subsystems electromechanical models using the output based Phasor Measurements Units (PMUs) data while disregarding any inside data. The research develops state space models and estimates their parameters and states. The research tests the developed algorithms against models of a higher and of the same complexity as the estimated models.

The dissertation explores two estimations approaches using the PMUs data: i)non-linear Kalman filters namely the Extended Kalman Filter (EKF) and then the Unscented Kalman Filter (UKF) and ii) Least Squares Estimation (LSE) with Finite Differences (FN) and then with System Identification. The EKF based research i) establishes a decoupling technique for the subsystem the rest of the power system ii) finds the maximum number of parameters to estimate for classical machine model and iii) estimates such parameters . The UKF based research i) estimates a set of electromechanical parameters and states for the flux decay model and ii) shows the advantage of using a dual estimation filter with colored noise to solve the difficulty of some simultaneous state and parameter estimation.

The LSE with FN estimation i) evaluates numerically the state space differential equations and transform the problem to an overestimated linear system whose parameters can be estimated, ii) carries out sensitivity studies evaluating the impact of operating conditions and iii) addresses the requirements for implementation on real data taken from the electric grid of the United States. The System Identification method i) develops a linearized electromechanical model, ii) completes a parameters sub-set selection study using si8ngular values decomposition, iii) estimates the parameters of the proposed model and iv) validates its output versus the measured output.

CHAPTER 1: INTRODUCTION

1.1 Phasor Measurement Units

Phasor Measurement Unit (PMU) is a *fast* and *synchronized* measurement device for the positive sequence phasor data of voltages and currents [2]. The measurements sampling rate can be 1000 Hz and its reporting rate can be 60 Hz (even bigger sometimes) [2]. The synchronization is achieved by a precise time stamp attached to every measurement record. The time stamp comes from a clock augmented by Global Positioning System (GPS) in order to ensure its precision. PMU diagram block is shown in Fig. 1.1 (from [3]).

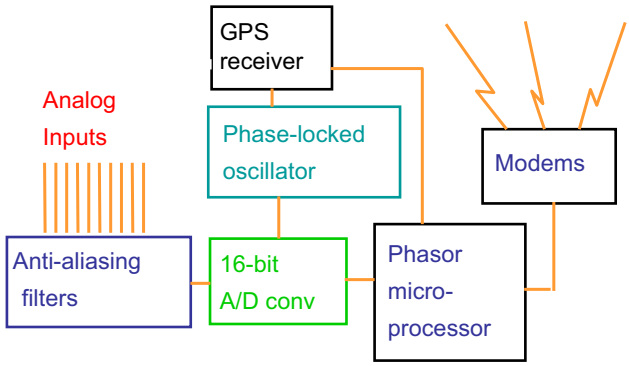

Figure 1.1. PMU block diagram. Note: from [3] ©2006 IEEE

Specifically, the voltage $v(t)$ (or the current) instantaneous value in a perfect sinusoidal form can be described as :

$$v(t) = V_m \cos(2\pi f t + \phi) \tag{1.1}$$

f is the frequency (50 or 60 Hz), V_m is the maximum value of $v(t)$, and ϕ is the angle. The PMU will provide both V and ϕ at the rate of 60 Hz. The timely and fast

availability of V_m and ϕ measurements becomes more important when the system is under transient condition and both V_m and ϕ are function of time. The combination of V_m and ϕ in one complex number is called the phasor $\widetilde{V}$ of $v(t)$:

$$\widetilde{V} = \frac{V_m}{\sqrt{2}} e^{j\phi} \qquad j \text{ is the complex number} \tag{1.2}$$

Phasor Measurement Units provide the phasor $\widetilde{V}$ of $v(t)$ from which the angle ϕ and magnitude V_m can be extracted.

1.1.1 Phasor Measurement Techniques

The theoretical approach to provide phasor data from the instantaneous one is built around Discrete Fourier Transform (DFT). The voltage or current (referred to as signal in this section) is sampled at a frequency Nf where N is an integer number ($N = 12$ has been used in the literature). The phasor value $\widetilde{V}_N$ of the fundamental frequency is extracted from the sampled signal using N samples (v_n $n = 0...N-1$) [2]:

$$v_n = V_m \cos(2\pi n/N + \phi) \tag{1.3}$$

$$\widetilde{V}_N = \frac{\sqrt{2}}{N} \sum_{n=0}^{N-1} [v_n(\cos(2\pi n/N) - j\sin(2\pi n/N))] \tag{1.4}$$

The value $\widetilde{V}_N$ is based on N samples. However a recursive formula can be found for $\widetilde{V}_N$ in the time window.

1.1.2 PMU Applications

The high reporting rate (60 Hz) compared to 0.5-1 Hz in existing measuring systems creates a whole new application area which had not been possible before. The measurements accompanied by the precise time stamps will allow for a constellation of PMUs implemented across the transmission network to generate the synchronized measurements necessary to estimate the state of the transmission network. Prior to the PMUs implemen-

tation, measurements taken every one or 2 second of the voltage magnitude and the active and reactive power flow were used to estimate the state of the power system [4]. Such low sampling rate did not allow to develop a dynamic situation awareness of the power systems. Such estimation was actually done every few minutes, a rate which can be greatly improved by the use of PMUs. An example of possible use of PMU is the FNET estimation of angle gradient map in the eastern part of the United States updated every 4 seconds (Fig. 1.2 available at `http://fnetpublic.utk.edu/anglecontour.html`).

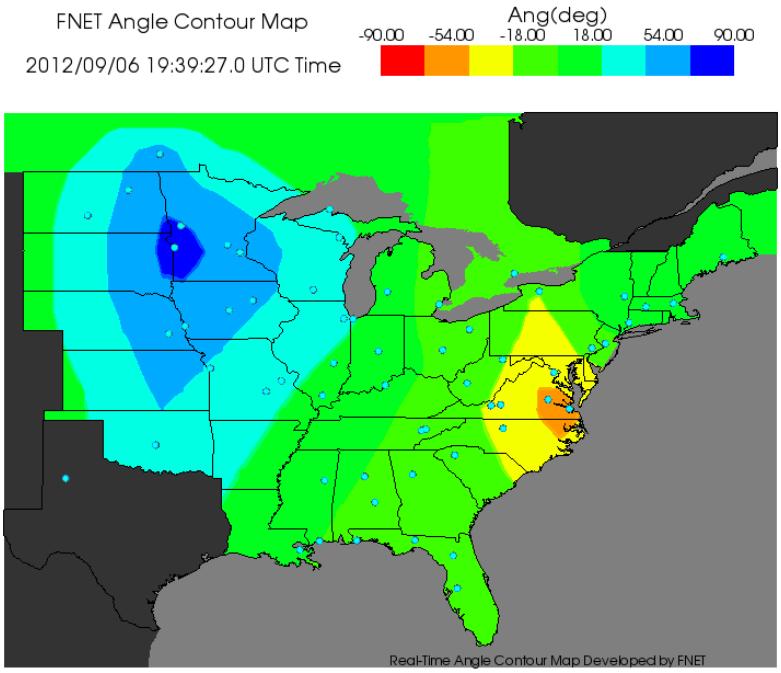

Figure 1.2. FNET angle contour map. Note: ©2012 Power Information Technology Lab, University of Tennessee

Several application areas can be built around PMUs in order to study the grid in a dynamic way. Such application areas include [5, 2, 6]:

1. Dynamic state estimation
2. Wide Area Monitoring systems (WAMS)
3. Power systems protection
4. Power systems control

5. Monitor system oscillations

6. Monitor the stress on the electric transmission system

7. Available transmission capacity

8. Identifying the corrective actions (such as damping) needed in case of discrepancies

9. Various stability studies including angular stability and voltage stability.

PMUs have already proven to be useful in WAMS applications.In China for example, the use of PMUs has shown an angle difference of a transmission line to be 6 degrees whereas simulation studies indicated a difference of 20 degrees. In Mexico WAMS studies using the PMUs were able to study a very critical oscillation problems which happened when two power systems were connected for the first time and ensuing oscillations were going to lead to a complete collapse of the whole power systems [5].

1.2 Parameter Estimation and Power Systems

1.2.1 The Need for Parameter Estimation in Power Systems

Outages like the one of Aug. 10th, 1996 and the one of Aug. 14th, 2003 have propelled the need for parameter estimation of synchronous generators and for situational awareness of the transmission system.

Following the 1996 blackout investigation, Western Systems Coordinating Council (WSCC) developed guidelines on synchronous machine model validation as a response to North American Electric Reliability Corporation (NERC) report on the outage [7]. Amongst the findings of the report, it was brought forward that machines parameters and states estimation play an important role in power system stability studies [8, 7]. Factors such as aging and repairs modify with time the generators parameters values from those provided by the manufacturers which could lead to serious deviation between machine simulated response and the actual response response to an event (Fig. 1.3). The WSCC

model validation guidelines call for periodic verification of the synchronous machine key parameters. These parameters include machines reactances, time constants, inertia, and stator resistance, among other parameters.

The United States Department of Energy report on the 2003 blackout advised on several factors contributing to this blackout including: i) lack of ability to identify emergency conditions, and ii) inappropriate awareness of the power system situation on the regional level [9].

Moreover, unit-specific dynamic data should be filed in order to comply with NERC MOD-013 [10] standard. This standard covers power generating systems inclusive of generators (inertia constant, damping coefficient, direct and quadrature axes reactances and time constants), excitation systems, voltage regulators, turbine-governor systems, power system stabilizers. Currently, the generating unit is brought offline and is subject to tests in order to provide the data required by NERC. The research problem investigated in this dissertation have a practical application by providing some of the data required by NERC MOD-013 while the generating unit is connected online and without interrupting its power supply to the electric grid.

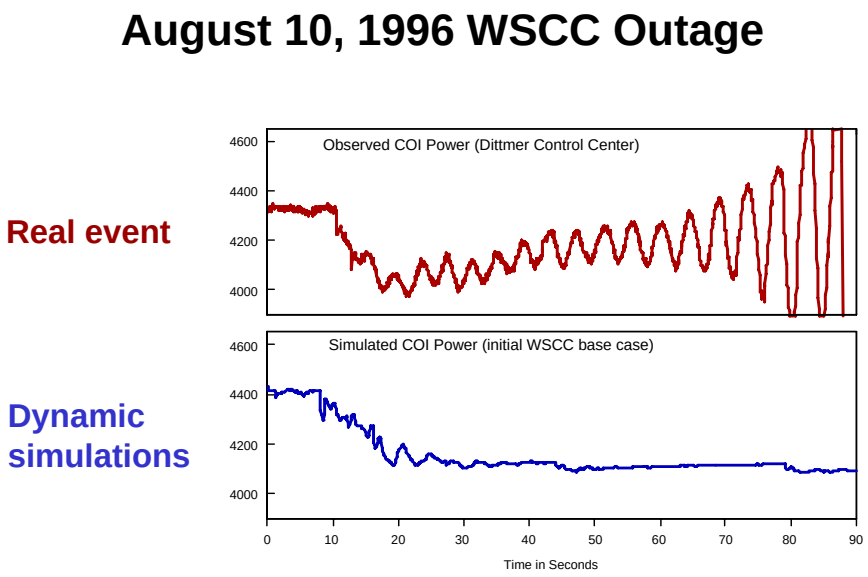

Figure 1.3. Deviation between real events and simulated ones. Note: ©NERC

1.2.2 Parameter Estimation in Power Systems

Parameter estimation comes from our endeavor to give physical systems mathematical representation. Often, such mathematical representation is under the form [11]:

$$f(m) = d \tag{1.5}$$

In engineering, the mathematical representation usually looks like:

$$\begin{cases} \dot{x} &= f(x, u, m) \\ y &= g(x, u, m) \end{cases} \tag{1.6}$$

f is a linear or a non-linear function, m is a constant vector (referred to as parameter set), x is a time varying vector representing the internal states of the system, u is an external time varying vector representing the control (or input) to the system, y is a time varying vector representing the measurements, and g is the observation function of the system. The problem of finding x given f and m is referred to as the forward problem which can be solved by Kalman filter, the problem of finding f (inclusive of m) given g, u and y is called system identification.The problem of finding m given y, g, u and f is an inverse problem (as opposed to the forward problem) or simply a parameter estimation problem [11, 12].

Power systems are dynamic systems spanning over various time periods. These dynamic phenomena have been classified according to their time scale under instantaneous response, short-term dynamics, and long-term dynamics [13]. Power system network response is assumed to be instantaneous. The network dynamics are of electromagnetic nature and considered to be very fast compared to the other power system phenomena and are usually modeled in algebraic forms. Long-term dynamics of several minutes are associated with some protective devices and controllers which by design do not interact with short-term dynamics. Short-term dynamics of few seconds are mainly due to the heart of power systems, the synchronous machines and their voltage and power controls, and they are referred to as electromechanical dynamics. Fig. 1.4 by [14] shows the synchronous ma-

chine related dynamics (inertial, prime mover, and excitation) compared with other power system dynamics. Among the short term oscillations, [15] points out that the local mode oscillations have a frequency of 0.7 - 2 Hz whereas the more important inter-area modes have oscillations in the order of 0.1 - 0.8 Hz. It is this kind of oscillations (0.1 - 2 Hz) that this dissertation is researching. PMUs with a reporting rate of 60 Hz are a good choice to capture the short-term dynamics with frequency of 10 Hz or less as evidenced [2].

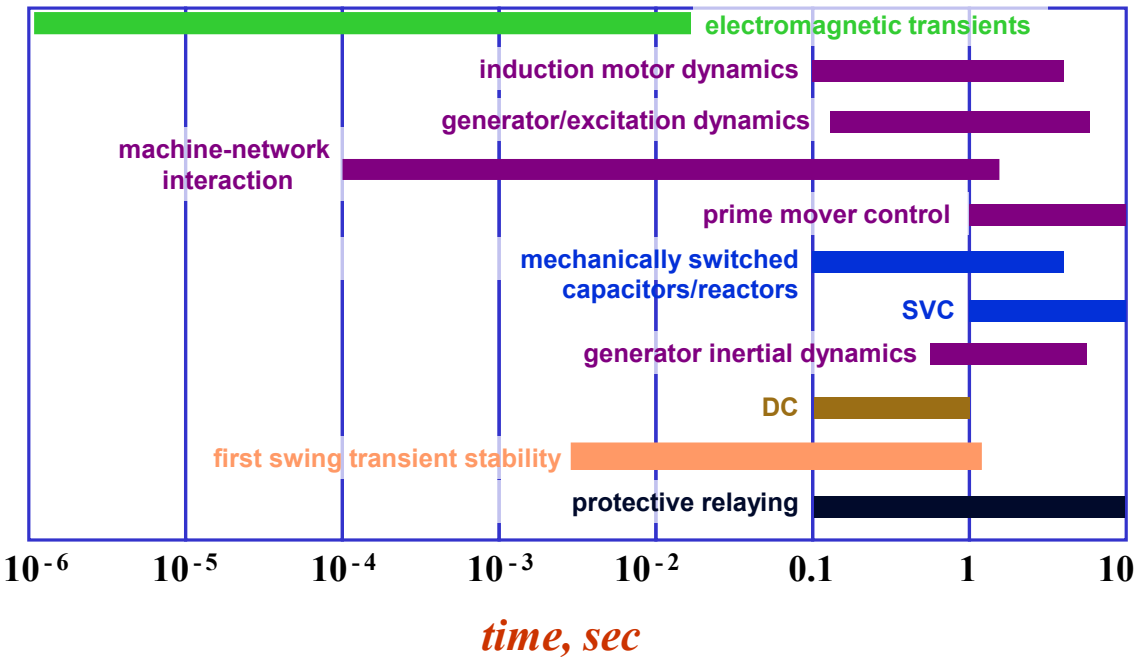

Figure 1.4. Time scale of power systems dynamics. Note: ©2002 - 2012 George Gross, University of Illinois at Urbana-Champaign

The choice of which model to use in studying synchronous machine depends on the objective of the study [16]. A synchronous machine two-axis model with no governor nor exciter controls and ignoring the sub-transient dynamics [17] is described by (The symbols are explained in Appendix A):

$$\frac{\partial \delta'}{\partial t} = \omega - \omega_0 \tag{1.7}$$

$$\frac{2H}{\omega_0}\frac{\partial \omega}{\partial t} = P_m - P_e \tag{1.8}$$

$$T'_{do}\frac{\partial E'_q}{\partial t} = -E'_q - (x_d - x'_d)I_d + E_{fd} \tag{1.9}$$

$$T'_{qo}\frac{\partial E'_d}{\partial t} = -E'_d - (x_q - x'_q)I_d \tag{1.10}$$

$$[E'_d + (x'_d - x'_q)I_q + E'_q] = jx'_d(I_d + jI_q) + Ve^{j(\theta-\delta'+\pi/2)} \tag{1.11}$$

A classical model for the synchronous machine can be derived from (1.11) by removing the dynamics of electromagnetic nature and keeping the electromechanical dynamics. Specifically, T'_{qo} is set to zero and T'_{do} to infinity. Classical model is a good choice to study inter-area stability because a power subsystem made of multiple coherent machines can be represented by one classical model machine [18]. Accordingly, PMU based methodologies can be developed to estimate individual machines parameters and such methodologies can be scaled to estimate power subsystems equivalent machines parameters.

The extraction of the machine parameters can be accomplished either through offline testing or during online operations following a disturbance. Offline testing has the disadvantage of disconnecting the machine from the transmission system, while online estimation works while the machine is connected to the power system during normal operation.

1.3 Statement of the Problem

The purpose of this dissertation is to research the estimation of power systems models with PMU data, specifically:

1. To explore the use of PMU data in System Identification

2. To investigate the use and effectiveness of various parameter estimation methods for the purpose of online system identification including models, states, and parameters. The parameters estimation methods include methods specific to power systems or general methods applicable to various engineering systems

3. To establish models of power systems electromechanical dynamics which can be reflected by PMUs data and are suitable for parameters estimation

4. To develop various parameters estimation applications on various synchronous generators models such as classical model system identification or flux decay

model parameter estimation. Such applications can be extended in the future to other power systems such as wind farms.

5. To propose methods to select the parameters involved in power systems electromechanical dynamics which can be estimated based on PMUs data.

1.4 Organization of the Dissertation

The dissertation is organized as follows:

1. Chapter 1 introduces the importance of model and parameter estimation in power systems.

2. Established research in power system parameters estimation based on Kalman Filter and Least Squares Estimation is exhibited in Chapter 2. The chapter highlights the limitations and assumptions of such research and points out to specific objectives to be attained by this dissertation providing an incremental contribution to the established research in the literature.

3. Kalman Filter based research is shown in Chapter 3. Section 3.3 carries out parameters estimation for non-linear systems of the synchronous machine classic model based on the linearization approach of Extended Kalman Filter. Section 3.4 shows the sampling approach of Unscented Kalman filter for solving the non-linearity related anomalies found in the synchronous machine flux decay model.

4. Chapter 4 presents two Least Squares Estimation based applications on synchronous machine and on power subsystem estimation. Finite differences technique is used in conjunction with Least Squares Estimation to estimate the parameters of synchronous machine classic model in Section 4.3 where the impact of various operating conditions and machine controls were studied. Section 4.4 develops a linearized model for the synchronous machine, studies the selec-

tion criteria for the parameters to be estimated and proceeds with a parameters sub-set estimation using System Identification.

5. Chapter 5 concludes the dissertation with the main results drawn from the research and proposes future work by extending the research of parameter estimation to other types of power systems.

CHAPTER 2: REVIEW OF RELEVANT LITERATURE AND RESEARCH

Generators parameters estimation has been an active research topic and has been clearly mandated by NERC. In order to classify the estimation methods, several criteria are used based on: the nature of the data (Section 2.1 and Section 2.2), data processing (Section 2.3 and Section 2.4), the measurements domain, machine offline testing or online connection, and the scope of the parameters (Section 2.5).

2.1 Parameter Estimation Measurement Equipment: DFRs and PMUs

Digital Fault Recorders (DFRs) are fast measurement devices designed to record the three phase instantaneous response of an electric system to faults. Due to the fast response of electric systems to faults, DFRs have high sampling rate which can reach 10 KHz [19].

Phasor Measurements Units (PMUs) are introduced in Section 1.1. Compared to DFRs, PMUs are part of Wide Area Monitoring Systems (WAMS) which prompts the establishment of PMUs data network covering interconnection areas such as FNET (see Fig. 1.2), and the establishment of North American SynchroPhasor Initiative (NASPI) aiming at improving the electric grid reliability. On the technical side, DFRs provide three phase instantaneous values versus the positive sequence phasor values with PMUs, and DFRs have a higher sampling rate.

Generators parameters include parameters of electric nature usually associated with fast electromagnetic and electric states (e.g. impedances associated with magnetic fluxes) and parameters of mechanical nature associated with slow mechanical states (e.g. inertia associated with rotor speed). Accordingly, electric parameters and states estimation necessitates the use of fast measurement equipment, e.g. the Digital Fault Recorder (DFR),

whereas equipment with lower measuring rates, e.g. PMUs, can be used in the estimation of the electro-mechanical parameters and states. Data from a PMU installed at the output of power generation area, as part of WAMS, can also be used to estimate the parameters of the equivalent of machine of the generation area.

DFR instantaneous data were used to estimate machine electrical parameters predominantly found in fast electromagnetic dynamics which have small time constants [17]. Such estimation for (L_{ad}, L_{aq}, and r_f) was carried out by Kyriakides *et al* [20], for the armature circuit parameters by Melgoza *et al* [21], and for x_{md}, x_{mq}, and r_f by Valverde *et al* [22]. In [20] and [21] the field circuit voltage and current need to be available in addition to the output voltage.

PMU data were used by Chow *et al* [23] to study of a radial transfer path and by Huang *et al* [24] to estimate the states in a multi machine system. It was also used by Wehbe and Fan for the estimation of synchronous machine classical model connected with a shunted transfer path[25].

Other methodologies based on measurements from inside the machine could also be used to assess the machine states. Humer [26] used contact-less sensors on the shaft of the rotor to find the rotor mechanical angle, rotational speed, and rotational acceleration. These dynamic parameters are used to find the torsion oscillations of the shaft through second order system. Operators need to know how much torsion oscillations the synchronous machines are subject to because such oscillations increase the fatigue of the machines and decrease their lifespan. This method does not seek to find electrical parameters like machine internal reactances or resistances, although the mechanical states of the machines are tightly associated with the electrical ones like frequency and rotor angle. Such method requires that the synchronous machine be equipped with sensors on its shaft increasing the cost of the machine.

As a summary, DFRs are used for the estimation of parameters built in the fast electromagnetic dynamics. The focus of this dissertation is on using PMU data for electromechanical dynamics related estimation.

2.2 State of the Art Approaches on PMU Data Based Estimation

Chow *et al.* [23] method uses two PMUs on the extremity of radial transmission line, which makes the method dependent on the network topology. Wehbe and Fan estimation of the classical machines parameters connected by a shunted transmission line in 2.2 depends also on the transfer.

Huang *et al.* [27] apply a Kalman filter based method to estimate generator parameters (inertia H, transient reactance x'_d, and damping D) using PMU data. However, the method was not tested for robustness since the simulated machine and the estimated machine have the same simplified complexity and the same simplified dynamics.

Ghahremani and Kamwa [28, 29] use EKF and UKF to estimate the dynamic states only of a synchronous machine where the parameters of the machines are assumed available. Huang *et al* [27, 24] used Extended Kalman Filter (EKF) and PMU data to estimate the states and parameters of a classical generator model (rotor angle, rotor speed, H, D and x'_d). The input mechanical power and the internal voltage of the machine are assumed to be known. The algorithm was tested against a simulation model exactly same as the estimation model.

As a summary, the PMU data used for estimation of synchronous machines has been supplemented either by simplifying assumptions or extra measurements. This dissertation will improve on the dynamic estimation using PMU data. Approaches which can be applied to any system topology will be developed. Robustness of the approaches will be tested against unmodeled dynamics. Both states and parameters will be estimated.

2.3 Least Squares Estimation and System Identification

The processing of the Differential and Algebraic Equations (DAEs) representing the machine model by the estimation methods, along with the data provided by the DAEs, can either be batch processing like the approach of Least Squares Estimation (LSE) methods

or recursive processing as used by Kalman Filter (KF). LSE was used by the frequency domain data based methods in [30, 31] and by time domain data based methods.

In the time domain data based methods, LSE coupled with DFR were used to estimate machine d and q axis inductances and field resistance, (L_{ad}, L_{aq}, and r_f) by Kyriakides *et al.* [20], the armature circuit parameters by Melgoza *et al.* [21]. Both [20] and [21] use data provided by DFRs (high sampling frequency) in addition to field circuit voltage which is not an output data and is not available usually when the machine is operating under normal circumstances.

The differential equations describing the machine under transient conditions can be tackled during LSE problem by numeric techniques like finite differences. Finite differences technique has been used in power systems research such as in [32] and [20] in order to compute derivatives wrt. time. The research in this dissertation will explore the possibilities o using finite differences in estimating power systems parameters.

Least squares estimation is a part of System Identification framework. System identification is another non-Bayesian approach used to find systems structures and estimate their parameters [12]. The objective of system identification is to use experimental or measured data as input and output of proposed model structure describing a physical system in order to estimate the proposed model parameters and order. System identification has been used in power electronics research in order to identify power converters [33, 34], to model large signal power electronics systems [35], and to estimate DC link model parameters in VSC-HVDC system [36]. It has also been used in power systems research in the design of probing signals for the estimation of inter-area electromechanical modes [37], and in finding the state space system for multi-input-multi-output models of power systems [38]. [38] uses system identification in order to identify the dominant modes of the systems based on their responses to pulse excitations.

System output sensitivity matrix based on singular value analysis is used to study which parameters can be estimated using Least Squares Estimation [39] with specific set of measurements (observations). [40] has used the similar approach of studying the Hes-

sian matrix for the synchronous machines parameters sub-set selection using synchronous machine voltage, current, rotor angle, and field voltage. Such set of data used by [40] is not usually available for synchronous machines in online operation as opposite to the continuous availability of PMU data. The dissertation will address the use of the sensitivity matrix of the PMU data for the purpose of parameters sub-set selection for estimation.

It is one of the objectives of the paper to extend system identification to estimate synchronous machines and power systems parameters based on the output data provided by PMUs only.

2.4 Kalman Filter Based Estimation

2.4.1 Kalman Filter

Kalman filter (KF) is a digital optimal linear data processor used to estimate the states of a system subject to process noise and to measurement noise [41]. KF approach is a Bayesian recursive method compared to the LSE which uses a non Bayesian methods considering the complete data set in the time window.

The states can be constant (parameters) or dynamic (time varying) states when using Kalman Filter and are modeled as random variables with mean $\hat{x}$ and a covariance P. What the filter needs to know is:

1. System and measurements descriptive equations
2. Process and measurements noise variances Q and R
3. Initial values of states with their initial covariances x_0 and P_0

Kalman filtering process in the discrete model at a time step starts with a prediction of the states and their probability moments (variance and mean) in the next time step using the recursive system, followed by a correction of the predicted moments using measured observations. It can be summarized as follows:

1. Find the system and measurements descriptive equations:

$$\begin{cases} x_k &= Ax_{k-1} + Bu_k + w_k \\ z_k &= Cx_k + Du_k + v_k \end{cases} \tag{2.1}$$

where x_k: state value at time k, u_k: control function, w_k: process noise, z_k: measurement, and v_k: measurement noise.

2. Predict the value of x_k and P_k:

$$\begin{cases} \hat{x}_k^- &= Ax_{k-1} + Bu_k \\ P_k^- &= AP_{k-1}A^T + Q \qquad A^T \text{ is the transpose of } A \end{cases} \tag{2.2}$$

3. Find Kalman Gain $G_k = P_k^- C^T (CP_k^- C^T + R)^{-1}$

4. Find the measurement deviation $\Delta z_k = z_k - (C\hat{x}_k^- + D\hat{u}_k)$

5. Correct the estimates for x_k and P_k:

$$\begin{cases} \hat{x}_k &= \hat{x}_k^- + G_k \Delta z_k \\ P_k &= (I - G_k C)P_k^- \qquad I \text{ is the identity matrix} \end{cases} \tag{2.3}$$

6. repeat steps 2.through 5. above until the estimation is stable.

Fig. 2.1 shows the workflow of Kalman Filter.

The state space system (2.1) is linear. When the state space system is non-linear then KF can still be used after getting modified to become either Extended Kalman Filter (EKF) or Unscented Kalman Filter (UKF). EKF linearizes the states and observations equations in order to deal with non-linearity issues [42] whereas UKF calculates the probability moments, of both a number of projected states samples and their projected observations, in order to address the non-linearity anomalies [43].

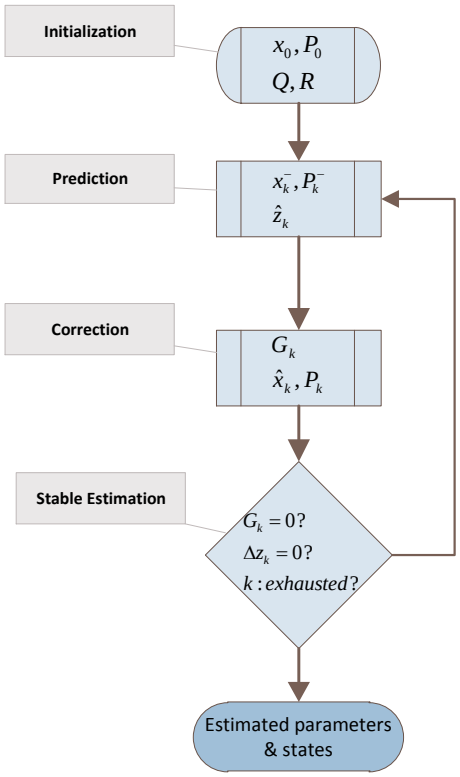

Figure 2.1. Kalman Filter workflow

KF is suitable for parameter estimation of synchronous machines, because synchronous machines can be formulated according to (2.1) where the state x can be either a variable (like rotor angle) or simply a parameter (like the machine inertia H).

2.4.2 Existing Research Using EKF and UKF in Machines Parameters Estimation

EKF and UKF have been used instead of the simple Kalman filter when the system model equations are non-linear. An example of the such non-linearity is the power flow equation between the synchronous machine and a bus at the output of the machine [44]: $P = \frac{EVsin(\delta-\theta)}{x'_d}$ where: P is active power, E and δ are the internal voltage source and the angle of the machine, V and θ are the voltage and angle of the bus; δ is a state variable in this case. Both filters (UKF and EKF) have been used to estimate parameters of synchronous and induction machines.

Azad *et al* [45] estimated stator and rotor resistances and inductances (in addition to other electromagnetic states) of doubly fed induction generator (DFIG) used in wind turbine using rotor and stator d and q axis voltages and currents with UKF or EKF. UKF is used by Valverde *et al* [22] to estimate the d and q magnetizing reactances x_{md}, x_{mq}, and the field resistance r_f (with various electromagnetic states). Additional mechanical measurements not provided by PMUs or DFRs, i.e. rotor speed ω and rotor angle δ, are required in [22] and [45]. [22] highlights the difficulties in obtaining x_{mq} and δ simultaneously because of a relation between them, hence [22] uses either a sensor to measure δ or a fixed ration between x_{mq} and x_{md}. The simultaneous estimation of δ and x_q is similarly challenging because of the relation between x_q and x_{mq}, $x_q = x_{ls} + x_{mq}$, x_{ls} being the leakage reactance [17].

Kalsi [46] uses EKF to calibrate the inertia H and damping factor D for a classical synchronous machine. The algorithm needs terminal measurements (like PMU) and to explicitly know the system equations which can only be done if other machine parameters (like the transient reactance) are known. Huang *et al* [24] used Extended Kalman Filter (EKF) and PMU data to estimate the states in a multi machine system. [27] calibrates the parameters of a classical machine based on recorded terminal data. The simulated model used in [46] and [24] is a simple model and can differ substantially from the real machine which raises the challenge of using a sophisticated model in the simulation. Ghahremani *et al* [28] [29] uses EKF and UKF to estimate the dynamic d and q voltage transients for a synchronous machine where the parameters of the machines are available.

As a summary, in this dissertation KF application using PMU data will be improved. More parameters and states will be estimated and unmodeled dynamics will be tested.

2.5 Further Classification and Summary

Following the domain of the data, the methods can either be time domain data based methods [40, 47, 48, 49, 50, 51, 52, 53, 54, 21, 55, 56, 57] or frequency domain data

based methods [30, 31, 58, 59]. Since the machine subject to estimation connects to the electric grid, the methods can either require the machine to be offline as in the case of the frequency domain based methods [30, 31, 58, 59] or to be online as found by time domain based methods. NERC's suggested method [7] uses the response for step change injected into the voltage reference and calls for an offline testing of the machine. Interest in keeping the machine connected to the network has led to the development of online estimation methods for the synchronous machine.

The scope of the parameters to be estimated is another area addressed by estimation methods: some methods estimate electrical parameters only (e.g., d or q axis resistances and inductances) as in [47, 49, 53, 54, 30, 31, 58, 59, 21, 55, 56, 57] whereas other methods look at a combination of electrical and mechanical parameters [48, 50, 51, 52].

Burth *et al.* [40] points out to the difficulty in estimating synchronous machine parameters based on its output only. The reason is the complicated structure of the synchronous machine which incorporates lots of parameters yet the effect of each parameter is not clearly reflected in the output (recorded by PMU or DFR), i.e. the generator output observations are not rich. In order to circumvent such estimation difficulties, researchers have resorted to using various additional information in addition to the machine output data towards carrying out machine parameters estimation.

Fig. 2.2 shows the various estimation approaches for power systems parameters estimation.

2.6 Dissertation Contribution

This dissertation will identify PMU based generator model estimation problems and apply approaches such as least square estimation and Kalman filtering in estimation. Specifically, the contributions of the dissertation include:

1. Building the estimation process around data from one PMU only

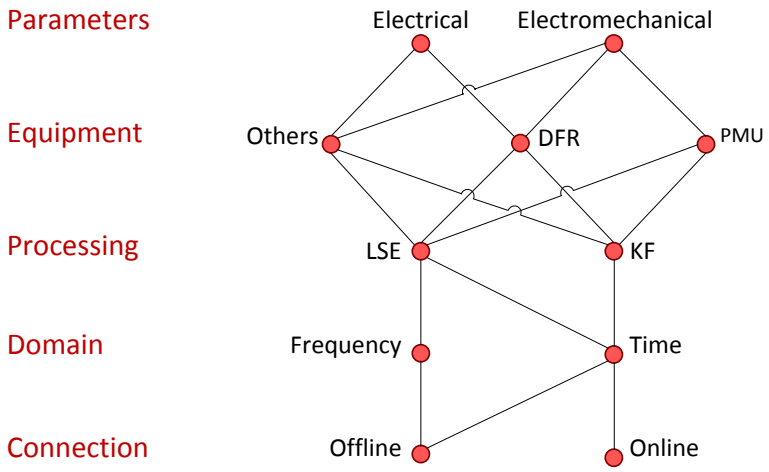

Figure 2.2. Various approaches in power systems parameters estimation

2. Extending System Identification Framework on synchronous machines and power subsystem in terms of developing a model, estimating its parameters, and validating its output against a sophisticated simulated system

3. Implement sensitivity matrix analysis using singular value decomposition on PMU data in order to select the parameters sub-set suitable for estimation by the PMU data

4. Exploring finite differences technique in conjunction with Least Squares Estimation as a parameter estimation method for the dynamic system representing a synchronous machines and using PMU data as measurements

5. Identify the issues facing the application estimation techniques on real PMU data

6. Developing subsystem decoupling technique as the interface between a power subsystem and the rest of the power system

7. Improving on the use of Extended Kalman Filter by increasing the accuracy and conversion of the estimations

8. Improving on the application of Unscented Kalman Filter by using dual filters on synchronous machine flux decay model and estimated q axis reactance with the rotor angle at the same time. Against other established research, the estimation of the rotor angle with the q axis reactance does not use any data other than the PMU data

9. Address the deviation resulting from machine high order models simulation subject to lower order model estimation

CHAPTER 3: KALMAN FILTER BASED ESTIMATION

3.1 Note to Reader

Portions of these results have been previously published (as a 1st author in [60]) or submitted for publication (as a 2nd author in[61]). The results are utilized with permission of the publisher.

3.2 Introduction

Kalman Filter was introduced in Section 2.4 as an estimation filter for linear systems. Extended Kalman Filter (EKF) and Unscented Kalman Filter (UKF) are the major improvements on KF in order to deal with non-linearity related discrepancies.

3.3 Extended Kalman Filter Based Estimation

3.3.1 Introduction

Phasor Measurement Units (PMU) equipped with GPS antennas measure three-phase instantaneous voltages and currents and calibrates phasors. These phasors are transmitted with time stamps and called synchrophasors. Synchrophasors have many applications that enhance situation awareness of the power grid. The Department of Energy has supported PMU installation around the US through the Smart Grid Investment Grant (SGIG) with a plan for thousands of PMUs to be installed in the US over the next several years. Effective use of the PMU data to enhance power system situation awareness and security is of key interest to power system operators.

State estimation can be generally classified into two categories: steady state and dynamic. Conventional state estimation belongs to the first category, where bus voltages

and phase angles are estimated every five minutes and the estimation handles *steady state* power flow problems. The measurements could be active power, reactive power and voltage magnitude. With phasor measurements, steady state estimation can incorporate direct phasor measurements and formulate least square estimation problems [62, 63, 64].

This research deals with dynamic state and parameter estimation employing PMU data. The current data in Eastern Interconnection collected by the RTDMS database [65] has a 30 Hz sampling rate. This is a much faster sampling rate compared to that of conventional state estimation (0.2 Hz sampling rate). With such a sampling rate, estimation of dynamic states and parameters related to critical low frequency electromechanical dynamics becomes feasible. Two applications can be envisioned for PMU data based dynamic estimation. The *first* one is in generator model and parameter estimation. NERC MOD-013 [10] compliance requires unit-specific dynamics data shall be reported. These data include generator (inertia constant, damping coefficient, direct and quadrature axes reactances and time constants), excitation systems, voltage regulators, turbine-governor systems, power system stabilizers, and other associated generation equipment. Currently, the data required by NERC have to be obtained by bringing a unit offline and conducting tests. The problem investigated in this research can provide some of the data required by NERC MOD-013 and therefore have a practical application in online generator parameter estimation without interrupting units operation. The *second* application is subsystem identification. Instead of just one generator unit, a subsystem consisting of multi units can be estimated with PMU data.

Synchronous generator parameter estimation has been investigated in the literature. Based on the data used, the methods can be classified into: time-domain data based [40, 47, 48, 49, 50, 51, 52, 53, 54, 21, 55, 56, 57] and frequency response data based [30, 31, 58, 59] methods. Based on the nature of the measurements, there are digital fault recorder data with high sampling rate based estimation for generator electrical parameters [21, 55, 56, 57], and other online tests based methods such as short circuit tests [47, 49], step or binary sequence inputs into excitation [48, 51, 52], and offline tests based [30, 31, 58, 59]

methods. Based on the scope of the estimation, some focus on electrical parameters (e.g., qd-axis resistances and inductances) only [47, 49, 53, 54, 30, 31, 58, 59, 21, 55, 56, 57], while [48, 50, 51, 52] estimate both electrical and mechanical parameters. Based on the estimation methods, then there are at least two major systematic methods to deal with differential equation model estimation: least square estimation [40, 47, 48, 49, 52, 54, 30, 31] and Kalman filter estimation [50, 51].

PMU data based estimation problems fall into the category of online, time-domain, and electro-mechanical dynamics related problems.

In the literature, a synchronous generators' parameters can be estimated accurately if given sufficient measurements. For example, in [48], a third-order machine model parameters (H, D, T'_{do}) are estimated based on the measurements of the terminal voltage, output power, angle given a step response in excitation system. In [51], electrical and mechanical parameters of a generator can be estimated given measurements from filed current, terminal current, terminal powers, rotor angle and rotor speed. In [52], electrical and mechanical parameters of a generator can be estimated given measurements of three-phase currents, line voltages, and field voltage. Reference [40] indicates that machine circuit parameters and mechanical system parameters can be estimated given different sets of measurements.

Unlike the estimation problems in the literature, PMU data are limited to voltage and current phasors. We cannot obtain measurements as much as we want such as in [51, 52]. Secondly, unlike the tests conducted in [48, 50, 52], the trigger of transients is unknown. Field current and voltage measurements are not available.

Therefore, PMU data based estimation problems are limited to state estimation only [66, 67] or state/parameter estimation for 2nd order mechanical system [24, 27, 46, 68, 69]. The above investigation all applies Kalman filtering technology in estimation. There are other methods in PMU data based estimation method designated for a special system, e.g., [23] investigates a radial system estimation problem. In this research, a general approach that can be applied for any system is sought.

EKF approach is adopted in this research to estimate a generator's model and parameters. Unlike least squared estimation which uses a time window of data, EKF estimation uses the current step measurements and prediction. Hence the data storage requirement is very low. This approach can also be used to estimate a reduced-order model which can represent a subsystem. In addition, to reduce the computation burden, instead of estimating the entire system, only a subsystem or a generator is estimated. The generator is however interconnected to the grid. Therefore, a model-decoupling method will be introduced in this research to decouple the subsystem model from the grid by treating a subset of measurements as inputs to the model.

Model decoupling technique has been employed in decentralized nonlinear control and subsystem model validation [70, 71, 68, 27]. A subsystem's model will be independent from the rest of the system as long as the interfacing variables with the rest of the system can be measured and used as the input for a local decentralized controller. In [70], terminal voltage is the interfacing variable. In [71], currents are the interfacing variables. In model validation, a technique used in subsystem model validation is called "event play back" [68, 27]. In "event play back," the objective is to estimate the parameters for a dynamic model which represents a synchronous generator or a subsystem. Measurements at the terminal bus will be separated into two groups. One group (voltage magnitude and phase angle) is treated as the input signals to the dynamic model and the other group (real and reactive power) is treated as the measurements in the EKF algorithm. Using such a technique, there is no longer the need to deal with the dynamic model of an entire power system; rather, second-order dynamic models will be used in the EKF in parallel.

This research will propose a model decoupling method and implement EKF to estimate dynamic states and parameters related to electromechanical dynamics. Compared to the most recent work on EKF implementation in PMU data for dynamic state estimation in [27, 66], the unique contribution of this research is two-fold:

1. The estimation can handle *more parameters*. The problem presented in this research is more comprehensive where two states and four unknown parameters

will be estimated. Estimated problem in [66] deals with four dynamic states (δ, ω, E'_q and E'_d) and one unknown parameter (excitation voltage E_{fd}). All other parameters such as inertia constant H, damping factor D and reactances are assumed to be known. Estimation of H and D have shown to be more difficult than other parameters [27] since nonlinearity is introduced and there will be more linearize error in EKF prediction. EKF-based estimation in [27] assumes the mechanical power for a generator is known and three parameters H, D and x'_d are estimated. This research will tackle four-parameter and five-parameter estimation problems.

2. The estimation can handle *modeling errors*. The model used in this research is the simplest for a synchronous generator. However the estimation will be tested against simulation data from more sophisticated model to demonstrate the robustness of the proposed estimation. This is a step further than research in [66, 67, 24, 27, 46, 68, 69] where estimation model is the same as the simulation model with white noise added in measurements. In this research, the estimation is tested against unmodeled dynamics which are no longer white noises.

The following sections will explain the basic EKF algorithm (Section 3.3.2), model decoupling and EKF implementation (Section 3.3.3). Case studies will be present in Section 3.3.4. Section 3.3.5 concludes this EKF based research.

3.3.2 Basic Algorithm of EKF

Kalman filter theory was developed by R. Rudolf Kalman in late 1950s and can be considered as a type of observers for linear dynamic systems perturbed by white noise by use of white noise polluted measurements [72]. Kalman filter is suitable for real time estimation since the estimation is done for any instantaneous time. EKF is a discrete Kalman filter adapting to nonlinear system estimation through linearization.

For a nonlinear dynamic system described by Differential Algebraic Equations (DAEs) in (3.1) and further in discrete form in (3.2), the purpose of EKF is to minimize the covariance of the mismatch between the estimated states and the states.

$$\begin{cases} \frac{d\boldsymbol{x}}{dt} = f_c(\boldsymbol{x}, \boldsymbol{y}, \boldsymbol{u}, \boldsymbol{w}) \\ 0 = g_c(\boldsymbol{x}, \boldsymbol{y}, \boldsymbol{u}, \boldsymbol{v}) \end{cases} \tag{3.1}$$

where the $\boldsymbol{x}$ vector represents the state variables, the $\boldsymbol{y}$ vector represents the algebraic variables, $\boldsymbol{u}$ is the vector of input variables, $\boldsymbol{w}$ and $\boldsymbol{v}$ are processing noise and measurement noise. The subscript "c" denotes the continuous form. The discrete form of (3.1) is:

$$\begin{cases} \boldsymbol{x}_k = \boldsymbol{x}_{k-1} + f_c(\boldsymbol{x}_{k-1}, \boldsymbol{u}_{k-1}, \boldsymbol{w}_{k-1})\Delta t \equiv f(\boldsymbol{x}_{k-1}, \boldsymbol{u}_{k-1}, \boldsymbol{w}_{k-1}) \\ 0 = g_c(\boldsymbol{x}_k, \boldsymbol{y}_k, \boldsymbol{u}_k, \boldsymbol{v}_k) \Rightarrow \boldsymbol{y}_k = h(\boldsymbol{x}_k, \boldsymbol{u}_k, \boldsymbol{v}_k) \end{cases} \tag{3.2}$$

The EKF problem can accommodate parameter estimation by adding "auxiliary states" where $x_k = x_{k-1}$. The EKF problem can be solved in a two-step process [73]:

$$Prediction: \begin{cases} \hat{\boldsymbol{x}}_k^- = f(\hat{\boldsymbol{x}}_{k-1}, \boldsymbol{u}_k, 0) \\ P_k^- = A_{k-1} P_{k-1} A_{k-1}^T + W_{k-1} Q_{k-1} W_{k-1}^T \end{cases} \tag{3.3}$$

$$Correction: \begin{cases} K_k = P_k^- H_{z,k}^T (H_{z,k} P_k^- H_{z,k}^T + V_k R_k V_k^T)^{-1} \\ \hat{\boldsymbol{x}}_k = \hat{\boldsymbol{x}}_k^- + K_k(\boldsymbol{z}_k - h(\hat{\boldsymbol{x}}_k^-, \boldsymbol{u}_k, 0)) \\ P_k = (I - K_k H_{z,k}) P_k^- \end{cases} \tag{3.4}$$

where the superscript $^-$ denotes a *priori* state, A_k and W_k are the process Jacobians at step k, P_k is a co-variance matrix of the state estimation error and is also called gain factor matrix, and Q_k is the process noise covariance at step k. $H_{z,k}$ and V_k are the measurement Jacobians at step k, and R_k is the measurement noise covariance at step k.

A, H_z, W, and V are formulated as follows:

$$A = \frac{\partial f}{\partial \mathbf{x}}, H_z = \frac{\partial h}{\partial \mathbf{x}}, W = \frac{\partial f}{\partial \mathbf{w}}, V = \frac{\partial h}{\partial \mathbf{v}}. \tag{3.5}$$

3.3.3 Model Decoupling and EKF Implementation

3.3.3.1 Model Decoupling

The technique used in subsystem model validation called "event play back" [68, 27] has the potential to decouple the EKF problem by better use of PMU data. One group is treated as the input signals to the dynamic model and the other group is treated as the measurements in the EKF problem. Using such a technique, there is no longer the need to deal with the dynamic model of an entire power system. Rather, *small-scale* dynamic models will be used in the EKF *in parallel*.

Each PMU provides voltage phasor and current phasor. From the provided data, active power P and reactive power Q can be computed. In this application, we consider PMU provides four data sets: voltage magnitude (V) , voltage phase angle (θ), active power (P_e) and reactive power (Q_e). Only positive sequence data from PMUs are used in this application since it is reasonable to assume that transmission systems are operated under balanced conditions for majority of the time. The dynamic model of each generator (modeled as a constant voltage behind a transient reactance) is expressed as follows:

$$\begin{cases} \frac{d\delta}{dt} = \omega - \omega_0 \\ \frac{d\omega}{dt} = \frac{\omega_0}{2H}(P_m - P_e - D(\omega - \omega_0) \\ = \frac{\omega_0}{2H}(P_m - \frac{EV}{x'_d}\sin(\delta - \theta) - D(\omega - \omega_0)) \end{cases} \tag{3.6}$$

The vector of the state variables is $\boldsymbol{x} = [\delta, \omega]^T$ (δ-rotor angle and ω-rotor speed). E and P_m are internal voltage and mechanical power. The coupling between a generator and network can be viewed at two levels: at electric level and at electro-mechanical level. At

electrical level, the generator is modeled as a voltage source behind impedance. A network voltage and current relationship can be setup $YV = I$.

At the electro-mechanical level, the machine speed is influenced by the electric network through the electric power exported. The mechanical power is assumed to be constant or the slow dynamics of the mechanical system is ignored. Fast dynamics in the damping windings are ignored. Further, field flux is assumed to be constant.

There are two ways to decouple the model using PMU measurements as shown in Fig. 3.1. Method A treats the terminal voltage phasor (V, θ) as the input and the power (P_e, Q_e) as the measurements. Method B treats the power as the input and the voltage phasor as the measurements. When P_e and Q_e are treated as the input for the model in (3.6), (3.6) can then be considered as a stand-alone dynamic model. On the other hand, if P_e and Q_e are not treated as the input, each generator will be dominated by its dynamic equation as (3.6). These equations are coupled by the expression of electric power.

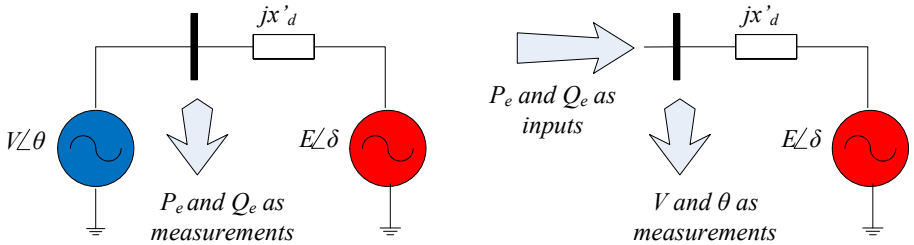

Figure 3.1. (a) model decoupling using V and θ as inputs while P_e and Q_e as measurements. (b) model decoupling using P_e and Q_e as inputs while V and θ as measurements

The relationship of P_eQ_e, $V\theta$ and other state can be found in the equations:

$$\begin{cases} P_e = \frac{EV}{X'_d} \sin(\delta - \theta) \\ Q_e = \frac{-V^2 + EV\cos(\delta - \theta)}{X'd} \end{cases} \tag{3.7}$$

Method A has been applied by the PNNL group in [68, 69]. Method B, however, has not been investigated. A significant difference between Method A and Method B resides

in the prediction step rotor speed computation:

$$\begin{cases} \omega_{k+1} &= \frac{\omega_0}{2H_k}\left(P_{m,k} - \frac{EV_k sin(\delta_k - \theta_k)}{x'_{d,k}} - D_k(\frac{\omega_k}{\omega_0} - 1)\right)\Delta t + \omega_k, \qquad \text{Method A} \\ \omega_{k+1} &= \omega_k + \frac{\omega_0}{2H_k}\left(P_{m,k} - P_{e,k} + D_k(\frac{\omega_k}{\omega_0} - 1)\right)\Delta t, \qquad \text{Method B} \end{cases} \tag{3.8}$$

Method A relies on the voltage measurement, phase angle measurement, and transient reactance estimation to compute the electric power in the prediction step. The expression for power is only accurate for a classical generator model. In addition, when the transient reactance is unknown, there will be significant errors in computing power. Compared to Method A, Method B uses the power measurements as the input for the model. The accuracy of the rotor speed prediction is greatly improved. Method A has been applied in [68, 27] and there are two limitations: 1) it cannot handle modeling error. In [68, 27], the simulation model and the estimation model are the same classical model. 2) it cannot handle four unknown parameters. It can only handle three parameters.

Therefore, in this paper, Method B is used as the model decoupling technique for EKF implementation. The EKF implementation is shown in Fig. 3.2 where PMU data are separated into two groups (P_eQ_e as inputs and $V\theta$ as measurements). The dynamics block performs prediction using system equations while the geometry block computes the estimated measurements based on the *priori* states. A Kalman filter gain is used to correct the *priori* state with the error between the measurements and their estimation.

3.3.3.2 EKF Implementation

In this section, detailed mathematical model of the EKF will be given. The states and parameters to be estimated are the rotor angle (δ), the rotor speed (ω), the mechanical power (P_m), the inertia constant H, the damping factor D and the transient reactance x'_d. PMU can give measurements for the terminal voltage magnitude, voltage phase angle, real power and reactive power. The real and reactive power are treated as the input. The voltage magnitude and voltage phase angle are treated as the outputs or measurements.

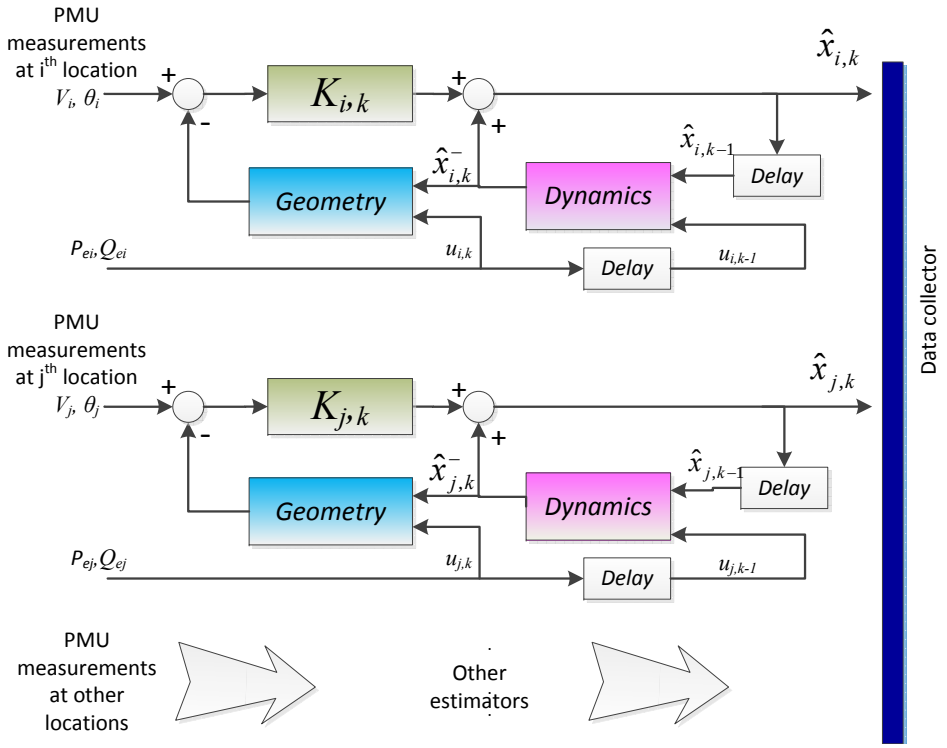

Figure 3.2. Kalman filtering technology using PMU data

The discrete model for the estimation system is describe as follow:

$$\begin{cases} \delta_{k+1} = \delta_k + (\omega_k - \omega_0)\Delta t + w_1 \\ \omega_{k+1} = \omega_k + \frac{\omega_0}{2H_k}(P_{m,k} - P_{e,k})\Delta t + D_k(\omega_k - \omega_0)\Delta t + w_2 \\ P_{m,k+1} = P_{m,k} + w_3 \\ H_{k+1} = H_k + w_4 \\ D_{k+1} = D_k + w_5 \\ x'_{d,k+1} = x'_{d,k} + w_6 \end{cases} \tag{3.9}$$

$P_{e,k}$ is the input of the system, w_i are the noise to represent un-modeled dynamics and ω_0 is the nominal frequency.

The Jacobian matrix A is given by

$$A = \begin{bmatrix} 1 & \Delta t & 0 & 0 & 0 & 0 \\ 0 & 1 - \frac{D\omega_0 \Delta t}{2H} & \frac{\omega_0 \Delta t}{2H} & A_{24} & A_{25} & 0 \\ 0 & 0 & 1 & 0 & 0 & 0 \\ 0 & 0 & 0 & 1 & 0 & 0 \\ 0 & 0 & 0 & 0 & 1 & 0 \\ 0 & 0 & 0 & 0 & 0 & 1 \end{bmatrix} \tag{3.10}$$

where:

$$A_{24} = -\frac{P_m - P_e - D(\omega - \omega_0)}{2H^2}\omega_0 \Delta t \tag{3.11}$$

$$A_{25} = \frac{-(\omega - \omega_0)}{2H}\omega_0 \Delta t \tag{3.12}$$

The measurement sensitivity matrix H_z can be found from the implicit functions (3.7).

$$\begin{aligned} H_z &= \begin{bmatrix} \frac{\partial V}{\partial \delta} & \frac{\partial V}{\partial \omega} & \frac{\partial V}{\partial P_m} & \frac{\partial V}{\partial H} & \frac{\partial V}{\partial D} & \frac{\partial V}{\partial x'_d} \\ \frac{\partial \theta}{\partial \delta} & \frac{\partial \theta}{\partial \omega} & \frac{\partial \theta}{\partial P_m} & \frac{\partial \theta}{\partial H} & \frac{\partial \theta}{\partial D} & \frac{\partial \theta}{\partial x'_d} \end{bmatrix} \\ &= \begin{bmatrix} 0 & 0 & 0 & 0 & \frac{\partial V}{\partial x'_d} \\ 1 & 0 & 0 & 0 & \frac{\partial \theta}{\partial x'_d} \end{bmatrix} \end{aligned} \tag{3.13}$$

where:

$$\frac{\partial V}{\partial x'_d} = \frac{\frac{-Q_e E^2 - 2x'_d P_e^2}{\sqrt{f_1}} - 4Q_e}{\sqrt{f_2}} \tag{3.14}$$

$$\frac{\partial \theta}{\partial x'_d} = \frac{2P_e f_2 - P_e x'_d \left(\frac{-4Q_e E^2 - 8x'_d P_e^2}{\sqrt{f_1}} - 4Q_e\right)}{f_2 \sqrt{E^2 f_2 - 4P_e^2 x'^2_d}} \tag{3.15}$$

where:

$$f_1 = -4Q_e x'_d E^2 + E^4 - 4x'_d P_e^2 \tag{3.16}$$

$$f_2 = 2\sqrt{f_1} + 2E^2 - 4Q_e x'_d \tag{3.17}$$

3.3.3.3 Iterated Extended Kalman Filter (IEKF)

In order to achieve better convergence, Iterative EKF [73] is adopted. For each time step in EKF there is one prediction and one update step. In Iterative EKF setup, for each time step, there will be several iterations to update the Jacobian matrices and calculate estimated measurements in the correction step. IEKF requires more computation time in correction step compared to EKF.

EKF algorithm expands the measurement function h_k in (2) in the *correction* stage around x_k^- obtained as the best estimation of x from the *prediction* phase:

$$h(x_k, u_k, v_k) = h(\hat{x}_k^-, u_k, 0) + H_z(\hat{x}_k - x_k^-) + v_k \tag{3.18}$$

Accordingly, after the correction phase we have a better estimate of x_k as in $\hat{x}_k$. Using such estimate $\hat{x}_k$ in (3.18) instead of $\hat{x}_k^-$ could decrease the linearization errors in the rest of the estimation process and improve the estimate $\hat{x}_k$ of the correction phase. Iterative Extended Kalman Filter (IEKF) is based on repeating the linearization of h and the *correction* phase on the improved estimate $\hat{x}_k^i$ where i is the number of the iteration.

A comparison of the estimation results obtained by EKF and iterative EKF for the case study presented in Section 3.3.4 is shown in Fig. 3.3.

Two initial guesses of H are used for each estimation. It is found that Iterative EKF can significantly increase the convergence rate towards the accurate parameter. The initial guess of H is set to be 4 pu.s or 8 pu.s. In both cases, IEKF can find the accurate estimation within two seconds. EKF however cannot reach the accurate estimation in ten

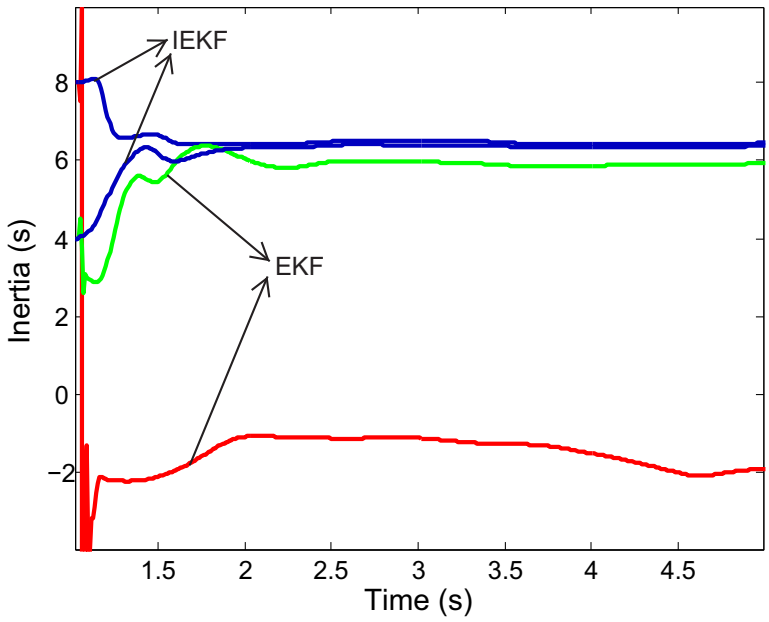

Figure 3.3. Estimation results of the inertia constant based on Set 1 data using EKF and iterative EKF

seconds. In addition, when the initial guess is 8 pu.s, EKF gives an estimation of a negative number.

In the following case studies, IEKF will be used.

3.3.4 Case Studies

The study system is the classic two-area four-machine system in the literature [15] (Fig. 3.4). A three-phase fault occurs at t=1 second on Load 1 bus. Load 1 is tripped after 0.1 second. Voltage phasor data and current phasor data from a generator terminal bus will be recorded. The sampling interval is 0.01s. The simulation is carried by Power System Toolbox [74]. The recorded data will be used to test the EKF methods. Four sets of simulation data will be recorded. To determine electromechanical states and parameters, the data contain obvious electromechanical oscillations are desired. On the other hand, measurements from digital fault recorders with high sampling rates and lasting less than 1 second are dominated by electromagnetic dynamics and hence are not suitable for the proposed method.

1. Set 1: In the first set, classical generator models are used in simulations. Hence the Kalman filter dynamic model is exactly same as the simulation model. The machine parameters are $H = 6.5s$, $D = 6$ pu, $x'_d = 0.25$pu, $E = 1.08$pu, and $P_m = 0.85$pu.

2. Set 2: In the second set, the damping is reduced to zero in the swing equation. The simulation model is same as the estimation model.

3. Set 3: In the third set, subtransient generator model [17] including dynamics in damping windings and field winding is used. The damping factor is zero. The simulation model is more sophisticated than the estimation model.

4. Set 4: In the fourth set, subtransient generator model is used. The damping factor is 6. Automatic voltage regulator (AVR) is enabled to get a stable system response.

When damping factor is zero, the system lacks damping and the PMU data in Fig. 3.5 presents obviously poor damped oscillations. Testing on those data can demonstrate that the proposed algorithm can converge well even the system is poorly damped.

At least two initial guesses will be used to demonstrate if EKF can converge to a same estimation or not. For the two states and four parameter estimation problem, Sets 1-4 are used. For the two states and five parameter estimation problem, Sets 1 and 4 are tested. Simulation data

The PMU data (V, θ, P_e, Q_e) for the four sets are plotted in Fig. 3.5. Among them, the power are used as input to the estimation model while the voltage phasor is treated as the measurements.

3.3.4.1 Two States and Four Parameters Estimation

In this section, the formulated EKF algorithm in Section 3.3.3 will be tested. The initial gain matrix P is the co-variance matrix of the estimate error and P will be updated in EKF and converge to zero if EKF works. Hence the parameters in P are not important.

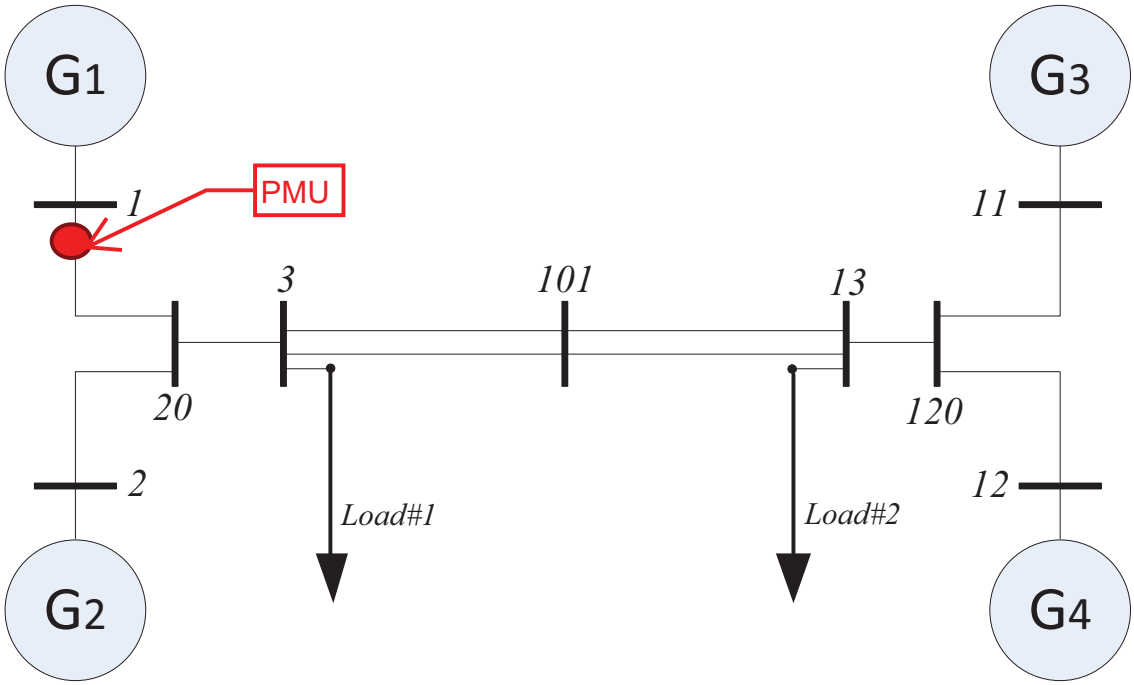

Figure 3.4. The study system

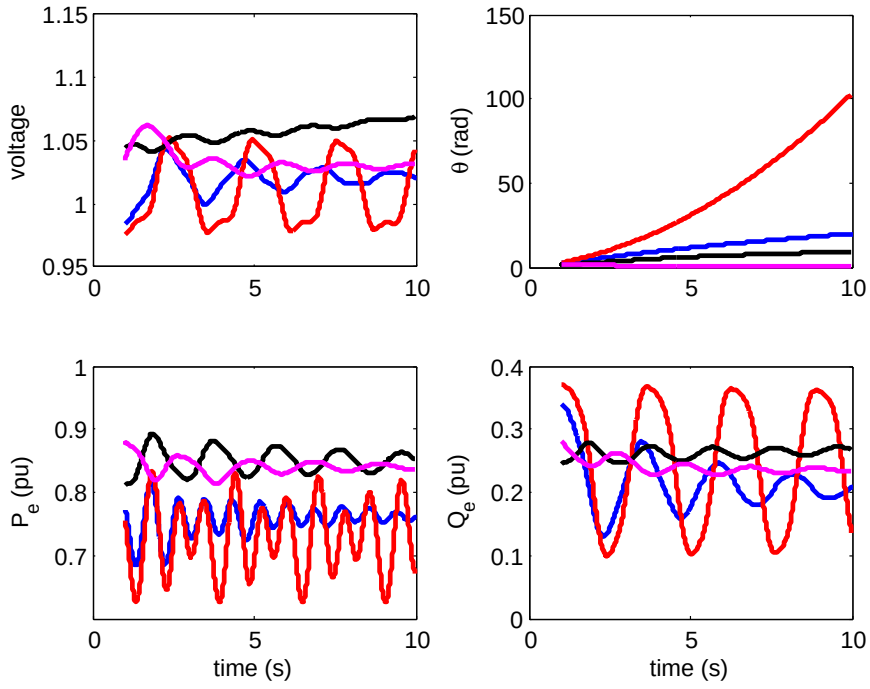

Figure 3.5. The PMU data V, θ, P and Q. P and Q are treated as the input to the estimation model while V and θ are treated as the measurement of the output of the estimation model. Set 1: red. Set 2: blue. Set 3: black. Set 4: magenta

However initial values of P matrix influence convergence rate. Therefore fine tuning is needed. Co-variance matrix Q represents noise co-variance. Noise includes processing noise and unmolded dynamics. Q is less deterministic. In often times superior filter performance can be obtained by "tuning" the filter parameters [75].

The co-variance matrix Q of the processing noise will be set differently for Sets 1&2 and Sets 3&4. Since Sets 1&2 are classical generator based simulation results and the internal voltage is fixed, there is no unmodeled dynamics in H, D and x'_d. Hence Q_{44}, Q_{55}, and Q_{66} are set to zero. On the other hand, Sets 3&4 are subtransient model based simulation data. Hence it is reasonable to model the unmodeled dynamics as noise in w_2, w_3, w_4, w_5, and w_6. The initial co-variance matrix is set to reflect the error in initial guess. Table 3.1 documents the parameters used in EKF estimation.

Table 3.1. Covariance matrices for two-state four-parameter estimation

P	Set 1&2	Set 3&4	Q	Set 1&2	Set 3&4
P_{11}	1	1	Q_{11}	$10^{-4}\Delta t$	$10^{-4}\Delta t$
P_{22}	30	30	Q_{22}	$10^{-3}\Delta t$	$10^{-3}\Delta t$
P_{33}	0.1	0.1	Q_{33}	0	0
P_{44}	5	5	Q_{44}	0	0
P_{55}	50	50	Q_{55}	0	0
P_{66}	1	1	Q_{66}	0	$0.01\Delta t$

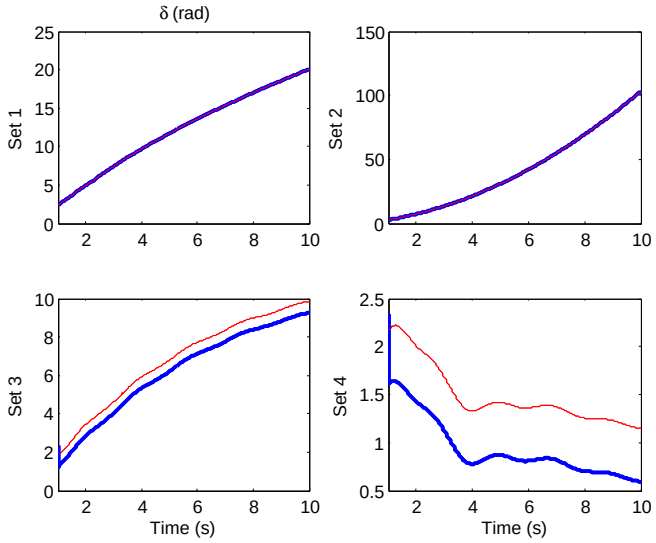

Figure 3.6. The estimated rotor angle compared to the simulated rotor angle

The rotor angle estimation matches very well with the simulated rotor angle in Set 1 and Set 2 scenarios. In Set 3 and Set 4, there is a discrepancy between the estimation and the real value though the dynamic trends match each other well. The discrepancy can be explained by comparing the classical machine model versus a two-axis machine model (Fig. 3.7).

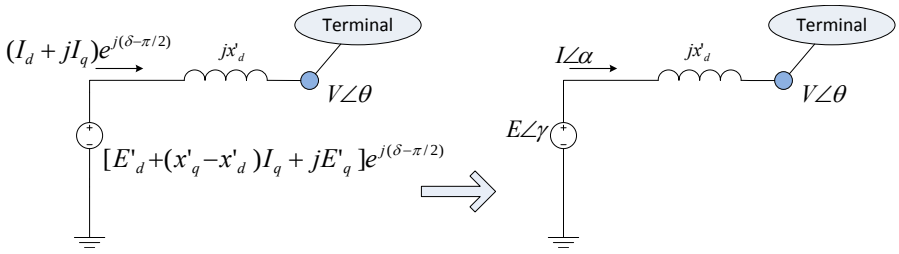

Figure 3.7. Two-axis model versus a classic generator model

The two voltage sources are equivalent to each other [17]. Hence the classic model voltage source can be expressed by:

$$E = \sqrt{(E'^o_d + (x'_q - x'_d)I^o_q)^2 + (E'^o_q)^2} \tag{3.19}$$

where x'_q is the q axis transient reactance; E'^o_d, E'^o_q, and I'^o_q are the d and q axis components of the voltage source and the current during steady state.

$$\delta'^o = tan^{-1}(\frac{E'^o_q}{E'^o_d + (x'_q - x'_d)I^o_q}) - \pi/2 \tag{3.20}$$

We notice that there is always a difference between the angle of the classical generator and the rotor angle ($\delta - \gamma = \delta'^o$)). Therefore, there is always a discrepancy (δ'^o) between the estimated rotor angle and the simulated rotor angle when the simulation model is subtransient model while the estimation model is a classical model.

The estimation of the rotor speed, the mechanical power, inertia constant, damping factor and transient reactance using Set1 and Set 2 data sets are found to be good matches of the simulation results. The results are shown in Figs. 3.8 - 3.12.

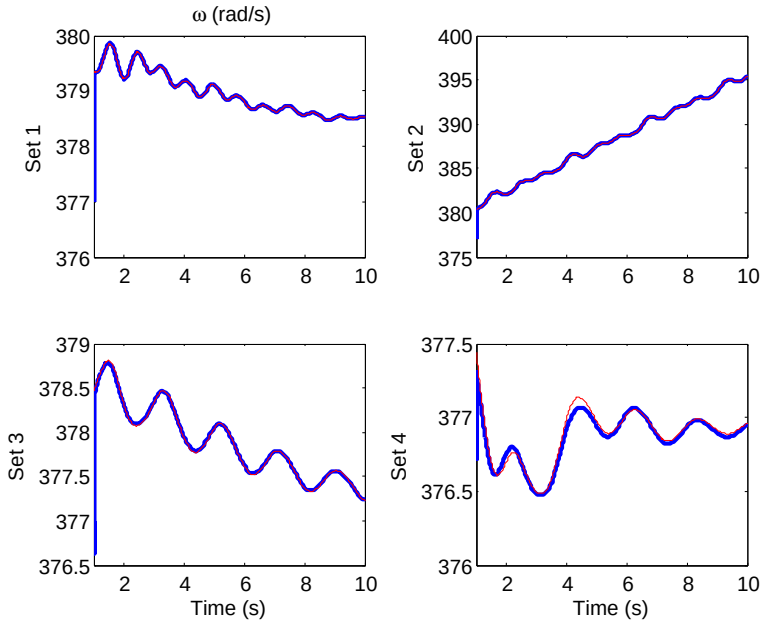

Figure 3.8. The estimated rotor speed compared to the simulated rotor speed

Set 3 and Set 4 data are simulation data from subtransient generator model. Excitation control is not modeled for Set 3 data. For Set 3 data, the estimation of H is higher than the real value while for Set 4 data, the estimation of H is lower than the real value.

When the field voltage E_{fd} is constant, the effect of the synchronous machine field circuit dynamics such as the field flux variations causes a slight reduction in the synchronizing torque component and increase in the damping torque component [76] at the electromechanical oscillation modes. The linearized swing equation for a classical generator can be expressed as:

$$s^2(\Delta\delta) + \frac{D}{2H}s(\Delta\delta) + \frac{K_s}{2H}\omega_0(\Delta\delta) = \frac{\omega_0}{2H}\Delta P_m. \tag{3.21}$$

where $K_s = \frac{\partial P_e}{\partial \delta}$, D is called the damping torque component while K_s is called the synchronizing torque component. Therefore, the characteristic equation is given by:

$$s^2 + \frac{D}{2H}s + \frac{K_s\omega_0}{2H} = 0 \tag{3.22}$$

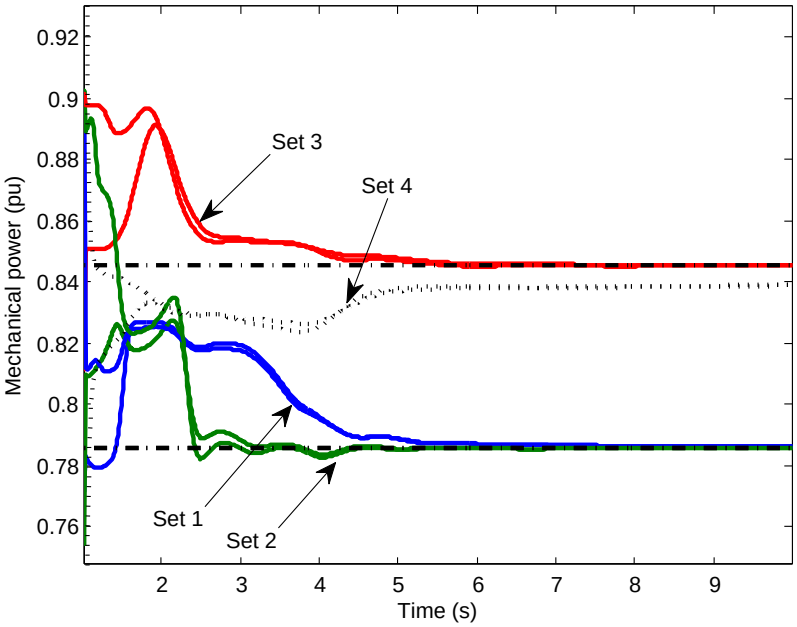

Figure 3.9. The estimated mechanical power

The effect of field flux variations will change the synchronizing torque component and the damping torque component by decreasing K_s and increasing K_D. Detailed explanation can be referred in [76] and [17]. A brief explanation is offered in this paper. Considering the field flux variation, the linearized system model is shown in Fig. 3.13 [76]:

K_1, K_2, K_3 and K_4 are constants related to operating conditions, T'_{d0} is the field winding time constant. From Fig. 3.13, we can find the contribution of K_s and K_D due to field flux variation or $\Delta E'_q$.

$$\frac{\Delta T_e}{\Delta \delta}|_{dueto\Delta E'_q} = \frac{-K_2 K_3 K_4}{1 + sK_3 T'_{d0}} \tag{3.23}$$

Substituting s by $j\omega$ and we have:

$$Re\left[\frac{\Delta T_e}{\Delta \delta}\right] = \frac{-K_2 K_3 K_4}{1+\omega^2 K_3^2 T'^2_{d0}} \tag{3.24}$$

$$Im\left[\frac{\Delta T_e}{\Delta \delta}\right] = \frac{K_2 K_3^2 K_4 T'_{d0}}{1+\omega^2 K_3^2 T'^2_{d0}} \tag{3.25}$$

$$\approx \frac{K_2 K_4}{\omega T'_{d0}} \tag{3.26}$$

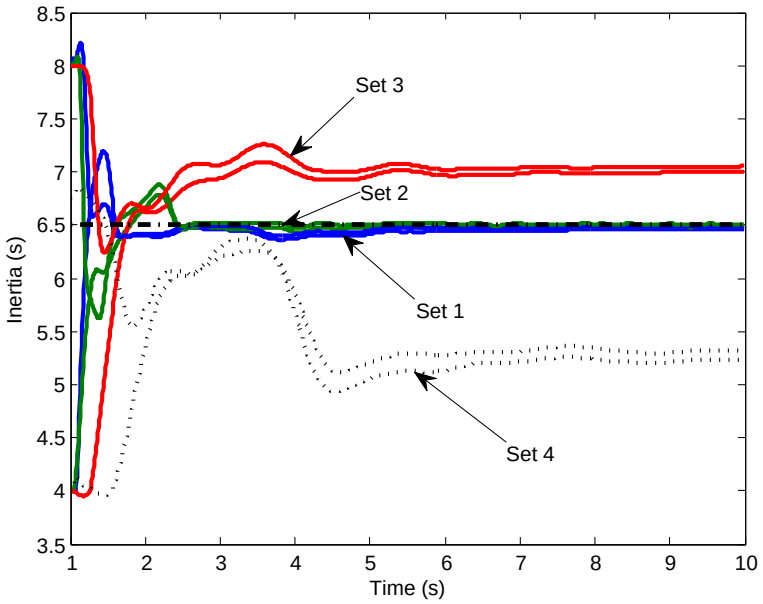

Figure 3.10. The estimated damping factor

K_2, K_3 and K_4 are positive numbers. Therefore, the impact of field flux variation can cause a decreased synchronizing torque component due to armature reaction while an increased damping torque component.

For a classical generator model, it is assumed that $T'_{d0} \approx \infty$. When T'_{d0} is very large, there is no effect on the damping torque component.

The characteristic equation becomes:

$$s^2 + \frac{DK_{fD}}{2H}s + \frac{K_s K_{fs}\omega_0}{2H} = 0$$
$$Or: s^2 + \frac{D'}{2H'}s + \frac{K_s\omega_0}{2H'} = 0 \tag{3.27}$$

where $K_{fD} > 1$ (increase in the damping torque component), $K_{fs} < 1$ (reduction in the synchronizing torque component), $H' = H/K_{fs} > H$, and $D' = DK_{fD}/K_{fs} > D$.

Therefore, it is reasonable for EKF-based estimation to find the estimated inertia and damping constant greater than the real values for Set 3 data.

The excitation control's effect on damping and synchronizing torque components at the oscillation frequency depends on the gain of the AVR and the system operating

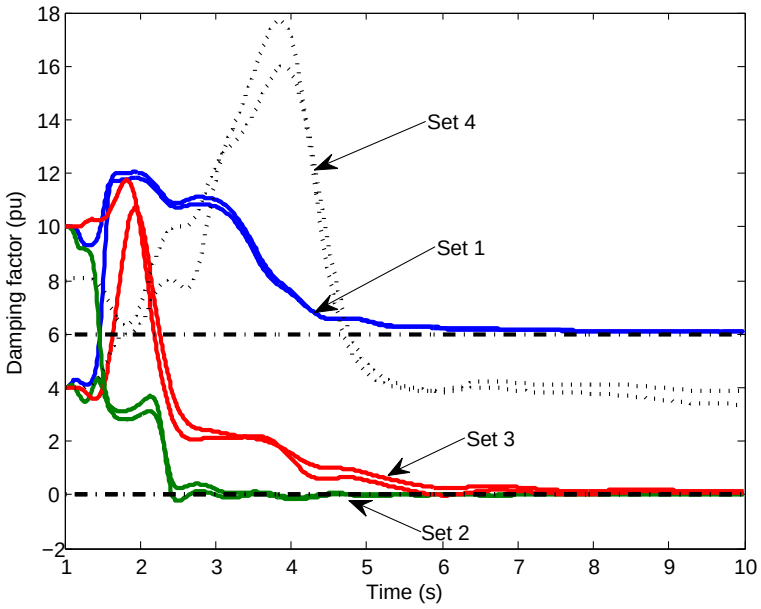

Figure 3.11. The estimated inertia constant

condition. In this case study, a high gain is chosen which introduces a positive synchronizing torque component and a negative damping torque component [76]. Compared to the effect of machine circuit dynamics, the effect of the AVR is much significant. Based on the same analysis carried out in (3.27), it can be found that $H' < H$ and $D' < D$. Therefore, for Set 4 data, it is reasonable that the estimated inertia constant and damping factor are less than the real values.

For this two-state four-parameter estimation problem, two initial guesses are used. Except for x'_d for Set 3, all parameter estimation converges to the same or close results within 10 seconds. Therefore, this EKF application is considered to be able to give converged and reasonable estimation.

3.3.4.2 Impact of the Assumption of E

The impact of E assumption is shown in Fig. 3.14. Set 1 data is used for this test. Different E values are assumed: 1.08, 1.1 and 1.2. The true value of E is 1.08 pu. It can be observed that the value of E impacts the estimation of x'_d a good deal. Its impact on the other parameters such as P_m, H and D are much less significant.

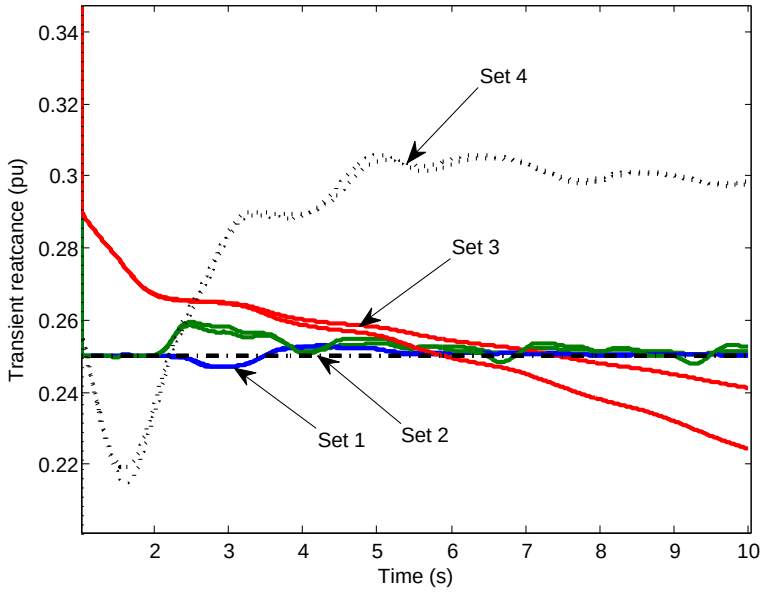

Figure 3.12. The estimated transient reactance

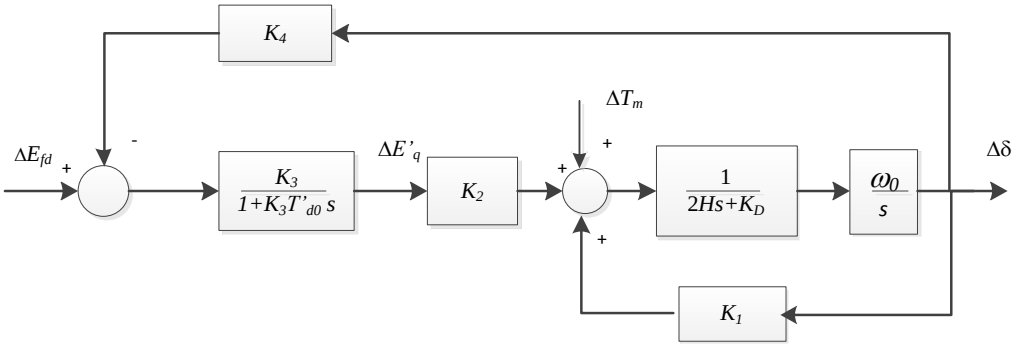

Figure 3.13. Linearized synchronous generator model considering field flux variation

3.3.4.3 Two-State Four-Parameter Estimation based on Measurements with White Noise

In this section, Set 3 data are assumed to be polluted by white noise. The measurements are presented in Fig. 3.15.

White noises are added on active power, reactive power and voltage. The estimated states and parameters are presented in Figs. 3.16 and 3.17.

It is found that the algorithm can estimate accurate states when there is noise. All parameters except H can be estimated accurately in ten seconds. The estimation of H

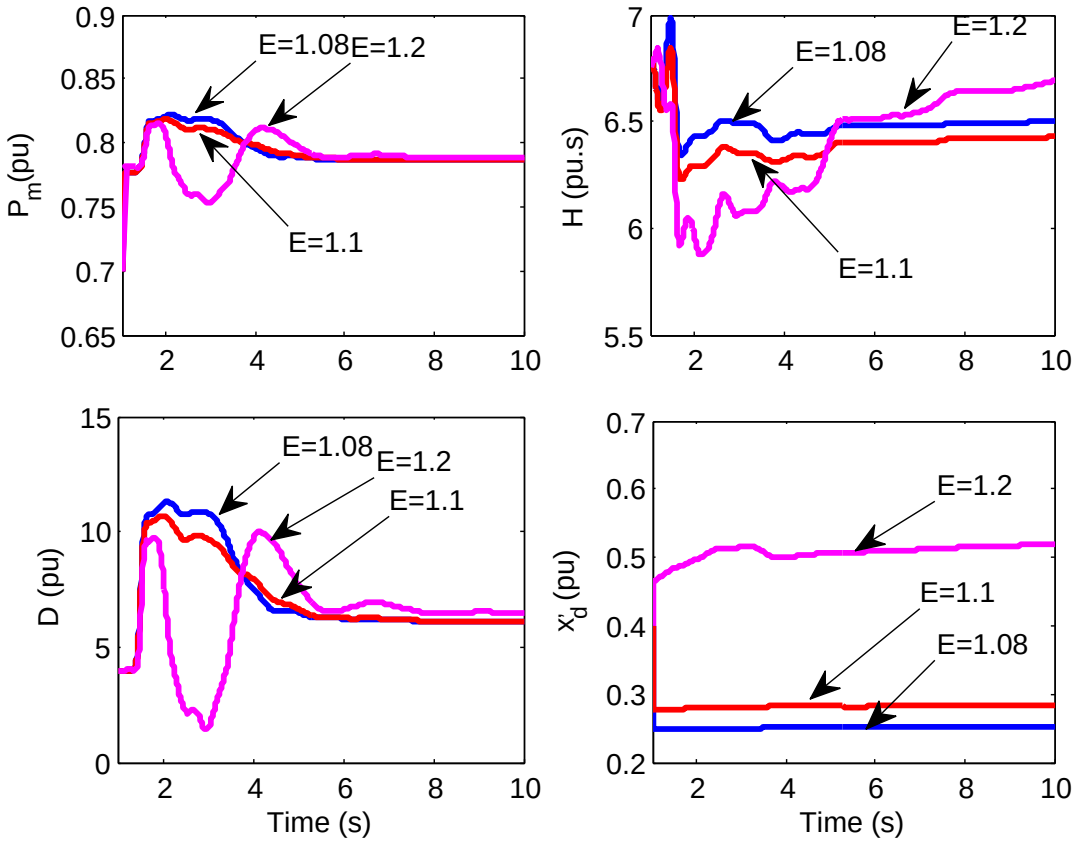

Figure 3.14. Impact of E assumption on estimation

is greater than the true value due to modeling error which has been explained in Section 3.3.4.1.

3.3.4.4 Two States and Five Parameters Estimation

In Section 3.3.4.1, four parameters are estimated along with the two states. In this section, estimation of two states (δ and ω) and five parameters (P_m, H,D,x'_d and E) are carried out using iterative EKF. Two sets of simulation data are used for EKF estimation.

The co-variance matrix Q of the processing noise will be set differently for Set 1 and Set 4. Since Set 1 is classical generator based simulation results and the internal voltage is fixed, there is no noise in $E_{k+1} = E_k$. Hence Q_{77} is set to zero. On the other hand, Set 4 is subtransient model based simulation and there is no fixed internal voltage. Hence it is reasonable to write $E_{k+1} = E_k + w_7$ and the noise co-variance is set to $0.001\Delta t$ where Δt

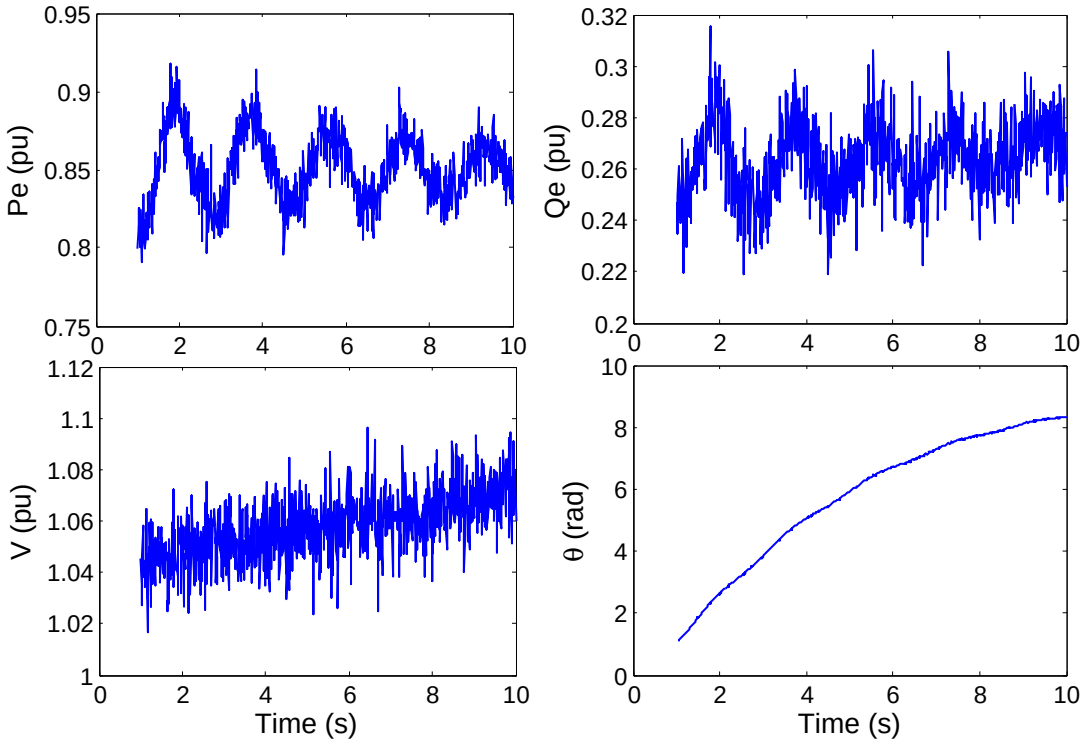

Figure 3.15. The measurements

is the sampling data time step. In addition, to make EKF's co-variance matrix P converge to zero as much as possible, the elements of P are also adjusted for two different test data.

Table 3.2. Covariance matrices for two-state five-parameter estimation

P	Set 1	Set 4	Q	Set 1	Set 4
P_{11}	1	10	Q_{11}	$10^{-6}\Delta t$	$10^{-6}\Delta t$
P_{22}	50	50	Q_{22}	$10^{-2}\Delta t$	$10^{-2}\Delta t$
P_{33}	1	1	Q_{33}	0	$10^{-6}\Delta t$
P_{44}	5	5	Q_{44}	0	$10^{-4}\Delta t$
P_{55}	100	50	Q_{55}	0	$10^{-4}\Delta t$
P_{66}	3	3	Q_{66}	0	$10^{-5}\Delta t$
P_{77}	3	3	Q_{77}	0	$10^{-3}\Delta t$

Four sets of initial guess of estimated state variables X shown in Table 3.3 are used for EKF estimation.

The estimation results for Set 1 data are plotted in Figs. 3.18 and 3.19. The estimation results for Set 4 data are plotted in Figs. 3.20 and 3.21.

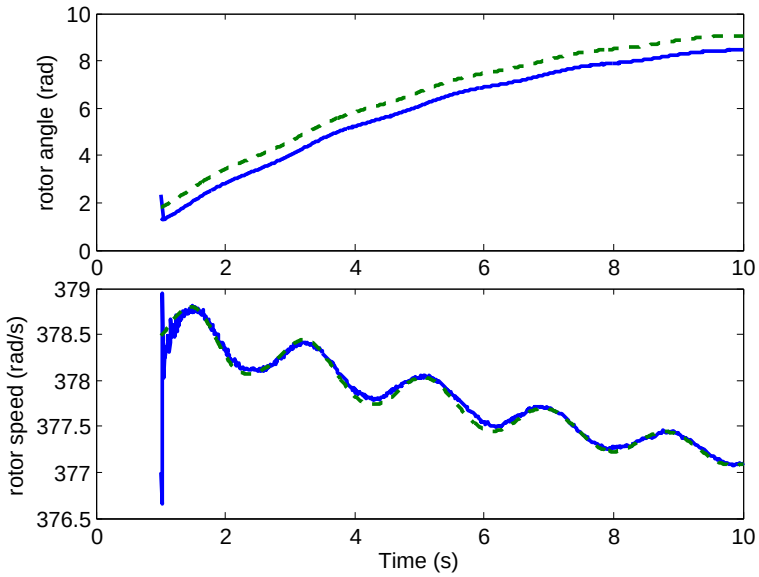

Figure 3.16. The estimated states

Table 3.3. Initial guess of estimation

X	Case 1	Case 2	Case 3	Case 4
X_1	2.34	2.34	2.34	2.34
X_2	ω_0	ω_0	ω_0	ω_0
X_3	0.6	1	1	1
X_4	8	4	4	8
X_5	6	4	4	8
X_6	0.3	0.1	0.2	0.4
X_7	1.0878	1.0878	1.0878	1.1

From both cases, it is found that to estimate an additional E, EKF will reach different sets of E and x'_d with different initial estimated states. This is apparently not wanted. In addition, a quick check of the co-variance matrix shows that the co-variance matrix elements are approaching zero. Therefore, the EKF is converging. An explanation can be offered by observing the power equations of (3.7). Given P, Q, V, θ, and two equations in (7), two unknowns among E, δ, and x'_d can be determined. This is based on the knowledge that N-unknowns can be determined from n-equations if the Jacobian matrix is not singular.

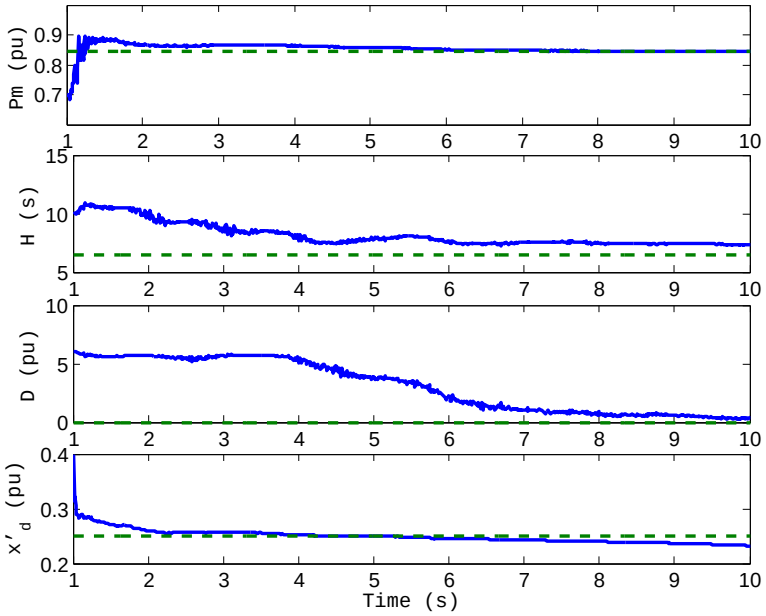

Figure 3.17. The estimated parameters

Therefore, for the EKF problem investigated in this paper, where a two-order swing equation and classical generator model are used to describe the system, the maximum parameters we can estimate are limited to four.

3.3.5 Conclusion

In this paper, an EKF-based dynamic state and parameter estimation using model decoupling technique is investigated. The application can perform real-time dynamic estimation for subsystems using PMU data where the real and reactive power are treated as the input to the estimation model while the voltage and phase angle are treated as the output from the estimation model. Based on a classic generator estimation model, the proposed EKF method can successfully estimate the states and parameters related to electromechanical dynamics. Simulation data generated from classical model, subtransient model and subtransient model equipped with AVR are used to test the estimation. It is demonstrated that the EKF-based estimation can give reasonable estimation for two-state four-parameter estimation. It is also demonstrated that this EKF-based estimation has a limited capability to handle the two-state five-parameter estimation.

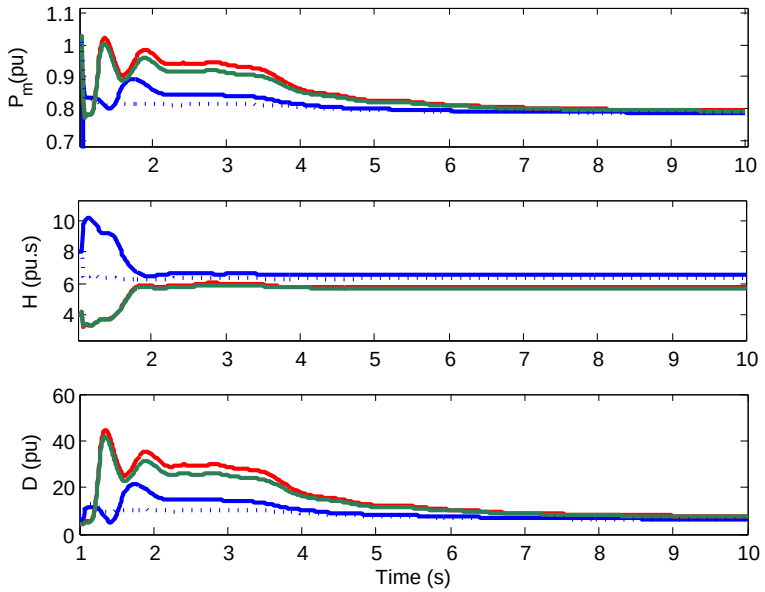

Figure 3.18. Estimated P_m, H and D for Set 1 data using four different initial $X(0)$. Case 1: blue; Case 2: red; Case 3: green; Case 4: blue dot

3.4 Unscented Kalman Filter Based Estimation

The research proposes an algorithm to estimate the electromechanical parameters and states of synchronous machines. The algorithm is based on Unscented Kalman Filter and uses observations or measurements available at the output terminal of the machine and polluted by colored noise. Testing of the algorithm was conducted against a model of the same complexity and a model of a higher complexity. The contribution of this research is twofold:1) Ability to estimate electromechanical parameters such as H and D which have not been investigated in other machine estimation research and 2) a dual UKF filter is set up to carry out the estimation.

Previous research has already engaged the Unscented Kalman Filter with parameter estimation in of electric machines. Yet the estimations have required more data to be available than the data provided by PMUs at the output of the machine. Valverde *et al* [22] estimate magnetizing reactances x_{md} and x_{mq} and field resistance r_f (and various electromagnetic states) using DFR and Unscented Kalman Filter (UKF). Azad *et al* [45] estimate stator and rotor resistances and inductances (in addition to other electromagnetic

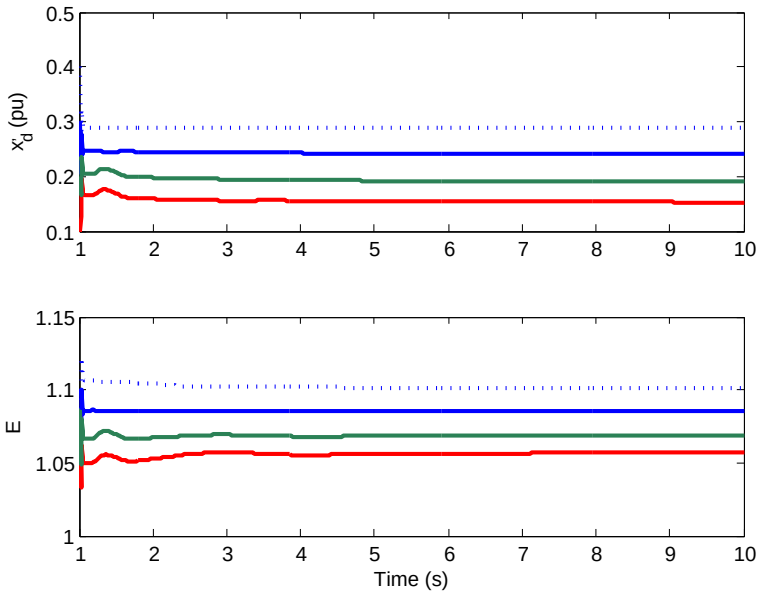

Figure 3.19. Estimated E and x'_d for Set 1 data using four different initial $X(0)$. Case 1: blue; Case 2: red; Case 3: green; Case 4: blue dot

states) using rotor and stator d and q axis voltages and currents with UKF or Extended Kalman Filter (EKF). Additional mechanical measurements, i.e. rotor rotational speed ω and rotor angle δ, are required in order for the estimation techniques to work in [22] [45]. [22] highlights the difficulties in obtaining both x_{mq} and the rotor angle at the same time because there is a linear relationship between x_{mq} estimation and the rotor angle estimation, hence [22] uses either a sensor to measure the rotor angle or a fixed ration between x_{md} and x_{mq}. The simultaneous estimation of the rotor angle and the q axis reactance x_q is similarly challenging because of the linear relationship between x_q and x_{mq}, $x_q = x_{ls} + x_{mq}$ [17].

The research carried out in this dissertation aimed at providing an online estimation of the synchronous machine electromechanical parameters and states while observing terminal phasor states in the case where access to mechanical measurements (δ and ω) or parameters (i.e. ration of x_{md} and x_{mq}) are not available. The parameters to be estimated are: the inertia H, the damping factor, D, the mechanical power P_m, and the q axis reactance x_q and the states to be estimates are the angle rotor δ and the angle rotational

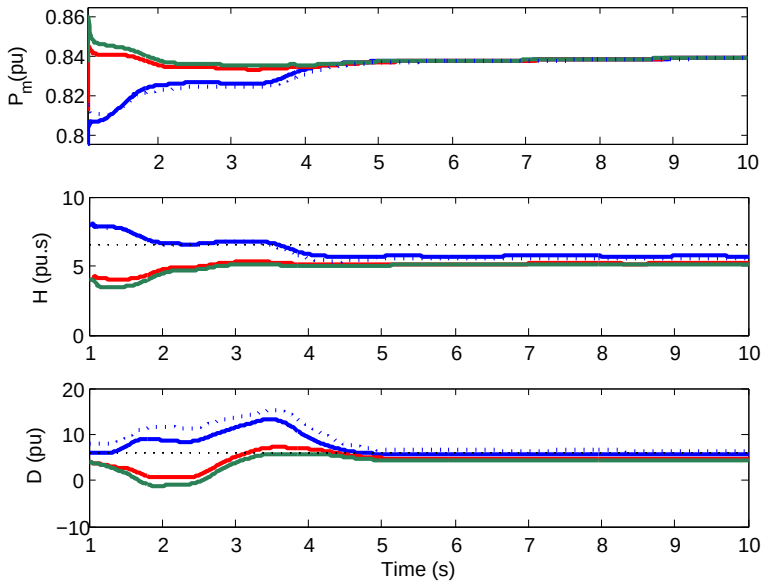

Figure 3.20. Estimated P_m, H and D for Set 4 data using four different initial $X(0)$. Case 1: blue; Case 2: red; Case 3: green; Case 4: blue dot

speed ω. The algorithm applied UKF on the available observations. The contribution of the research is twofold : The simultaneous estimation of x_q and δ and the complete estimation of the electromechanical states and parameters all based on the minimum set terminal phasor observations. The research use of UKF is due to its excellent processing of non-linearity anomalies in non-linear state space systems [42]. The choice of electromechanical parameters and states is due to their importance in the estimation of electrical parameters as evidenced by [22] [45].

3.4.1 Synchronous Machine Flux Decay State Space System

Synchronous machines are studied according to various state space systems or models varying in the level of details or insights on the synchronous machine behavior. Sauer *et al* [17] classify synchronous machines models based on the time constants used in the relevant state space system and following the dynamic phenomena the model aims to study. The estimation of electromechanical parameters and states calls for the study of the slow transient dynamics. The slow transient dynamics can be studied between 0.1 s and 10 s [17], in other words dynamics lasting less than 0.1 s can be ignored (although their effect

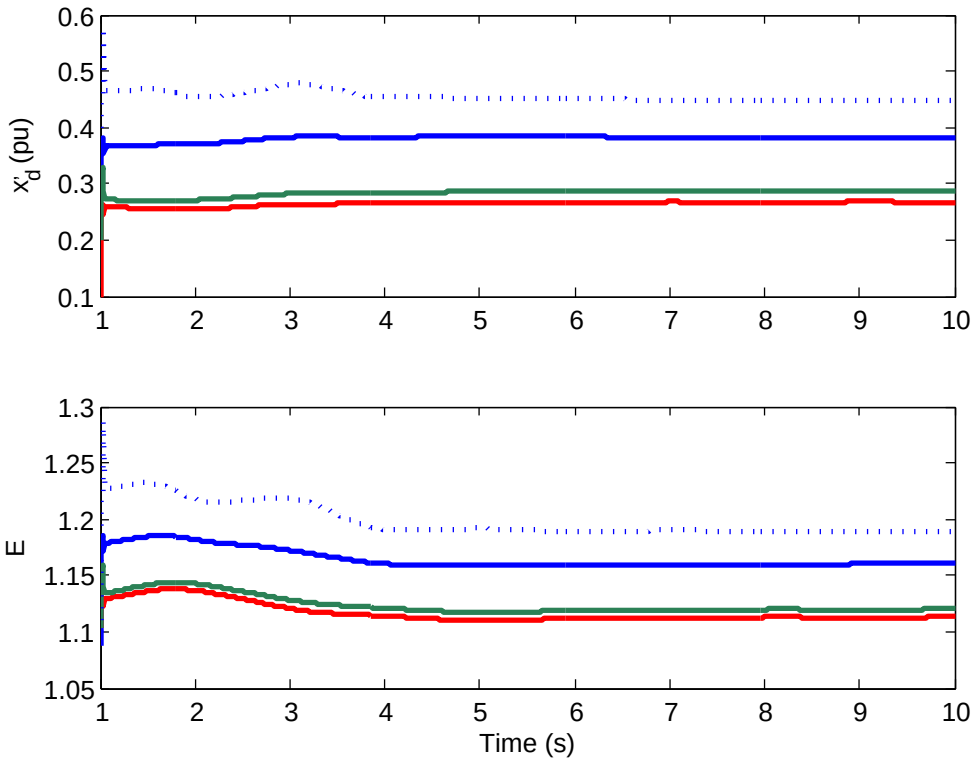

Figure 3.21. Estimated E and x'_d for Set 4 data using four different initial $X(0)$. Case 1: blue; Case 2: red; Case 3: green; Case 4: blue dot

will be modeled as process noise in the UKF). Such dynamics are related to electromagnetic interactions among the rotor (field and damping circuits) and stator circuits.

Kundur [76] suggests to simplify the model of the synchronous machine by eliminating the impact of rotor speed change and neglecting the damping circuits. Such system can be described as follows (while neglecting the stator losses) [17]:

$$T'_{do}\frac{dE'_q}{dt} = -E'_q - (x_d - x'_d)I_d + E_{fd} \tag{3.28}$$

$$\frac{d\delta}{dt} = \omega - \omega_b \tag{3.29}$$

$$\frac{2H}{\omega_b}\frac{d\omega}{dt} = P_m - P_e - D(\frac{\omega}{\omega_b} - 1) \tag{3.30}$$

$$\tilde{E}' = [(x_q - x'_d)I_q + jE'_q]e^{j(\delta - \pi/2)} \tag{3.31}$$

$$\tilde{E}' = \tilde{V} + jx'_d\tilde{I} \tag{3.32}$$

The output power at the terminal can be found to be:

$$P_e + jQ_e = \tilde{V}(\tilde{I})^* \tag{3.33}$$

$$P_e = E'_q I cos(\delta - \alpha) + \frac{(x_q - x'_d)I^2 sin(2\delta - 2\alpha)}{2} \tag{3.34}$$

$$Q_e = E'_q I sin(\delta - \alpha) + (x'_d - x_q)I^2 cos^2(\delta - \alpha) - x'_d I^2 \tag{3.35}$$

The state space system (3.28) .. (3.30) has one unobserved variable (E_{fd}), three dynamic states E'_q, δ, ω and six parameters H, D, P_m, x_q, x'_d, and T'_{do}, while considering all the terminal quantities I, α, V, P_e, and Q_e to be observed or available. (3.34) and (3.35) can further be simplified by eliminating E'_q between them:

$$P_e = (Q_e + x_q I^2)cot(\delta - \alpha) \tag{3.36}$$

By simplifying (3.34) and (3.35) into (3.36) there will be no need to use (3.28) and the number of parameters is reduced to four H, D, P_m, and x_q and that of dynamic states to two δ and ω, in addition to eliminating the unknown variable E_{fd}. Such reduction decouples the electromechanical system from the electromagnetic system (including the excitation system) except for x_q. The state space system in discrete mode is now:

$$\delta^{k+1} = \delta^k + h\omega^k - h\omega_b + \zeta^k_\delta \tag{3.37}$$

$$\omega^{k+1} = \omega^k + h\frac{\omega_b(P^k_m - P^k_e) - D^k(\omega_b - \omega^k)}{2H^k} + \zeta^k_\omega \tag{3.38}$$

$$H^{k+1} = H^k + \zeta^k_H \tag{3.39}$$

$$P^{k+1}_m = P^k_m + \zeta^k_{P_m} \tag{3.40}$$

$$D^{k+1} = D^k + \zeta^k_D \tag{3.41}$$

$$x^{k+1}_q = x^k_q + \zeta^k_{x_q} \tag{3.42}$$

ζ represents the additive process noise.

The observation Z of P_e (3.36) with additive noise ϑ will be used to correct the estimation of the parameters ans states in the Kalman filter:

$$Z^k = P_e^k + \vartheta^k \tag{3.43}$$

$$Z^k = [Q_e^k + x_q^k (I^k)^2] cot(\delta^k - \alpha^k) + \vartheta^k \tag{3.44}$$

3.4.2 The Unscented Kalman Filter

The Unscented Kalman Filter (UKF) is another extension to the recursive Kalman filtering developed to deal with non-linear systems. UKF is part of the Sigma-Point Kalman Filters family (SPKF) [43] which calculates the probability moments (variance and mean) of a number of samples to address non-linearity anomalies when moving from one recursion to the next recursion. This approach is different from the other non-linear Kalman filter extension, the Extended Kalman Filter (EKF), which linearizes the non-linear functions, through Jacobian matrices, around the current recursion in order to calculate the variance and mean of the system of the next recursion.

UKF follows the general filtering process of the linear Kalman Filter: A prediction of the states and their moments (variance and mean) in the next time step using the recursive system, followed by a correction of the predicted moments using observation equations. The main difference comes in the prediction state where the predicted moments are based on a number of deterministic samples (called Sigma Points) of the states. The variance and mean of the Sigma Points going through a non-linear transformation give a very good representation of the states exact mean and variance going through the same non-linear transformation. In other words, when dealing with non-linear function in discrete recursive state space systems, it is better to find the Sigma Points of the state estimated value, perform the non-linear transformation on the Sigma Points, find the mean and variance of the transformed the Sigma Points which are now the predicted mean and variance of the state. Such transformation is called Unscented Transformation (UT).

Table 3.4. Unscented Transformation

Unscented Transformation Steps:
$\lambda = a^2(n+\kappa) - n$
n :number of states in the system
a :scaling factor $\quad 0 \leq \alpha \leq 1$
κ :scaling factor $\quad \kappa \geq 0$
Sigma Points χ_i :
$\chi_0 = \hat{X}^k$
$\chi_i = \hat{X}^k + \left(\sqrt{(n+\lambda)P}\right)_i \quad i = 1, \ldots, n$
$\chi_i = \hat{X}^k + \left(\sqrt{(n+\lambda)P}\right)_i \quad i = n+1, \ldots, 2n$
Weights of Sigma Points :
$W_0 = \frac{\lambda}{n+\lambda}$
$W_i = \frac{\lambda}{2(n+\lambda)} \quad i = 1, \ldots, 2n$
Weights of covariance matrix :
$W_0^c = \frac{\lambda}{n+\lambda} + 1 - a^2 + b$
$W_i^c = \frac{\lambda}{2(n+\lambda)} \quad i = 1, \ldots, 2n$
Propagated mean and covariance
$\hat{X}_i^{k+1} = f(\chi_i, U^k) \quad i = 0, \ldots, 2n$
$\hat{X}^{k+1(-)} = \sum_{i=0}^{2n} W_i \hat{X}_i^{k+1}$
$P_{XX} = \sum_{i=0}^{2n} W_i^c (\hat{X}_i^{k+1} - \hat{X}^{k+1(-)})(\hat{X}_i^{k+1} - \hat{X}^{k+1(-)})^T$

Note: from Wehbe and Fan [60] ©2012 IEEE

The general scaled unscented transformation with the Unscented Kalman Filter can be summarized as in Table 3.4 and in Table 3.5 and as described by [43, 42, 72] for a given n state X non-linear recursive system f with a non-linear observation g:

$$\begin{cases} X^{k+1} & = f(X^k, U^k) + \zeta^k \\ Z^k & = g(X^k, U^k) + \vartheta^k \\ X^k & \sim (\hat{X}^k, P^k) \\ \zeta^k & \sim (0, Q^k) \\ \vartheta^k & \sim (0, R^k) \end{cases} \tag{3.45}$$

Table 3.5. Unscented Kalman Filter

Unscented Kalman Filter:
$Prediction:$
$[X^{k+1(-)}, P_{XX}, \chi_i] = UT(X^{k(+)}@f)$
$X^{k+1(-)}$:predicted state
$P^{k+1(-)} = P_{XX} + Q^k$
$Correction:$
$[\hat{Z}^{k+1}, P_{ZZ}, \chi_i] = UT(X^{k+1(-)}@g)$
$P_{XZ} = \sum_i W_i^c(\chi_i - X^{k+1(-)})(g(\chi_i) - \hat{Z}^{k+1})^T$
$G_k = P_{XZ}P_{ZZ}^{-1}$ Kalman Gain
$P^{k+1(+)} = P^{k+1(-)} - G_K P_{ZZ} G_K^T$
$X^{k+1(+)} = X^{k+1(-)} - G_k(Z_{k+1} - \hat{Z}^{k+1})$
$X^{k+1(+)}$:corrected state

Note: from Wehbe and Fan [60] ©2012 IEEE

3.4.3 Implementing UKF

Implementing UKF on the system described in Section 3.4.1 required the setting UKF various parameters $X, U, Z, n, a, \kappa, \beta$ and the nature and the statistical moments of the noise variables ϑ and ζ representing the process and measurement uncertainties in the recursive and observation equations (3.37...3.44).

The initial states and parameters vector X should include $\delta, \omega, H, D, P_m$, and x_q. Noise variables in Kalman filters are usually set to be additive white Gaussian noise with mean of zero. However, the recursive equation of δ (3.37) requires the correct initial value in order for the recurrent estimates to be correct. Since the initial value of δ is assumed to be unavailable hence the relevant error ζ_δ will set to be colored noise with mean different from zero. The rest of the process noise variables $\zeta_{(.)}$ will be set to white noise of mean equal zero. Simon [42] shows that dealing with colored noise with mean other than zero is addressed by adding one new parameter representing this noise variable to the Kalman filter. Accordingly, X will be amended to include ζ_δ as a parameter to be estimated.

Looking at (3.37)...(3.44) we noticed that x_q is not used in the dynamic states recursive equations (3.37) and (3.38) and it is used in the observation equation (3.44). It is possible hence to estimate x_q separately from the other parameters and states. We set up

two dual parallel filters, and we divided X into $X1$ and $X2$. $X1$ includes $\delta, \omega, H, D, P_m$, and $X2$ includes x_q.

The UT parameters were set as follows $\kappa = 0$, $a = 0.24$, and $\beta = 2$ [43]. The choice of a was critical because of the severe non-linearity of the observation function (3.53) which contains the function cotangent. A small value of a will keep the sigma points of δ close to each other and hence avoids the sever error caused by the the function cotangent of (3.44) when the sigma points are spread over more than one period.

The input functions U to be available for the filter are: Q_e, I and α. The measurement is P_e.

The two UKF filters are set up as follows:

$$X1^k \sim (\hat{X1}^k, P1^k) \tag{3.46}$$

$$X2^k \sim (\hat{X2}^k, P2^k) \tag{3.47}$$

$$\zeta^k \sim (0, Q^k) \tag{3.48}$$

$$\zeta_\delta^k \sim (\hat{\zeta_\delta^k}, Q^k) \tag{3.49}$$

$$\vartheta^k \sim (0, R^k) \tag{3.50}$$

Filter 1 is formed of:

$$X1 = [\delta, \omega, H, P_m, D, \zeta_\delta]^T \tag{3.51}$$

$$X1^{k+1} = f1(X^k, U^k)$$

$$f1(X^k, U^k) = \begin{bmatrix} \delta^k + h\omega^k - h\omega_b + \zeta_\delta^k \\ \omega^k + h\dfrac{\omega_b(P_m^k - P_e^k) - D^k(\omega_b - \omega^k)}{2H^k} + \zeta_\omega^k \\ H^k + \zeta_H^k \\ P_m^k + \zeta_{P_m}^k \\ D^k + \zeta_D^k \\ \zeta_\delta^k + \zeta_{\zeta_\delta}^k \end{bmatrix} \tag{3.52}$$

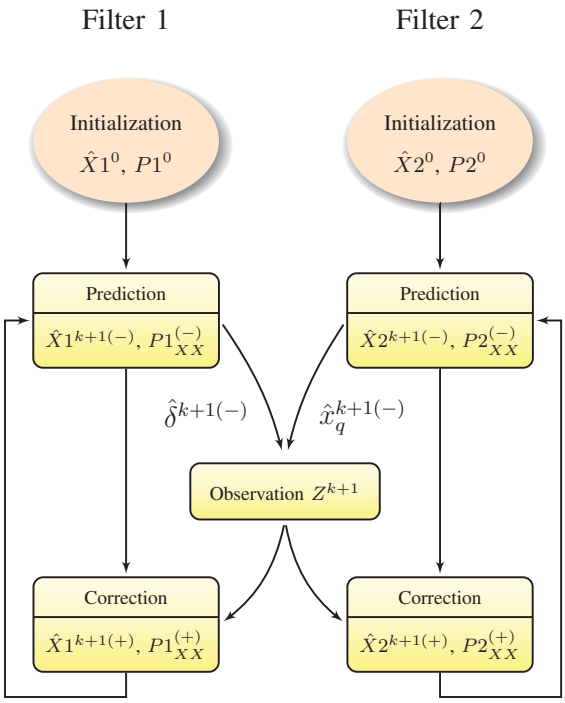

Figure 3.22. Implementation of UKF dual filters. Note: from Wehbe and Fan [60] ©2012 IEEE

$$\begin{aligned} Z^k &= Pe^k + \vartheta^k \\ &= [Q_e^k + x_q^k (I^k)^2] cot(\delta^k - \alpha^k) + \vartheta^k \end{aligned} \tag{3.53}$$

Filter 2 is formed of:

$$X2 = [x_q] \tag{3.54}$$

$$X2^{k+1} = f2(X2^k) = X2^k + \zeta_{x_q}^k \tag{3.55}$$

$$\begin{aligned} Z^k &= Pe^k + \vartheta^k \\ &= [Q_e^k + x_q^k (I^k)^2] cot(\delta^k - \alpha^k) + \vartheta^k \end{aligned} \tag{3.56}$$

Filter 1 and Filter 2 parallel estimations are shown in Fig. 3.22.

3.4.4 Case Studies

Two cases were studied using the proposed algorithm. The first case (Section 3.4.5) estimates the electromechanical parameters of a synchronous generator modeled as flux decay system, as in (3.28)-(3.32). In the second case (Section 3.4.6) the algorithm estimates the electromechanical parameters of a synchronous generator modeled as sub-transient system. The purpose of the case in Section 3.4.6 is to test the proposed algorithm against the more complex system closer to physical machine system.

Each case study involves performing a three phase balanced fault on a synchronous machine in the two area four machine system. One second following the clearance of the fault, phasor measurements for the next 14 seconds were taken at a rate of 1000 Hz. Power System Toolbox [77] under MATLAB was used in the simulations (see Appendix B for the simulation data).

3.4.5 Case 1: Flux Decay Model

Flux decay model of a synchronous generator was simulated in this case. Since the machine model is the same as the model used in the algorithm the process noise covariance was set to 10^{-13} but for the rotor angle it was set to 10^{-10}. The observation noise was set to 10^{-7}.

The choice of the initial values for the parameters was far from the simulated values unless there is a way to estimate them. The initial values were taken as follows: δ^0 slightly $> \theta^0$, ω^0 slightly $> \omega_b$, and $P_m^0 = P_e^0$. Table 3.6 shows the initial values for the rest of the parameters.

Table 3.6 shows the simulated parameters along with their estimated values while Fig. 3.23 shows how the estimation errors are converging.

3.4.6 Case 2: Sub-transient Model

Sub-transient models have closer resemblance to real synchronous especially because of the modeling of the fast sub-transient dynamics. In this case, the same param-

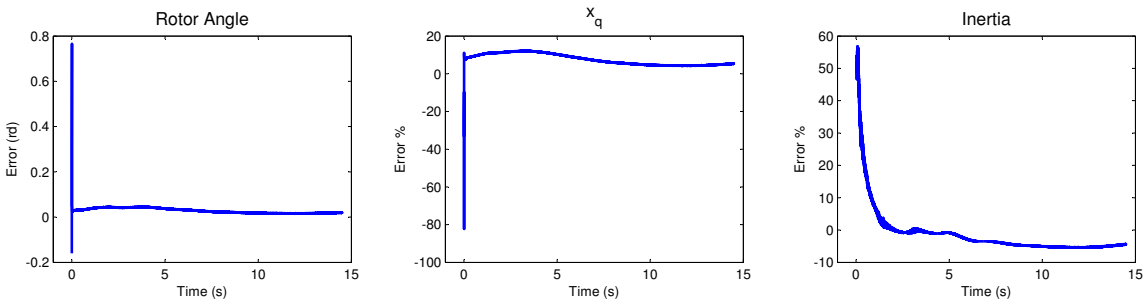

Figure 3.23. Convergence of parameters estimation errors for flux decay model. Note: from Wehbe and Fan [60] ©2012 IEEE

Table 3.6. Results of case 1

Parameter	Init value	Sim. value	Est. value	Error
H	10	6.5	6.24	-4.1%
D	0	3	2.95	-1.8%
x_q	1	1.5	1.61	+7.2%
P_m	0.71	0.797	0.795	-1.1%

Note: from Wehbe and Fan [60] ©2012 IEEE

eters of Case 1 (Section 3.4.6) were used with the addition of parameters and dynamics describing the additional phenomenons. The state space system (3.52) is still valid in the sub-transient model; however (3.34) and (3.35) will have errors leading to bigger errors in (3.36) and the observation equation (3.53). Accordingly, the observation error ϑ of (3.53) was substantially increased to 2×10^{-1} whereas the process error was slightly increased to 10^{-6}.

The choice of the initial values stayed the same as in Section 3.4.5: for the parameters, it was far from the simulated values unless there is a way to estimate them: δ^0 slightly $> \theta^0$, ω^0 slightly $> \omega_b$, and $P_m^0 = P_e^0$.

The estimated values of the simulated parameters are shown in Table 3.7 while Fig. 3.24 shows how the estimation errors are converging.

The following *remarks* can be made:

1. The parameters estimated values are very close to the simulated values

2. x_q and δ estimations are highly correlated

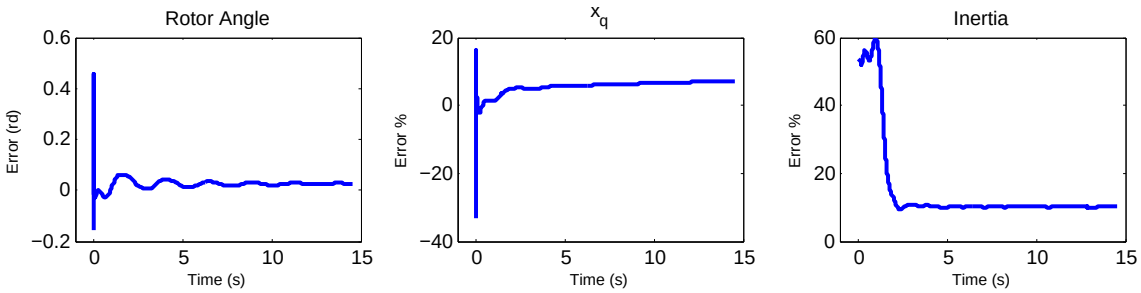

Figure 3.24. Convergence of parameters estimation errors for the sub-transient model. Note: from Wehbe and Fan [60] ©2012 IEEE

Table 3.7. Results of case 2

Parameter	Init value	Sim. value	Est. value	Error
H	10	6.5	7.15	+10.1%
D	0	3	3.02	+0.8%
x_q	1	1.5	1.61	+7.2%
P_m	0.72	0.787	0.792	+0.7%

Note: from Wehbe and Fan [60] ©2012 IEEE

3. The first few recursions show a spike in ζ_δ estimation agreeing with the proposal of this research that the error of δ has a mean $\neq 0$

4. The modeling of the error (as colored pr white noise) in any approximated state space system plays a pivotal role in converging towards correct values.

3.4.7 Conclusion on UKF Based Estimation

In this research we showed an algorithm to be used to estimate the electromechanical parameters and states of a synchronous generator. We demonstrated that a UKF algorithm can give very good results for such estimations when it is based on flux decay model of the synchronous machine while only the output data from the machine are available. We also showed that the modeling of error as colored error plays an important role when the used state space system is an approximation of the simulated state space system.

CHAPTER 4: LEAST SQUARES BASED ESTIMATIONS

4.1 Note to Reader

Portions of these results have been previously published (as a 1st author in [78]), or submitted for publication (as a 3rd author in [79]), or will be published. The results are utilized with permission of the publisher.

4.2 Introduction

Least squares based estimation (LSE) was made possible by the introduction of digital computers which can process large amount of data. The main idea of least squares estimation is to minimize the total error between a measured data set and proposed observations of the model subject to estimate. In its simplest forms LSE is a technique to fit a certain polynomial, of the parameters to be estimated, to a certain time series of data points [80]. In a more sophisticated approach, LSE forms the estimation basis for system identification [12].

LSE approach has been used in power systems in the measurements based states estimation [4]. In its simplest way, the approach is based on the availability of n measurements z (such as active and reactive power P_e and Q_e), then m states x (like voltage angle θ and magnitude V) when a linear relation A exists between z and x:

$$z = Ax \tag{4.1}$$

$$\text{where:} \begin{cases} z \text{ is } [m \times 1] \text{ vector} \\ A \text{ is } [m \times n] \text{ matrix} \\ x \text{ is } [n \times 1] \text{ vector} \\ m \geq n \end{cases}$$

$$\Rightarrow \hat{x} = (A'A)^{-1}A'z \qquad A' \text{ is the transpose of } A \tag{4.2}$$

This LSE technique provides the estimation $\hat{x}$ of x where the error $|H\hat{x} - z|^2$ is minimized, or simply the curve $H\hat{x}$ is fitted to the measurements z. It is noticed here that the relation H is linear and algebraic. Section 4.3 will show how to supplement the LSE with finite differences techniques in order to solve dynamic systems.

System Identification is used when we want to propose dynamic model to represent a physical system based on measurements at the output of the system (Fig. 4.1). System Identification estimate the parameters in the proposed model and validate its output[81]. Model and parameters estimation for synchronous machines and power subsystems is shown in Section 4.4.

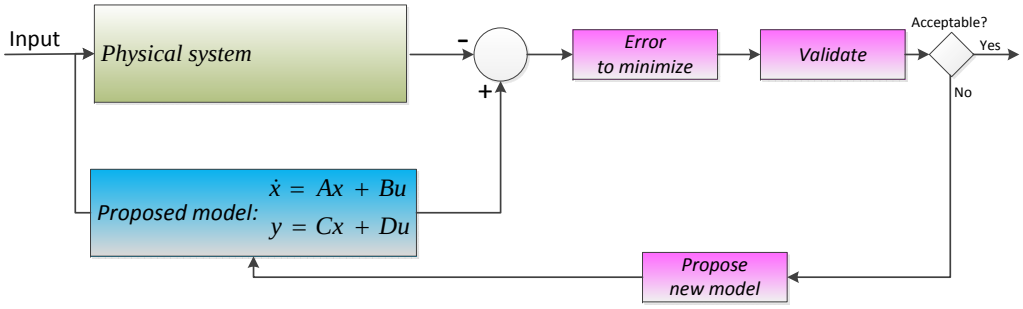

Figure 4.1. Basic implementation of System Identification

Basic differences also exist between System Identification and Kalman filter approach when it to comes to processing input and measurements data since System Identification does batch processing of the data whereas KF does recursive processing of such data.

4.3 Finite Differences Based Estimation

The research in this section investigates the estimation of synchronous generator states and parameters related to angular stability using PMU data. The method proposed in this research uses finite difference technique and least squares method to evaluate differential equations governing the synchronous machine using a time window of PMU measurements. Sensitivity studies have been carried out to evaluate the impact of system strength, transmission line length, machine controls (exciter and governor) and local load on estimation accuracy. The simulation studies demonstrate the feasibility of the proposed method in dynamic states and parameters estimation.

Synchronous machines equations involve differential and algebraic equations as shown in (1.11). Finite differences can be used to transform the differential equations into algebraic ones and hence simplifying the parameter estimation process.

This research aimed at providing an online estimation the synchronous machine electromechanical parameters and study angular stability dynamics through the use of time window of PMU recorded data. It was intended to use less input data and provide an online method, while providing a less computing intensive method. In general, parameter estimation problem falls within the bigger family of system identification. System identification methods can be divided into two sets: non parametric models (e.g. Fourier Analysis) and parametric methods such as Least Squares [82]. We used Least Squares and Finite Difference techniques to estimate the electromechanical parameters and related state dynamics and study the effect of various operational conditions. This approach could be developed to use parallel computation and run on multiple machines connected to the same power system and hence run stability studies because the PMUs offer synchronized data.

4.3.1 Proposed Algorithm

The research aims to estimate the synchronous machine electromechanical parameters and angular stability dynamics through the use of PMU recorded data. The syn-

chronous machine is connected to a transmission network (Fig. 4.2) and the parameters to be estimated are: transient reactance x'_d rotor angle δ, rotor speed, inertia H, and turbine Power P_m.

The model to be estimated is the equivalent classical model as defined by Anderson *et al* [83] and assumes: constant voltage behind a transient reactance, mechanical power is constant, no losses in the machine.

The time period during which this classical model, according to [76], is valid if the study period is less than the time constant T'_{d0}, which is in the order few seconds for synchronous machines.

Accordingly, we have:

$$\tilde{E} = (jx'_d)\tilde{I} + \tilde{V} \tag{4.3}$$

or,

$$E\angle\gamma = (jx'_d)I\angle\alpha + V\angle\theta \tag{4.4}$$

where: E is the magnitude of the voltage source behind the transient reactance, γ is the angle of the voltage source, x'_d is the transient reactance of the stator, I and α are the magnitude and angle of stator current, V and θ are the magnitude and angle of machine terminal voltage.

This research uses data recorded by a PMU (the RMS and angle of both the voltage and the current) at the terminal of the synchronous machine after a disturbance to find the internal machine parameters within few seconds. The study period of few seconds is required in order to cope with the requirements of study time validity for classical model.

The algorithm (Fig. 4.3) provided in this research follows these steps:

1. Find the transient reactance
2. Estimate the magnitude and angle of the machine electromagnetic force
3. Provide an estimation for the machine inertia and mechanical power

In order to find the transient reactance, the research will develop a non-linear relationship between the measured data by the PMU and the unknown voltage source magnitude and the transient reactance of the machine. The fact of quasi constant value of the voltage source magnitude will be used in order to transform the relationship to involve one unknown parameters, the transient reactance, which will be estimated through least squares fitting.

Once the transient reactance is found, the magnitude and angle of the voltage source can be found.

The swing equation will allow the estimation of the unknown parameters inertia and turbine power. Finite differences [84] will be used to estimate the rotor angle dynamics, then we will have an overdetermined system which will be solved by least square estimation (LSE). LSE has been used by power systems for state estimation as shown by Monticelli [4].

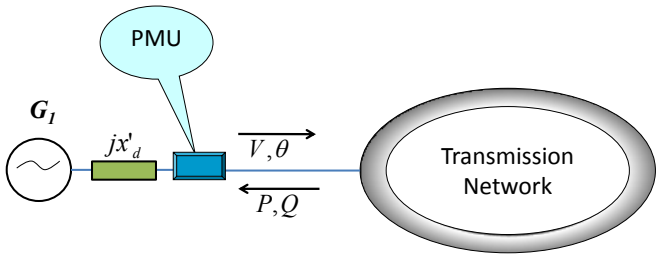

Figure 4.2. Synchronous machine connected to a transmission network. Note: from Wehbe *et al.* [78] ©2012 IEEE

Let's consider a synchronous generator connected to a transmission network as in Fig. 4.2. A PMU is installed at the output of the synchronous generator G_1 connected to a load to measure the interaction between this machine and the network in terms of angle and magnitude of both the voltage and current. In steady state, the differential equations governing the synchronous machine behavior does not give much information since all the time derivatives are equal to zero. However, upon a disturbance, the machine is in transient mode and the states' time derivatives are no longer equal to zero, a fact which allows us to build a system of equations and then solve this system.

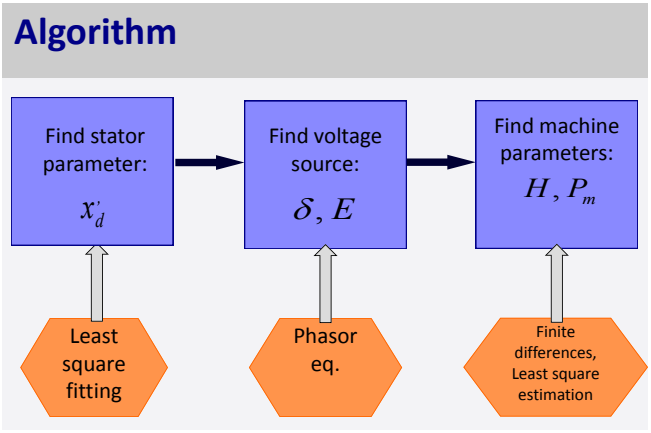

Figure 4.3. Algorithm to find synchronous machine parameters. Note: from Wehbe *et al.* [78] ©2012 IEEE

4.3.1.1 Estimating the Stator Transient Reactance

At the terminal of the synchronous generator we apply the phasor equation (4.4). The unknown variable γ can be eliminated by calculating the magnitude of E and the reactive power intercepted by the PMU Q:

$$E^2 = V^2 + (x'_d I)^2 + 2x'_d Q \tag{4.5}$$

or, for every time step i where we consider x'_d as constant:

$$E^2 = V_i^2 + (x'_d I_i)^2 + 2x'_d Q_i \tag{4.6}$$

Since we want to consider E to be quasi constant, we solve this problem by fitting $V_i^2 + (x'_d I_i)^2 + 2x'_d Q_i$ into a constant value of E^2 by manipulating x'_d.

We can say:

$$E \approx \ constant \Rightarrow E^2 \approx \ constant$$

$$\Rightarrow Var(E^2) \approx 0 \Rightarrow \overline{(E^2 - \overline{E}^2)^2} \approx 0 \tag{4.7}$$

where Var() means the variance and the bar sign over a variable denotes the mean of that variable.

Hence and according to (4.7) the problem comes down to fitting E^2 into $\overline{E^2}$. However, both E^2 and $\overline{E^2}$ have unknown values we do the following transform in order to solve the problem.

We use (4.6) to find $\overline{E^2}$:

$$\overline{E^2} = \overline{V_i^2 + {x'_d}^2 I_i^2 + 2x'_d Q_i} \tag{4.8}$$

$$\Rightarrow \overline{E^2} = \overline{V_i^2} + {x'_d}^2 \overline{I_i^2} + 2x'_d \overline{Q_i} \tag{4.9}$$

Fitting E^2 into $\overline{E^2}$ means, according to (4.6) and (4.9):

$$[\overline{V_i^2} + {x'_d}^2 \overline{I_i^2} + 2x'_d \overline{Q_i}] - [V_i^2 + (x'_d I_i)^2 + 2x'_d Q_i] \approx 0 \tag{4.10}$$

$$[{x'_d}^2 \overline{I_i^2} + 2x'_d \overline{Q_i} - (x'_d I_i)^2 - 2x'_d Q_i] - [V_i^2 - \overline{V_i^2}] \approx 0 \tag{4.11}$$

$$[{x'_d}^2 \overline{I_i^2} + 2x'_d \overline{Q_i} - (x'_d I_i)^2 - 2x'_d Q_i] \approx [V_i^2 - \overline{V_i^2}] \tag{4.12}$$

The problem has become according to (4.12) the fitting of the function $[{x'_d}^2 \overline{I_i^2} + 2x'_d \overline{Q_i} - (x'_d I_i)^2 - 2x'_d Q_i]$ into the data series $[V_i^2 - \overline{V_i^2}]$ by manipulating the value of x'_d. We can do such fitting with least square techniques and obtain x'_d.

4.3.1.2 Finding the Electromagnetic Force Magnitude and Angle

Looking back at (4.4), we will use the value of x'_d found by (4.12) in addition to the measured values of $I\angle\alpha$ and $V\angle\theta$ by the PMU, in (4.4) in order to obtain E and the voltage source angle (γ).

$$E\angle\gamma_i = jx'_d I_i \angle\alpha_i + V_i\angle\theta_i \tag{4.13}$$

4.3.1.3 Estimating the Machine Inertia and Turbine Power

The synchronous machine electromechanical coupling is governed by the swing equation:

$$\frac{2H}{\Omega}\frac{\partial^2\delta}{\partial t^2} = P_m - P_e \tag{4.14}$$

where H is the inertia of the machine, P_m is the mechanical power delivered to the machine through the turbine, Ω is the synchronous speed and is equal to 377 rad/s, δ is the rotor angle, and P_e is the electrical power delivered to the stator and is equal to:

$$P_e = Re(VI^*) \tag{4.15}$$

In (4.15) all the terms are now known, hence P_e can be calculated at all time steps.

We substitute the calculated values of P_e in (4.14) which will have two unknown machine parameters H and the mechanical power delivered to the machine P_m. On the other hand, P_m is constant for a short period of time.

$\frac{\partial^2\delta}{\partial t^2}$ can be calculated numerically by finite difference techniques since the value of γ is available at all sampling numbers i thanks to (4.13). In the case of classic machine $\delta = \gamma$ and in the case of subtransient machine model, $\delta = \gamma + constant$. Finite difference has been used in [32] and [20] in order to compute derivatives.

The swing equation at various time steps (i) can be rearranged as follows:

$$\frac{2}{\Omega}\frac{\partial^2\delta_i}{\partial t^2}H - P_m = P_{ei} \tag{4.16}$$

Then, it can be treated as overestimated system written as follows:

$$A \times X = Z \tag{4.17}$$

where:

$$A = \begin{bmatrix} \frac{2}{\Omega}\frac{\partial^2\delta_1}{\partial t^2} & -1 \\ . & . \\ \frac{2}{\Omega}\frac{\partial^2\delta_i}{\partial t^2} & -1 \\ . & . \end{bmatrix}, X = \begin{bmatrix} H \\ P_m \end{bmatrix}, Z = \begin{bmatrix} -P_{e1} \\ . \\ -P_{ei} \\ . \end{bmatrix}$$

The overdetermined system (4.17) can be solved by finding the least squares estimation $\widehat{X}$ of X given by [4] in order to find the optimum values for H and P_m:

$$\widehat{X} = (A'A)^{-1}A'Z \tag{4.18}$$

where A' is the transpose of A.

4.3.2 Simulations

We simulate the transmission network of Fig. 4.2 by two synchronous machines connected by a radial system with: G_1 represents the power system to be studied, x'_{d1} represents the transient reactance of G_1, , x_1 represents line reactance between the terminal of G_1 and Bus_{10}, x_l represents the reactance of the transmission line, G_2 represents the transmission network power system, $Load_2$ represents a load connected to the transmission network between the machine and the PMU. The sampling period we used in the simulation was 0.01 s, the total time study was 10 seconds, and the time used for the estimation was 6 s, 2 s after the disturbance.

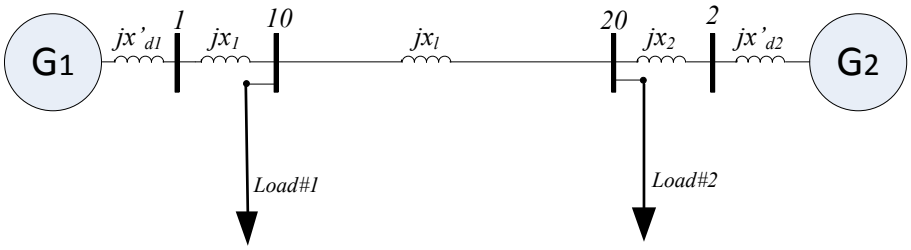

Figure 4.4. Two machines detailed system. Note: from Wehbe *et al.* [78] ©2012 IEEE

The machine G_1 was simulated by two-axis model (sub-transient model) as in [17]. The load is represented by constant active power P_l sink neglecting the sensitivity to the voltage or to frequency, hence the load can also be represented by a constant resistance $(r + jx)$. The transmission network will be represented by a bigger synchronous machine G_2 also connected with a load (Fig. 4.4). See Appendix B for the simulation data

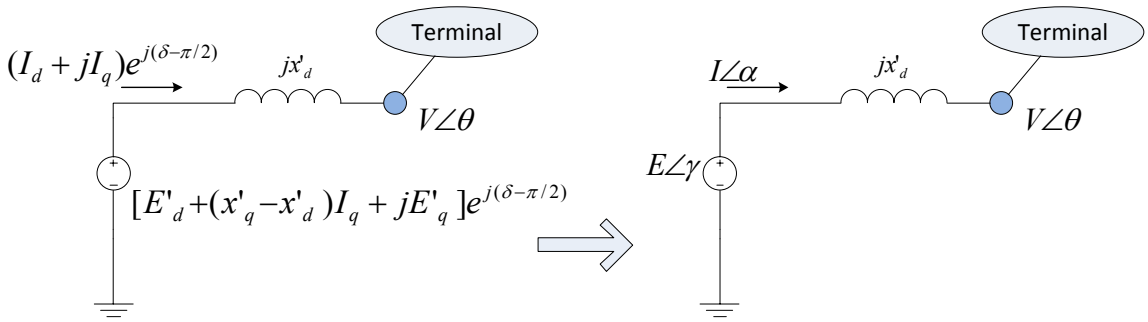

Figure 4.5. Two-axis sub-transient model of synchronous machine versus a classical generator mode. Note: from Wehbe *et al.* [78] ©2012 IEEE

The algorithm will find the classical machine equivalent (Fig. 4.5) of the simulated two-axis sub-transient model G_1. The main difference between the classical equivalent and the two-axis model reside in the magnitude of the voltage source behind the transient reactance x'_d and the rotor angle calculations. For the classical machine the magnitude of the voltage source is considered constant, whereas for the two-axis model, the component E'_d shows small variations only after the q-axis open-circuit time constant (T'_{qo} generally few hundreds of milliseconds) and the component E'_q stabilizes after that especially with the use of an exciter and as evidenced in Chow *et al* paper[23]. The angle of the voltage source between the two model is also different as shown by Sauer *et al* [17]; in the two-axis model it is $\delta - \pi/2$, δ being the rotor angle, whereas in the classical model the angle is $\gamma = \delta + \delta'^o$. The classic model voltage source parameters are as follows [17]:

$$E = \sqrt{(E'^o_d + (x'_q - x'_d)I^o_q)^2 + (E'^o_q)^2} \tag{4.19}$$

where x'_q is the q axis transient reactance; E'^o_d, E'^o_q, and I'^o_q are the d and q axis components of the voltage source and the current during steady state.

$$\delta'^o = tan^{-1}(\frac{E'^o_q}{E'^o_q + (x'_q - x'_d)I^o_q}) - \pi/2 \tag{4.20}$$

We notice that the difference in the angle between the classical equivalent and the two-axis model ($\delta'^o + \pi/2$) is constant. Consequently, the dynamics (time derivatives) of the two angles should be very close to each other and we can substitute the value of second derivative of γ as the value of the second derivative of (δ) in the swing equation (4.14).

4.3.2.1 Impact of System Inertia

In this set of simulations we install the PMU at Bus 1 and we remove the $Load_1$ connected to the machine G_1. We estimate the machine transient reactance, inertia and turbine power. We vary the inertia of the system (machine G_2) and we record estimations in Table 4.1. The reactance of the transmission line x_l is 1.17 .

Table 4.1. Impact of system inertia on estimated parameters

Parameter	Simulated	Estimated	Estimated	Estimated
x'_{d1}	0.25	0.204	0.365	0.39
H_1	6.5	7.35	6.81	6.74
P_{m1}	4.2	4.24	4.2	4.2
H_2		16.5	60	100

Note: from Wehbe *et al.* [78] ©2012 IEEE

The following *remarks* can be made:

1. The estimation of H_1 gets closer to the real H_1 when H_2 increases. This can be attributed to the fact that when H_2 is big (100 s) then the machine G_2 behaves like an infinity bus. In this case the PMU is estimating the overall inertia of the system which is $(H_1 \times H_2)/(H_1 + H_2)$ which is very close to H_1. In the case when the system inertia gets smaller (16.5 s) the two machines show greater coherency (as evidenced by the rotor angles of G_1 (δ) and G_2 (δ_2) in Fig. 4.6. We can see as the system inertia H_2 increases the rotor angle difference between the two

machines also increases and becomes less constant which means less coherency and the system inertia gets closer to $(H_1 \times H_2)/(H_1 + H_2)$ [44].

2. We notice that the estimated x'_{d1} increases with H_2. This can be understood by looking at the angle of Fig. 4.6, as H_2 increases, the angle $\delta - \delta_2$ increases, the reactance x_t of the line, which is equal $(x'_{d1} + x_1 + x_l + x_2 + x'_{d2})$, between E_1 and E_2 increases, as shown in Fig. 4.7, hence the estimated (x'_{d1} also increases).

3. The two variables in the swing equation $\ddot{\delta}$ and $-P_e$ behave as shown in Fig. 4.8 where they oscillate in phase to show the linear relationship between them shown in (4.14).

4. Fig. 4.9 shows how the estimated voltage source magnitude closely follows the simulated voltage source magnitude and is more constant than another estimation of x'_d (in this case $x'_d = 0.23$).

As a summary, the greater the system inertia is the better the estimation of the synchronous machine inertia is.

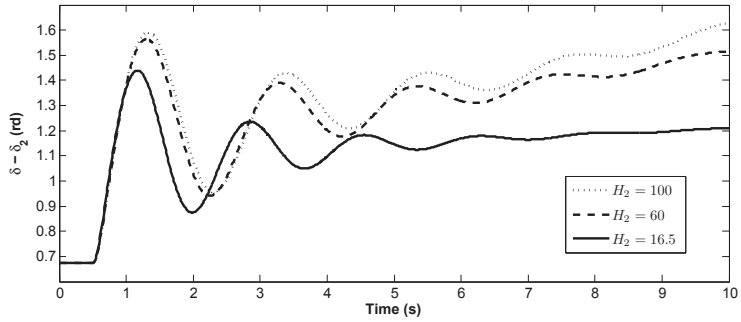

Figure 4.6. Variation of rotor angle difference with the system inertia. Note: from Wehbe *et al.* [78] ©2012 IEEE

4.3.2.2 Impact of Machine Controls

In this simulation (PMU at Bus 1 and no $Load_1$) we equipped the machine G_1 with some controls namely an exciter and a governor and we kept the reactance of the transmission line x_l at 1.17 . The results are summarized in Table 4.2.

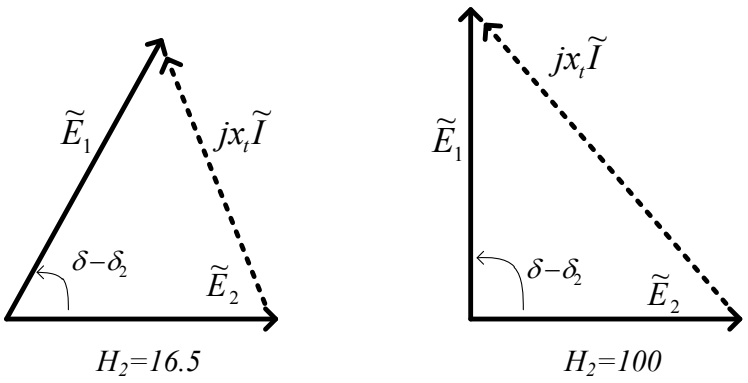

Figure 4.7. Impact of system inertia H_2 on estimated x_t. Note: from Wehbe *et al.* [78] ©2012 IEEE

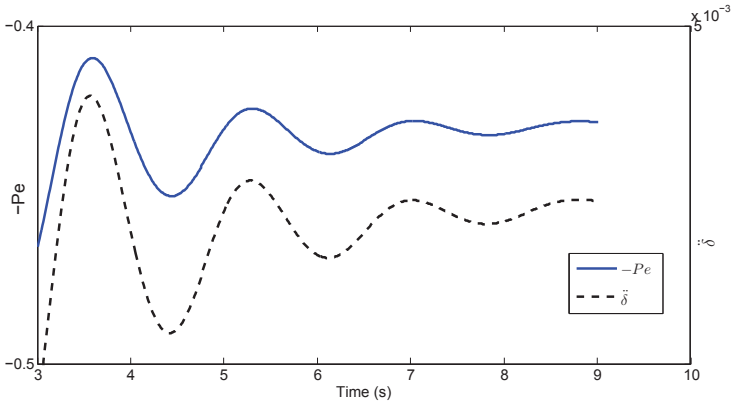

Figure 4.8. Oscillations of electric power of the machine and the rotor angle dynamics / $H_2 = 16.5$ Note: from Wehbe *et al.* [78] ©2012 IEEE

The following *remarks* can be made:

1. The estimation of x'_d gets smaller when the machine controls are used. This can be attributed to the fact that the exciter is stabilizing the machine terminal voltage hence the point of constant voltage inside the machine will get closer to the terminal which projects a smaller transient reactance.

2. The estimated H_1 gets closer to the simulated H_1 with the use of machine controls. The reason could be the governor which will try to stabilize the rotor speed around one pu . Consequently, governor control has the similar effect as an infinite bus which ensures the machine having a constant rotating speed (Fig. 4.10).

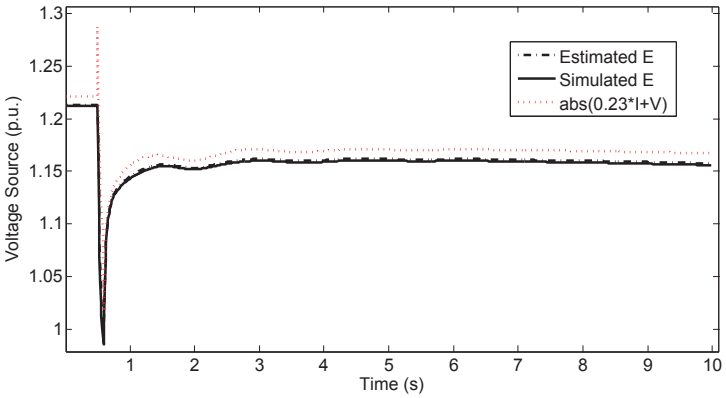

Figure 4.9. Comparison between the simulated and estimated voltage source / $H_2 = 16.5$. Note: from Wehbe *et al.* [78] ©2012 IEEE

Table 4.2. Impact of machine controls on estimated parameters

Parameter	Simulated	Estimated (no controls)	Estimated (with controls)
x'_d	0.25	0.204	0.186
H_1	6.5	7.35	7.09
P_{m1}	4.2	4.24	4.18
H_2	16.5		

Note: from Wehbe *et al.* [78] ©2012 IEEE

3. The assumption of the mechanical power being quasi constant is also investigated. Fig. 4.11 shows the variation of the mechanical power of the simulated machine G_1 as a function of time which shows very small ripples. As a matter of fact, the statistical variance of this mechanical power is in the order of $1e^{-4}$ which is very small compared with the mean of P_m of 4.2 pu .

As a summary, machine controls (especially the governor) will make the estimation of the synchronous generator inertia more accurate.

4.3.2.3 Impact of Transmission Line Length

In this simulation we change the reactance of the transmission line to simulate a weaker or a stronger connection to the system. The results are summarized in Table 4.3.

The following *remarks* can be made:

1. We notice that the estimated $x'd$ decreases with the transmission line length.

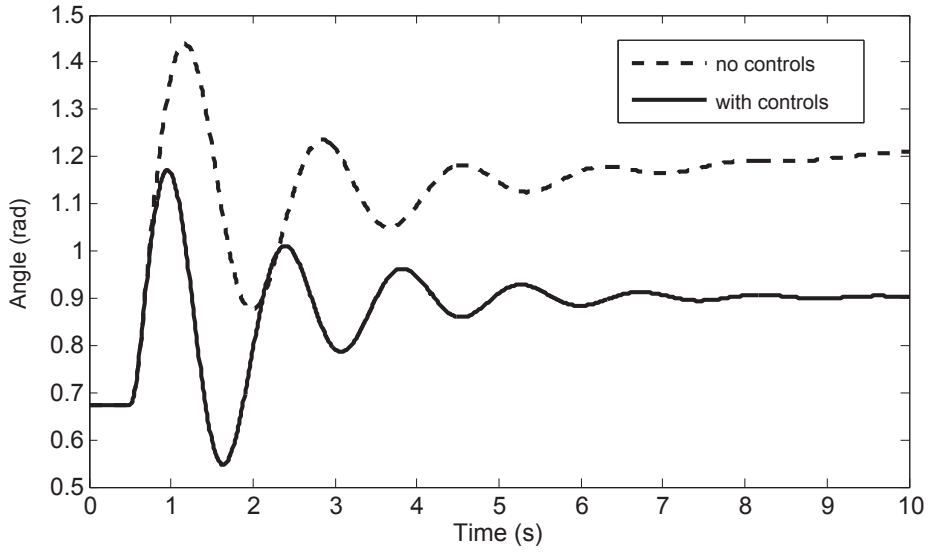

Figure 4.10. Variation of rotors angles difference with machines controls. Note: from Wehbe *et al.* [78] ©2012 IEEE

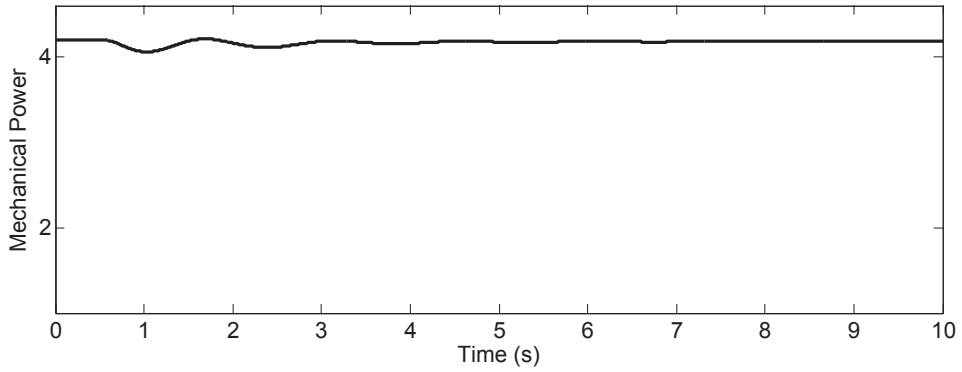

Figure 4.11. Variation of the mechanical power. Note: from Wehbe *et al.* [78] ©2012 IEEE

2. We notice that estimated H_1 increases while the transmission line length decreases.

In order to understand the impact of the transmission line reactance, we will look at the simple two machines shown in Fig. 4.12. Machine G_1 is connected through a short line (represented by the reactance x) to a Bus 10 and the bus is connected through a longer transmission line (represented by the reactance $x_l > x$) to a bigger machine. A PMU will be installed at Bus 10 and we will ignore the impact of machine reactances for simplification purposes. It is important to note that the system of Fig. 4.12 can also be represented by

Table 4.3. Impact of transmission line reactance on estimated parameters

Parameter	Sim.	Est.	Est.	Est.	Est.
x'_d	0.25	0.28	0.204	$1.5e^{-5}$	$3e^{-6}$
H_1	6.5	6.92	7.35	8.55	9.1
P_{m1}	4.2	4.22	4.24	4.28	4.29
$x_l =$		1.35	1.17	0.9	0.72

Note: from Wehbe *et al.* [78] ©2012 IEEE

a single machine connected to an infinity bus system ([23] and [44]). In order to study the electric characteristics of the system in Fig. 4.12, we will find the Thevenin equivalent of the machines G_1 and G_2 seen from the Bus 10. Such Thevenin equivalent is a machine G_{Th} with voltage source $\widetilde{E}_{Th}$. We will assume $E_1 \approx E_2$.

$$x_{Th} = \frac{x \times x_l}{x + x_l} \tag{4.21}$$

$$\widetilde{E}_{Th} = \frac{x\widetilde{E}_2 + x_l\widetilde{E}_1}{x + x_l} \tag{4.22}$$

Equation (4.21) says that the equivalent reactance will decrease with smaller x_l, this could be the reason for x'_d decreasing.

We also note that in the case $x_l > 10x$ (4.22) becomes:

$$\widetilde{E}_{Th} \approx \frac{x_l\widetilde{E}_1}{x + x_l} \approx \widetilde{E}_1 \tag{4.23}$$

Equation (4.23) means that the machine $G_{Th}$is almost completely independent from the machine G_2 and the PMU at Bus 10 will measure G_1 only. In other words, if the transmission line increases then the equivalent machine G_{Th} will get closer to representing machine G_1 and its inertia only. If the transmission line decreases then the equivalent machine G_{TH} will represent both machines G_1 and G_2 and their inertias.

As a summary, the longer the transmission line to the system is the more accurate the estimation of the synchronous generator parameters.

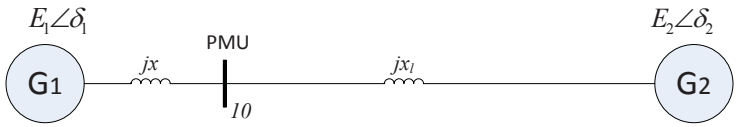

Figure 4.12. Two machines and simple radial line. Note: from Wehbe *et al.* [78] ©2012 IEEE

4.3.2.4 Impact of Load Level

In this set of simulations we put the PMU at Bus 10 we instate a load $Load_1$ between the PMU and the generator G_1 (Fig. 4.4), then we vary the real power transfer through the PMU from G_1 to G_2 by varying the load $Load_1$. We obtain the estimation results in Table 4.4:

Table 4.4. Impact of power transfer level on estimated parameters

Parameter	Sim.	Est.	Est.	Est.	Est.	Est.
$x(=x'_d+x_1)$	0.34	0.336	0.1	$4.8e^{-5}$	$3.1e^{-8}$	0.08
H_1	6.5	7.2	8.6	9.1	8.3	8.2
P_{m1}	3.8	3.82	3.4	2.9	1.93	1.93
$Load_1$		zero	0.5	1	2	2
$PowerTransfer$		3.55	3.1	2.68	1.76	1.88
H_2		16.5	16.5	16.5	16.5	66

Note: from Wehbe *et al.* [78] ©2012 IEEE

The following *remarks* can be made:

1. We notice that the estimated reactance x decreases as $Load_1$ increases

2. We notice that the estimated H_1 increases as the load $Load_1$ increases

The effect of the load between the PMU and G_1 can be understood from the Thevenin equivalent of the system (G_1 and $Load_1$ which is simulated as a resistance r) and as illustrated in Fig. 4.13. The Thevenin equivalent is now the machine G'_1 in series with a resistance R and a reactance jX. The resistive part R will introduce a quasi-constant active power loss in the swing equation which will be deducted from the mechanical power, that explains that the power of $Load_1$ added to the estimated mechanical power will almost equal the simulated mechanical power.

The magnitude of the voltage source of the machine G'_1, as per the Thevenin transformation will be equal to E' with:

$$E' = B \times E_1 \tag{4.24}$$

where $B < 1$ and is equal to:

$$B = \sqrt{\frac{r^2}{r^2 + x'^2_{d1}}} \tag{4.25}$$

Now that $Load_1$ is transformed into the linear impedance we can use (4.22) and replace x by $(-jR + X)$ and E_1 by E'_1 and we will get for the whole system:

$$\widetilde{E}_{Th} = \frac{(-jR + X)\widetilde{E}_2 + x_l\widetilde{E}'_1}{-jR + X + x_l} \tag{4.26}$$

$$\widetilde{E}_{Th} = \frac{(-jR + X)\widetilde{E}_2 + (x_l B) \times \widetilde{E}_1}{-jR + X + x_l} \tag{4.27}$$

In other words, the transmission line reactance has been reduced by the factor B which is less than 1. Since the transmission line reactance is now reduced then transmission line is shorter, the connection with the system is stronger, and as discussed in para 4.3.2.3 we expect a higher inertia estimation. Looking at (4.25) we realize, the higher the load is, the lower r is, the lower B is, the higher the reduction of the transmission line is, and the higher the estimation of the inertia will be, this is what we have in Table 4.4.

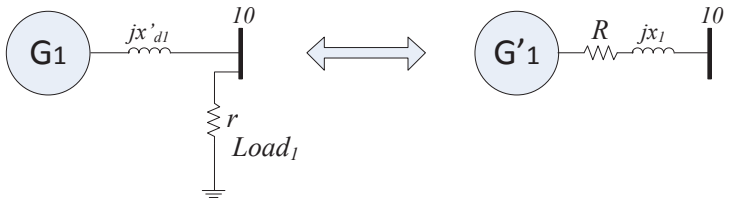

Figure 4.13. Thevenin equivalent of a machine with a load. Note: from Wehbe *et al.* [78] ©2012 IEEE

As a summary, the lower the local load is the more accurate the estimation of the synchronous generator parameters.

Observing the simulation results in this section, we conclude that the accuracy of the synchronous generator parameters increases when:

1. The system inertia is higher
2. Machine controls (especially governor) are used
3. The transmission line is longer
4. The local load is lower

4.3.3 Application on Real World Data

In this section, a variation of the finite difference method will be applied on real PMU data extracted from an operating PMU network on the electric grid.

A set of real world data of the Eastern Interconnection PMUs was recorded by NASPI Real Time Dynamics Monitoring System (RTDMS) regarding a generator trip event was obtained and analyzed using the finite differences for the purpose of dynamic state/parameter estimation. NASPI RTDMS shows significant oscillations. Frequency plots are shown in Fig. 4.14.

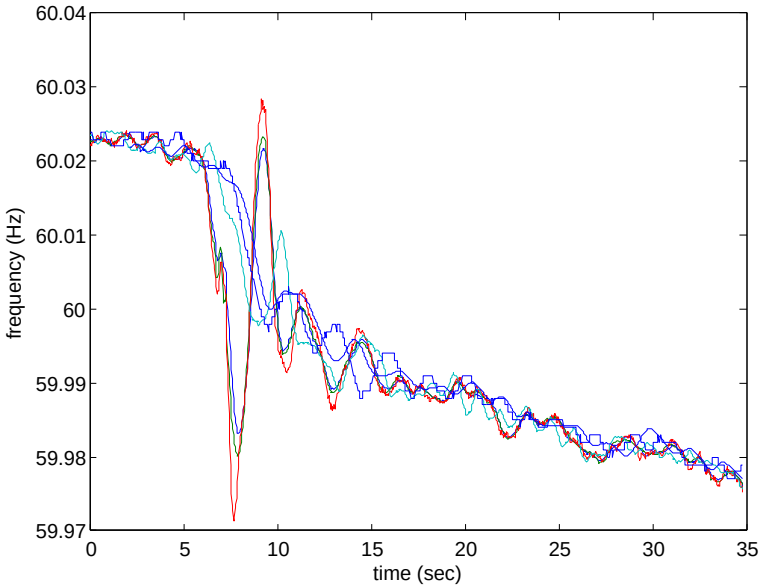

Figure 4.14. Frequency plots

Seven locations P_0 -P_7 are selected. They are located from west to east. The voltage phase angles are plotted in Fig. 4.15 and the voltage magnitudes are shown in Fig. 4.16. The voltage phase angles are reference angles. The reference bus is chosen to be a bus located in Tennessee Valley Authority.

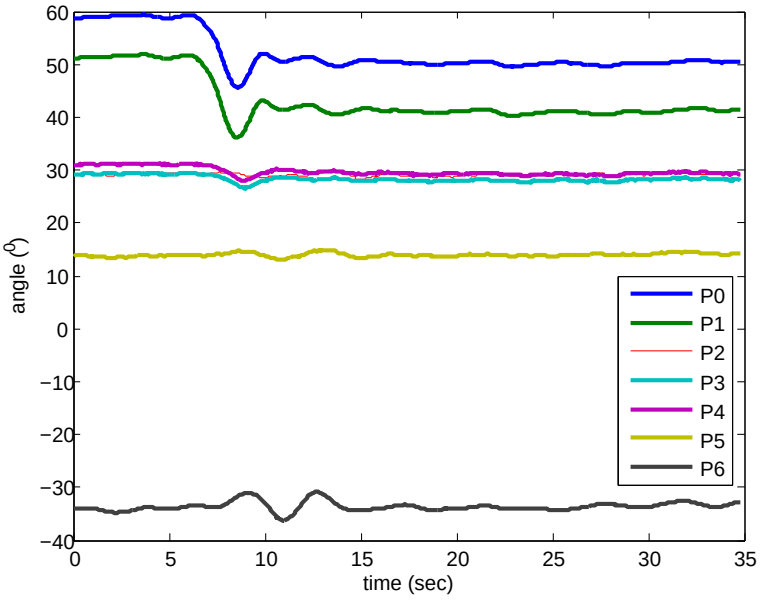

Figure 4.15. Voltage phase angles. Reference bus is located in TVA

From Fig. 4.15, we can observe that $\angle\bar{V}_0 > \angle\bar{V}_1 > ... > \angle\bar{V}_6$. Hence the power transfer direction is from west to east since the voltage phase angles decrease from west to east. This can also be confirmed by the power flow measurements on some PMUs. Note only few PMUs have data for real power and reactive power. Through majority of the PMUs have voltage phasor data. The frequencies measured at buses decrease. This shows that loads in the system exceeds generation. The event is a generator trip event at west.

Starting from $t = 8s$, it is obvious that the system suffers an active power unbalance since the frequencies decrease. Voltage phase angles of P_0 and P_1 have significant reduction (about 10 degree) while the voltage phase angles of the other locations (P_2 –P_6) have insignificant reduction.

Finite differences were applied in this section to the PMU data in order to calculate the derivatives wrt. time. First we applied the algorithm to the PMU data from P_0.

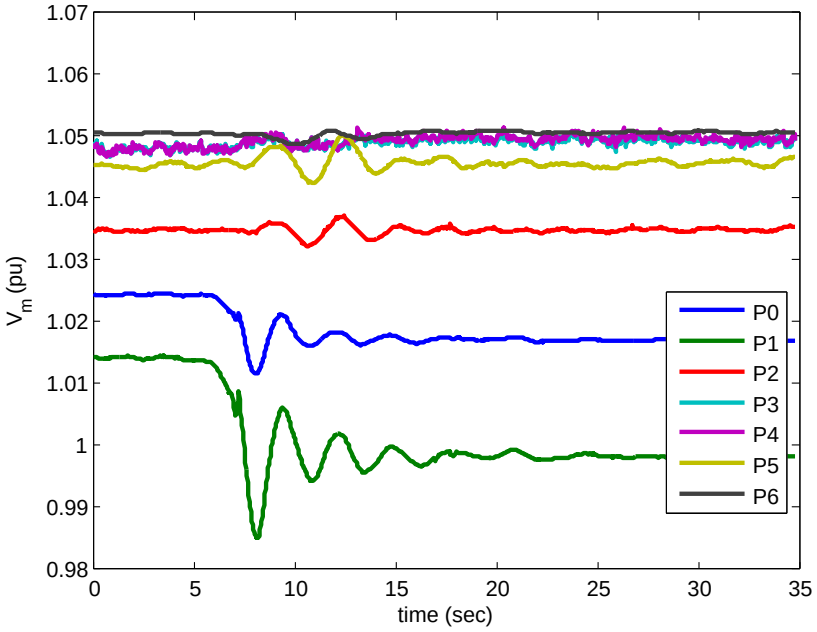

Figure 4.16. Voltage magnitudes

The inputs of the estimation algorithm are a time series of voltage phasors (angle and magnitude) and current phasor as shown in Fig. 4.17. The phase angles are all related to the voltage phase angle at Bus P1. The outputs of the estimation algorithm are internal generator voltage phasor (angle and magnitude), transient reactance and equivalent inertia.

The first step of the finite difference method is to estimate the transient reactance by curve fitting technique. We find that $x'_d = 0.0209$.

With x'_d available, the internal voltage phasor $\bar{E}$ can be estimated. Figs. 4.18 and 4.19 present the internal voltage magnitude and the phase angle. The measured voltage magnitude and phase angle are also presented in the figures.

In order to obtain the equivalent inertia, The swing equation for the synchronous machine classical model was used:

$$\frac{2H}{\omega_0}\frac{\partial^2\delta}{\partial t^2} = P_m - P_e \tag{4.28}$$

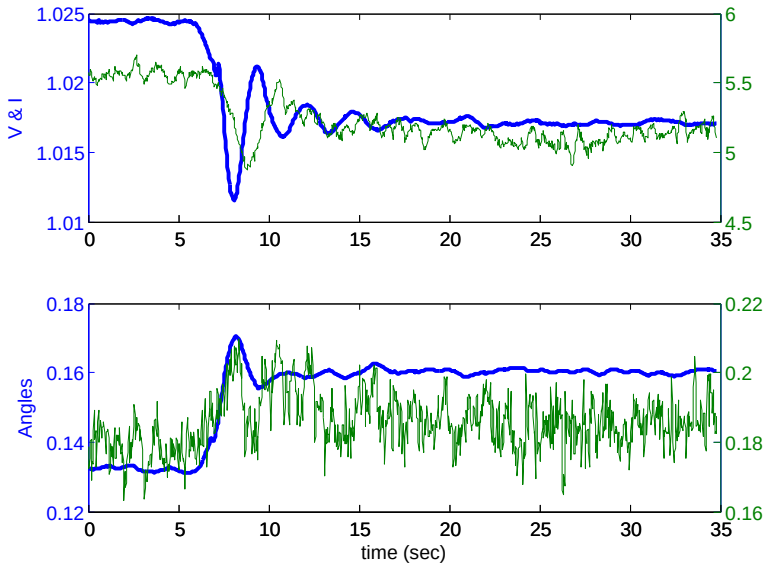

Figure 4.17. Inputs of the estimation algorithm: Finite Difference Method. Phase angles are relative to the ones of P_1

In the classical model, P_m is considered constant, hence deriving both side wrt. time leads to:

$$\frac{2H}{\omega_0}\frac{\partial^3\delta}{\partial t^3} = \frac{\partial P_e}{\partial t} \tag{4.29}$$

$$H = -\frac{\omega_0}{2}(\frac{\partial P_e}{\partial t})/(\frac{\partial^3\delta}{\partial t^3}) \tag{4.30}$$

The derivative of P_e and the 3rd derivative of δ should be obtained. When obtaining the numeric derivatives of real world data using finite differences, it is found that the derivative of δ is contaminated with white noise which is difficult to remove as shown in Fig. 4.20. With white noise presented, the computed inertia also presents significant white noise. White noise is the key issue that affects the accuracy of this algorithm.

To solve this issue, digital filter techniques is introduced to deal with the estimated rotor angle. Chebshev filter is used in this case with the sampling window set to be 64 sample to do the filter. The Chebshev filter time-domain and frequency domain function are shown in Fig. 4.22. With Chebshev filter applied, the internal angle waveform will be

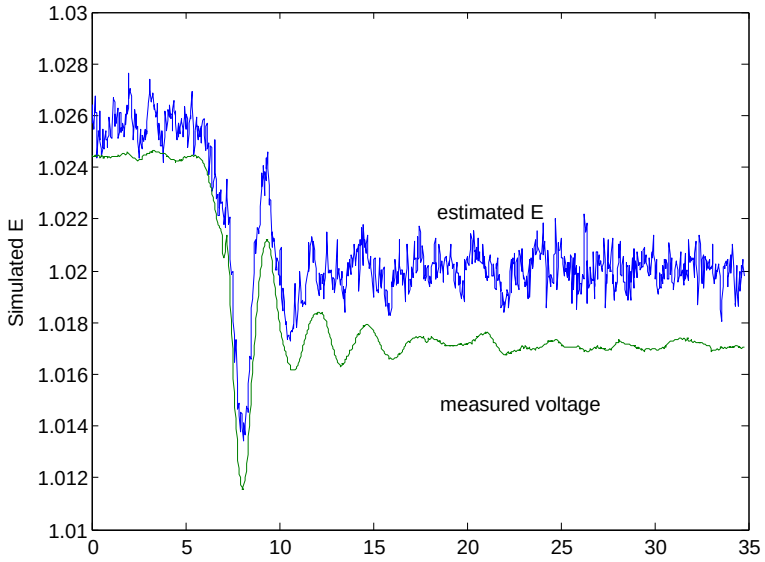

Figure 4.18. Estimated internal voltage magnitude compared with the measured voltage

smoothed out (shown in Fig. 4.21). Similarly, the power waveform is smoothed out (shown in Fig. 4.24).

With the smoothed waveforms, the first order derivative of P_e and the 3rd order derivative of δ are obtained and presented in Fig. 4.25. The equivalent system inertia can be computed from (4.31):

$$H = -\frac{\omega_0}{2}(\frac{\partial P_e}{\partial t})/(\frac{\partial^3 \delta}{\partial t^3}) \tag{4.31}$$

Fig. 4.25 presents the derivative of P_e and the denominator in (4.31). We select an instant at $t = 9.47$ second and find the $\frac{dP_e}{dt}$ and $\frac{d^3\delta}{dt}$. The inertia for the equivalent generator behind P_0 can be found to be 1300 seconds pu.

4.3.4 Conclusion on Finite Difference Based Estimation

In this research we showed a method based on PMU measurements and least squares aimed at estimating the electrical and mechanical parameters and angular stability dynamics of synchronous generators under various operating conditions. We showed that under real conditions, where the system inertia is close to infinity, the proposed method provides accurate estimation of the parameters.

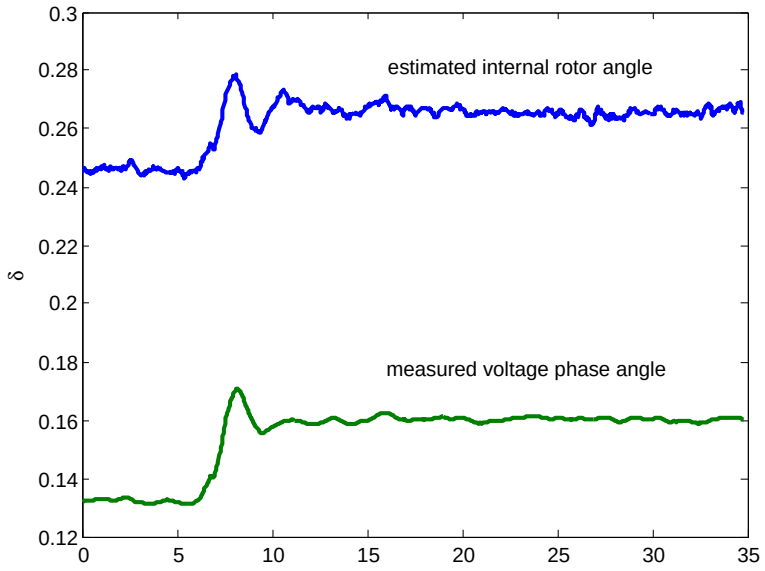

Figure 4.19. Estimated internal voltage phase angle compared with the simulated rotor angle

4.4 System Identification

This research proposes a new modified classical model for the synchronous machine based on the two-axis model having active and reactive power as input and voltage phasor magnitude and angle as output. The research will estimate the parameters of the proposed model and will validate its output using system identification methodology. The research will apply the proposed model on two cases involving a single machine and a power sub-system and will estimate the inertia and the transient reactance. The contribution of this research is the higher accuracy of the proposed model output compared with the classical model output due to the consideration of the effects of some disregarded dynamics in the classical model. The system matrix will be modified in order to ensure stability and prevent error propagation.

System identification is a non-Bayesian approach used to find systems structures and estimate their parameters [12]. The objective of system identification is to use experimental or measured data as input and output of proposed model structure describing a physical system in order to estimate the proposed model parameters. System identification

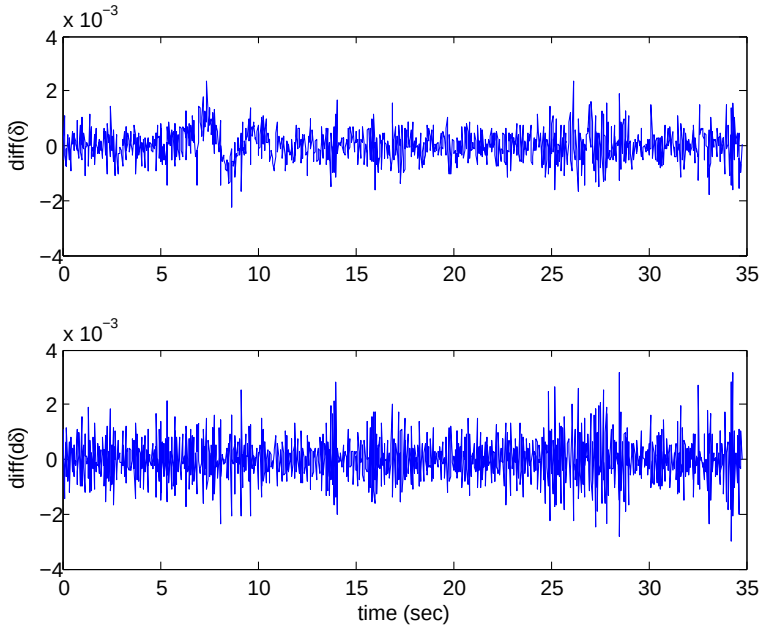

Figure 4.20. Derivatives with white noise

has been used in power electronics research in order to identify power converters [33, 34], to model large signal power electronics systems [35], and to estimate DC link model parameters in VSC-HVDC system [36]. It has also been used in power systems research in the design of probing signals for the estimation of inter-area electromechanical modes [37], and in finding the state space system for multi-input-multi-output models of power systems [38].

Burth *et al.* [40] points out to the difficulty in estimating synchronous machine parameters based on its output. The reason is the complicated structure of the synchronous machine which incorporates lots of parameters yet the effect of each parameter is not clearly reflected in the output (recorded by PMU or DFR), i.e. the generator output observations are not rich. In order to circumvent such estimation difficulties, researchers have used various additional information. Accordingly and in machine estimation, [22] and [45] use additional mechanical measurements, i.e. ω and δ, whereas [60] and [46] fix the process error covariance to specific values. Power area equivalent machine was estimated by [23] using the inter-area frequency in addition to the PMU measurements. Burth *et*

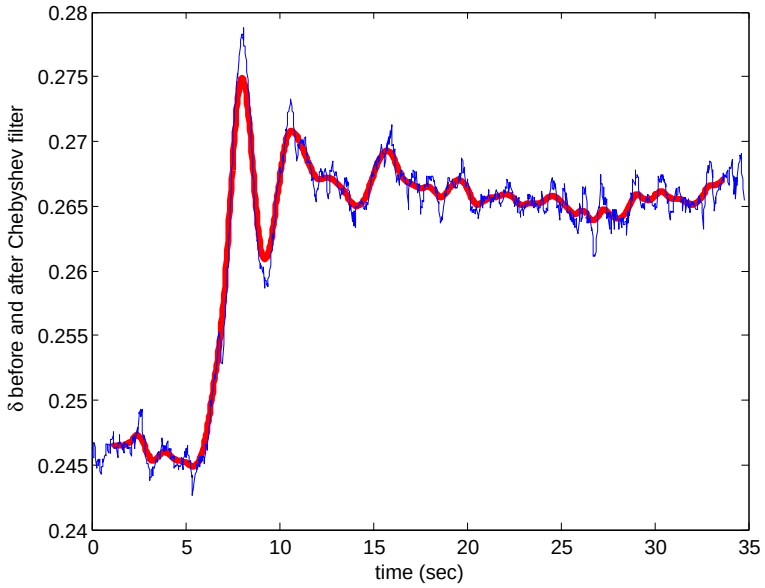

Figure 4.21. δ before and after Chebshev filter

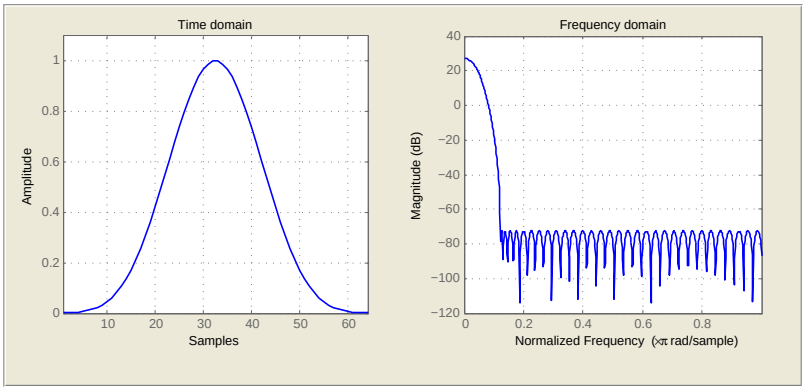

Figure 4.22. Chebshev filter

al. [40] suggests to apply parameters sub-set selection which focus on finding the best set of parameters which can be estimated with reasonable amount of precision for a specific problem formulation. [40] uses the Hessian matrix of the objective function to find the parameters sub-set. Another approach for sub-set selection is the study of sensitivity matrix as shown by Cintron-Arias *et al.* [39]. The two approaches are correlated and both based on Jacobian calculation. It is one of the objectives of this research to select a sub-set of parameters to estimate based on sensitivity matrix.

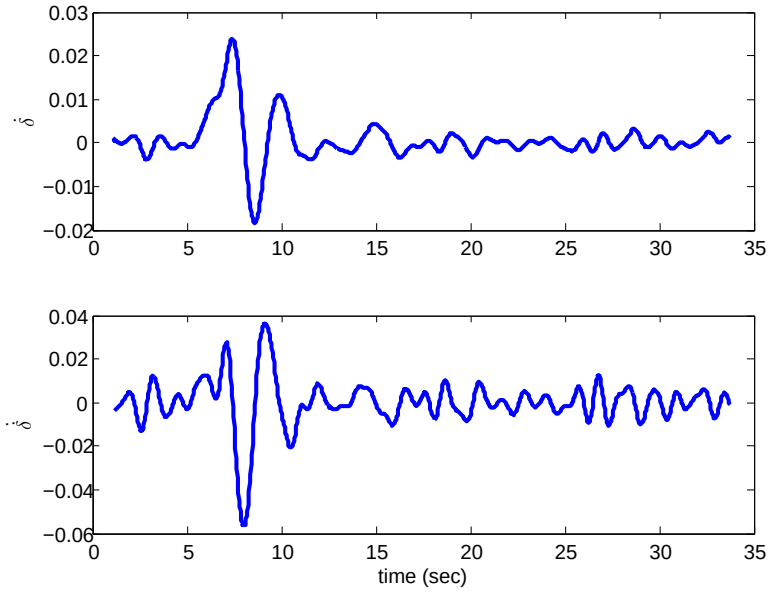

Figure 4.23. Derivatives of δ after Chebshev filter

It is one of the objectives of this research to extend system identification to estimate synchronous machines and power systems parameters based on the output data only provided by PMUs and to provide a systematic approach to immune such estimation from the impact of the process error. This research will carry out:

1. Derive a modified classical (electromechanical) synchronous machine model from the two-axis model by considering the effects of the eliminated dynamics. The proposed model will be validated against the classical model in order to show the improvements.

2. Identify the parameters which can be estimated with high confidence from those subject to low confidence estimation using sensitivity analysis based on PMU output

3. Estimate the parameters of the modified model using system identification on PMU data.

4. Analyze the origin of the model error and study ways to mitigate its impact on the estimated parameters and the output of the proposed model

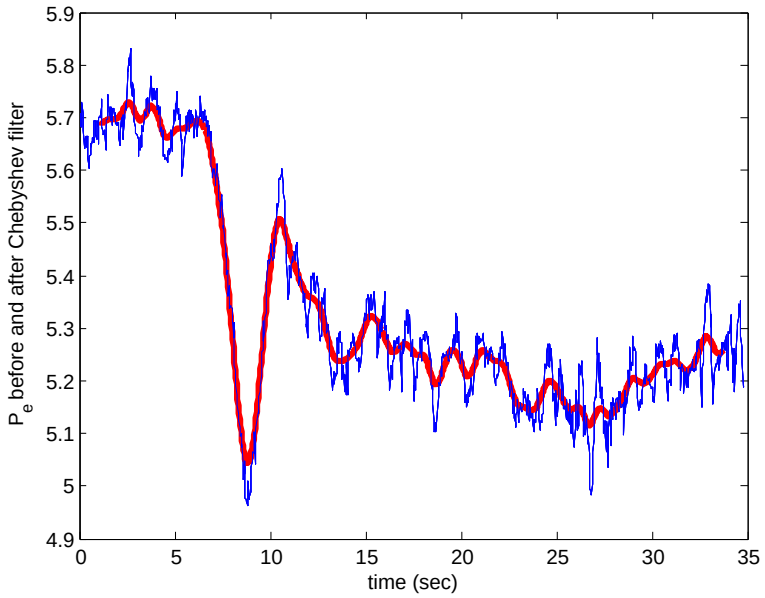

Figure 4.24. P_e before and after Chebshev filter

The rest of this chapter is organized as follows: Section 4.4.1 will derive the small signal model of the proposed modified classical machine and analyze the impact of the model error, Section 4.4.2 will introduce system identification grey box, and Section 4.4.3 will show the simulation and output validation of a single synchronous machine and of a power sub-system.

4.4.1 Small Signal Linearized Model Suitable for PMUs

The purpose of this section in to build a linearized ste-space model having ΔPe and ΔQe as input and ΔV and $\Delta\theta$ as output as shown in Fig. 4.26.

4.4.1.1 Linearized System for the Two-axis Model

Synchronous machine two-axis model with no governor nor exciter controls and ignoring the sub-transient dynamics [17] can be described by:

$$\frac{\partial \delta'}{\partial t} = \omega - \omega_0 \tag{4.32}$$

$$\frac{2H}{\omega_0}\frac{\partial \omega}{\partial t} = P_m - P_e \tag{4.33}$$

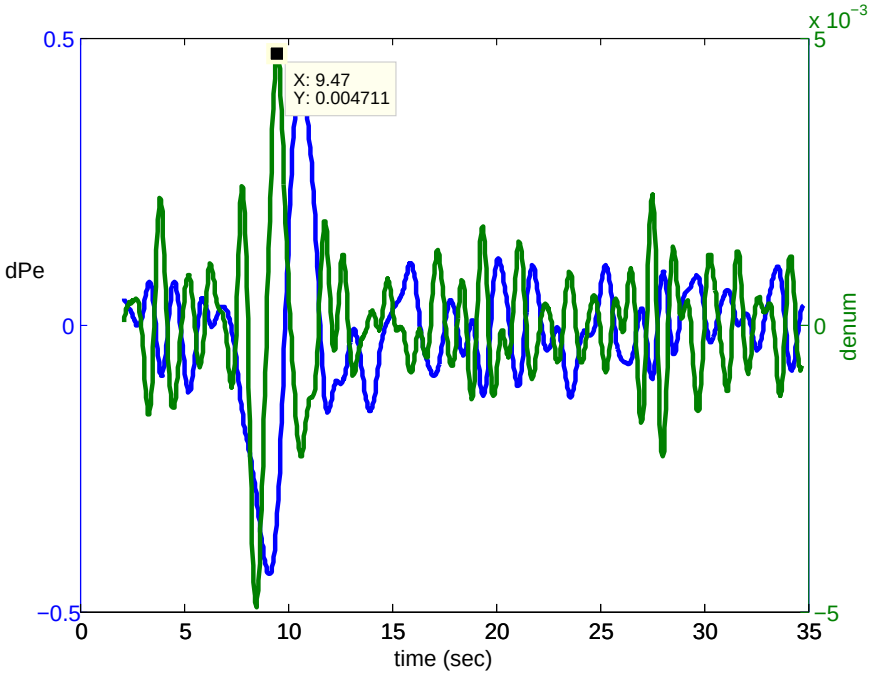

Figure 4.25. Nominator and denominator for inertia computation

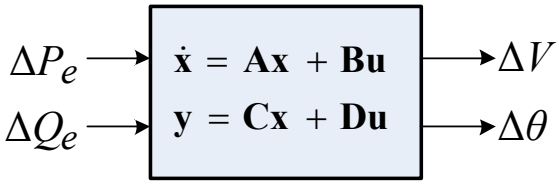

Figure 4.26. Proposed state space model

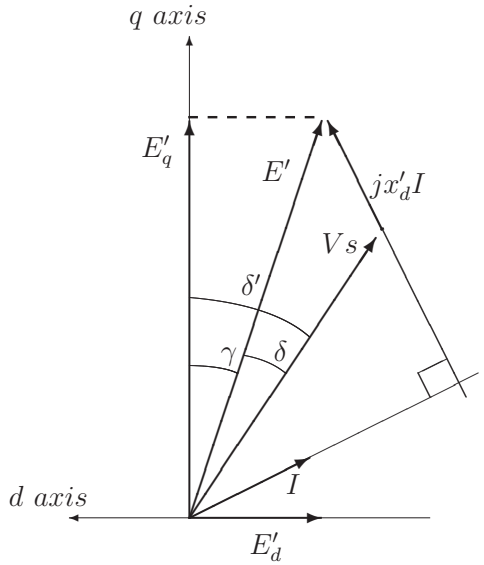

Figure 4.27. Phasor diagram for a classical model from [1]

$$T'_{do}\frac{\partial E'_q}{\partial t} = -E'_q - (x_d - x'_d)I_d + E_{fd} \tag{4.34}$$

$$T'_{qo}\frac{\partial E'_d}{\partial t} = -E'_d - (x_q - x'_q)I_d \tag{4.35}$$

$$[E'_d + (x'_d - x'_q)I_q + E'_q] = jx'_d(I_d + jI_q) + Ve^{j(\theta-\delta'+\pi/2)} \tag{4.36}$$

The the power expressions can be found:

$$\begin{cases} P_e &= I_d V\sin(\delta'-\theta) + I_q V\cos(\delta'-\theta) \\ Q_e &= I_d V\cos(\delta'-\theta) - I_q V\sin(\delta'-\theta) \end{cases} \tag{4.37}$$

Using (4.36) to find:

$$\begin{cases} I_d &= \frac{E'_q - V\cos(\delta'-\theta)}{x'_d} \\ I_q &= \frac{-E'_d + V\sin(\delta'-\theta)}{x'_q} \end{cases} \tag{4.38}$$

Then we find the power-voltage relationship in plugging (4.38) in (4.37):

$$\begin{cases} P_e &= \frac{V}{x'_d x'_q}\left\{x'_q E'_q\sin(\delta'-\theta) - x'_d E'_d\cos(\delta'-\theta) + \right. \\ & \qquad \left. 1/2\times(x'_d - x'_q)V\sin(2\delta'-2\theta)\right\} \\ Q_e &= \frac{V}{x'_d x'_q}\left\{x'_q E'_q\cos(\delta'-\theta) + x'_d E'_d\sin(\delta'-\theta) + \right. \\ & \qquad \left. 1/2\times[(x'_d - x'_q)V\cos(2\delta'-2\theta) - (x'_d + x'_q)V]\right\} \end{cases} \tag{4.39}$$

Simplifying by neglecting the transient saliency ($x'_d = x'_q$), (4.39) becomes:

$$\begin{cases} P_e &= \frac{E'_q V\sin(\delta'-\theta) - E'_d V\cos(\delta'-\theta)}{x'_d} \\ Q_e &= \frac{E'_q V\cos(\delta'-\theta) + E'_d V\sin(\delta'-\theta) - V^2}{x'_d} \end{cases} \tag{4.40}$$

On the other hand, the synchronous machine classical model can be obtained by reducing the two-axis model when setting T'_{qo} is set to zero (i.e. ignoring the quick q axis dampers dynamics) and T'_{do} is extended to ∞ (i.e. extending the effect of the d axis

where the field is located). Consequently, such simplification keeps the electromechanical dynamics in (4.32) and (4.33) and completely disregards E'_d and E'_q dynamics.

The simplified model in this research will be based on differential equations describing the voltage source angle δ and the rotor speed ω and will include the effect of E'_q and E'_d. According to [1] and [17] the difference γ between the rotor angle δ' and the voltage source angle δ is almost constant and is negligible when studying angle dynamics. Fig. 4.27 [1] shows γ, δ', and δ. Accordingly:

$$\delta' = \delta + \gamma \Rightarrow \tag{4.41}$$

$$\dot{\Delta\delta'} = \dot{\Delta\delta} + \dot{\Delta\gamma} \tag{4.42}$$

Careful attention at γ (Fig. 4.27)shows the following:

$$\gamma = tan^{-1}\left(\frac{E'_d}{E'_q}\right) \Rightarrow \tag{4.43}$$

$$(\dot{\Delta\gamma}) = -\frac{E'_{d0}}{{E'_{d0}}^2 + {E'_{q0}}^2}(\Delta\dot{E}'_q) + \frac{E'_{q0}}{{E'_{d0}}^2 + {E'_{q0}}^2}(\Delta\dot{E}'_d) \tag{4.44}$$

When E'_d and E'_q dynamics are ignored $\dot{\Delta\gamma} = 0$. Based on (4.42) and (4.44):

$$\begin{aligned} &\dot{\Delta\delta} = \dot{\Delta\delta'} - \dot{\Delta\gamma} \\ &\Rightarrow \dot{\Delta\delta} = \Delta\omega + \frac{E'_{d0}}{{E'_{d0}}^2 + {E'_{q0}}^2}(\Delta\dot{E}'_q) - \frac{E'_{q0}}{{E'_{d0}}^2 + {E'_{q0}}^2}(\Delta\dot{E}'_d) \end{aligned} \tag{4.45}$$

We need to find $(\Delta\dot{E}'_q)$ and $(\Delta\dot{E}'_q)$. Based on (4.34) and (4.35), we have:

$$(\Delta\dot{E}'_q) = \frac{1}{T'_{do}}[-\Delta E'_q - (x_d - x'_d)\Delta I_d + \Delta E_{fd}] \tag{4.46}$$

$$(\Delta\dot{E}'_d) = \frac{1}{T'_{qo}}[-\Delta E'_d - (x_d - x'_d)\Delta I_q \tag{4.47}$$

From (4.38) ΔI_d and ΔI_q are obtained and then plugged in (4.46) and (4.47) to formulate $(\Delta\dot{E}'_q)$ and $(\Delta\dot{E}'_d)$:

$$\begin{cases} \Delta I_d &= \frac{1}{x'_d} \begin{bmatrix} 1 \\ -\cos(\delta'_0 - \theta_0) \\ V_0 \sin(\delta'_0 - \theta_0) \\ -V_0 \sin(\delta'_0 - \theta_0) \end{bmatrix}^T \begin{bmatrix} \Delta E'_q \\ \Delta V \\ \Delta\delta' \\ \Delta\theta \end{bmatrix} \\ \Delta I_q &= \frac{1}{x'_q} \begin{bmatrix} -1 \\ \sin(\delta'_0 - \theta_0) \\ V_0 \cos(\delta'_0 - \theta_0) \\ -V_0 \cos(\delta'_0 - \theta_0) \end{bmatrix}^T \begin{bmatrix} \Delta E'_d \\ \Delta V \\ \Delta\delta' \\ \Delta\theta \end{bmatrix} \end{cases} \tag{4.48}$$

$$\begin{cases} (\Delta\dot{E}'_q) &= \frac{x_d - x'_d}{T'_{do} x'_d} \begin{bmatrix} -x_d/(x_d - x'_d) \\ \cos(\delta'_0 - \theta_0) \\ -V_0 \sin(\delta'_0 - \theta_0) \\ V_0 \sin(\delta'_0 - \theta_0) \\ x'_d/x_d - x'_d \end{bmatrix}^T \begin{bmatrix} \Delta E'_q \\ \Delta V \\ \Delta\delta' \\ \Delta\theta \\ \Delta E_{fd} \end{bmatrix} \\ (\Delta\dot{E}'_d) &= \frac{x_q - x'_q}{T'_{qo} x'_q} \begin{bmatrix} -x_q/(x_q - x'_q) \\ \sin(\delta'_0 - \theta_0) \\ V_0 \cos(\delta'_0 - \theta_0) \\ -V_0 \cos(\delta'_0 - \theta_0) \end{bmatrix}^T \begin{bmatrix} \Delta E'_d \\ \Delta V \\ \Delta\delta' \\ \Delta\theta \end{bmatrix} \end{cases} \tag{4.49}$$

The system (4.49) can be verified by looking at the special case of the machine connected to an infinity bus and neglecting both E'_d dynamics and resistances. In this

case, the quantities V_0 and θ_0 are considered those of the infinity bus and both x'_d and x_d will include the transmission line reactance, then (4.49) will transform to the system already shown by Anderson *et al.* [83]:

$$(\Delta\dot{E}'_q) = \frac{x_d - x'_d}{T'_{do}x'_d} \begin{bmatrix} -x_d/(x_d - x'_d) \\ -V_0\sin(\delta'_0 - \theta_0) \\ x'_d/x_d - x'_d \end{bmatrix}^T \begin{bmatrix} \Delta E'_q \\ \Delta\delta' \\ \Delta E_{fd} \end{bmatrix} \tag{4.50}$$

In (4.49) $\Delta\theta$ and ΔV are used as input to the state space model. However the interest is to formulate (ΔP_e and ΔQ_e) as the input because (ΔP_e and ΔQ_e) are representative to the changes of the transmission system the machine is connected to which can be done by obtaining the small signal model for P_e ans Q_e around an equilibrium point using (4.40):

$$\Delta P_e = \frac{1}{x'_d} \begin{bmatrix} E'_{q0}\sin(\delta'_0 - \theta_0) - E'_{d0}\cos(\delta'_0 - \theta_0) \\ E'_{q0}V_0\cos(\delta'_0 - \theta_0) + E'_{d0}V_0\sin(\delta'_0 - \theta_0) \\ -E'_{q0}V_0\cos(\delta'_0 - \theta_0) - E'_{d0}V_0\sin(\delta'_0 - \theta_0) \\ V_0\sin(\delta'_0 - \theta_0) \\ -V_0\cos(\delta'_0 - \theta_0) \end{bmatrix}^T \begin{bmatrix} \Delta V \\ \Delta\delta' \\ \Delta\theta \\ \Delta E'_q \\ \Delta E'_d \end{bmatrix} \tag{4.51}$$

$$\Delta Q_e = \frac{1}{x'_d} \begin{bmatrix} E'_{q0}\cos(\delta'_0 - \theta_0) + E'_{d0}\sin(\delta'_0 - \theta_0) \\ E'_{d0}V_0\cos(\delta'_0 - \theta_0) - E'_{q0}V_0\sin(\delta'_0 - \theta_0) \\ E'_{q0}V_0\sin(\delta'_0 - \theta_0) - E'_{d0}V_0\cos(\delta'_0 - \theta_0) \\ V_0\cos(\delta'_0 - \theta_0) \\ V_0\sin(\delta'_0 - \theta_0) \end{bmatrix}^T \begin{bmatrix} \Delta V \\ \Delta\delta' \\ \Delta\theta \\ \Delta E'_q \\ \Delta E'_d \end{bmatrix} \tag{4.52}$$

Solving (4.52) in order to find the small signal model for V and θ:

$$\begin{bmatrix} \Delta\theta \\ \Delta V \end{bmatrix} = \begin{bmatrix} 1 \\ 0 \end{bmatrix} \Delta\delta' + \begin{bmatrix} J_{\theta P_e} & J_{\theta Q_e} \\ J_{VP} & J_{VQ_e} \end{bmatrix} \begin{bmatrix} \Delta P_e \\ \Delta Q_e \end{bmatrix} + \begin{bmatrix} J_{\theta E'_q} & J_{\theta E'_d} \\ J_{VE'_q} & J_{VE'_d} \end{bmatrix} \begin{bmatrix} \Delta E'_q \\ \Delta E'_d \end{bmatrix} \tag{4.53}$$

$J_{\theta P_e}$, $J_{\theta Q_e}$, J_{VP_e}, J_{VQ_e}, $J_{\theta E'_q}$, $J_{\theta E'_d}$, $J_{VE'_q}$, and $J_{VE'_d}$ represent the Jacobian of $\Delta\theta$ and ΔV around the equilibrium point. They can be preliminary expressed as:

$$J_{\theta P_e} = \frac{x'_d[2V_0 - E'_{q0}\cos(\delta'_0 - \theta_0) - E'_{d0}\sin(\delta'_0 - \theta_0)]}{V_0 D} \tag{4.54}$$

$$J_{\theta Q_e} = \frac{x'_d[E'_{q0}\sin(\delta'_0 - \theta_0) - E'_{d0}\cos(\delta'_0 - \theta_0)]}{V_0 D} \tag{4.55}$$

$$J_{VP_e} = \frac{x'_d[E'_{q0}\sin(\delta'_0 - \theta_0) - E'_{d0}\cos(\delta'_0 - \theta_0)]}{D} \tag{4.56}$$

$$J_{VQ_e} = \frac{x'_d[E'_{q0}\cos(\delta'_0 - \theta_0) + E'_{d0}\sin(\delta'_0 - \theta_0)}{D} \tag{4.57}$$

$$J_{\theta E'_q} = \frac{[E'_{d0} - 2V_0\sin(\delta'_0 - \theta_0)]}{D} \tag{4.58}$$

$$J_{\theta E'_d} = \frac{[2V_0\cos(\delta'_0 - \theta_0) - E'_{q0}]}{D} \tag{4.59}$$

$$J_{VE'_q} = \frac{-E'_{q0}V_0}{D} \tag{4.60}$$

$$J_{VE'_d} = \frac{-E'_{d0}V_0}{D} \tag{4.61}$$

$$D = {E'_0}^2 - 2E'_0V_0\cos(\delta_0 - \theta_0) \tag{4.62}$$

Using (4.40) around the equilibrium point leads to simplified expressions (with only one unknown x'_d) which are used in the estimation process replacing (4.54), (4.55), (4.56), and (4.57):

$$J_{\theta P_e} = \frac{V_0^2 x'_d - Q_{e0}{x'_d}^2}{(P_{e0}x'_d)^2 + (Q_{e0}x'_d)^2 - V_0^4} \tag{4.63}$$

$$J_{\theta Q_e} = \frac{P_{e0}{x'_d}^2}{(P_{e0}x'_d)^2 + (Q_{e0}x'_d)^2 - V_0^4} \tag{4.64}$$

$$J_{VP_e} = \frac{P_{e0}V_0{x'_d}^2}{(P_{e0}x'_d)^2 + (Q_{e0}x'_d)^2 - V_0^4} \tag{4.65}$$

$$J_{VQ_e} = \frac{Q_{e0}V_0{x'_d}^2 + V_0^3x'_d}{(P_{e0}x'_d)^2 + (Q_{e0}x'_d)^2 - V_0^4} \tag{4.66}$$

We use (4.53) in (4.49) in order to get the small signal system for E'_q and E'_d:

$$\begin{bmatrix} \Delta\dot{E}'_q \\ \Delta\dot{E}'_d \end{bmatrix} = \begin{bmatrix} J_{\dot{E}'_q E'_q} & J_{\dot{E}'_q E'_d} \\ J_{\dot{E}'_d E'_q} & J_{\dot{E}'_d E'_d} \end{bmatrix} \begin{bmatrix} \Delta E'_q \\ \Delta E'_d \end{bmatrix} + \begin{bmatrix} J_{\dot{E}'_q P_e} & J_{\dot{E}'_q Q_e} \\ J_{\dot{E}'_d P_e} & J_{\dot{E}'_d Q_e} \end{bmatrix} \begin{bmatrix} \Delta P_e \\ \Delta Q_e \end{bmatrix} + \begin{bmatrix} 1/T'_{do} \\ 0 \end{bmatrix} \Delta E_{fd} \quad (4.67)$$

where:

$$J_{\dot{E}'_q E'_q} = \frac{-1}{T'_{do}} - \frac{(x_d - x'_d)}{x'_d T'_{do} D}[D + {V_0}^2(1 - \cos(2\delta'_0 - 2\theta_0)) + E'_0 V_0 \cos(2\delta'_0 - \delta_0 - \theta_0)] \quad (4.68)$$

$$J_{\dot{E}'_q E'_d} = \frac{-(x_d - x'_d)}{x'_d T'_{do}} \frac{V_0}{D}[E'_0 \sin(2\delta'_0 - \delta_0 - \theta_0) - V_0 \sin(2\delta'_0 - 2\theta_0)] \quad (4.69)$$

$$J_{\dot{E}'_d E'_q} = \frac{-(x_q - x'_d)}{x'_d T'_{qo}} \frac{V_0}{D}[E'_0 \sin(2\delta'_0 - \delta_0 - \theta_0) - V_0 \sin(2\delta'_0 - 2\theta_0)] \quad (4.70)$$

$$J_{\dot{E}'_d E'_d} = \frac{-1}{T'_{qo}} - \frac{(x_q - x'_d)}{x'_d T'_{qo} D}[D + {V_0}^2(1 + \cos(2\delta'_0 - 2\theta_0)) - E'_0 V_0 \cos(2\delta'_0 - \delta_0 - \theta_0)] \quad (4.71)$$

$$J_{\dot{E}'_q P_e} = \frac{(x_d - x'_d)[2V_0 \sin(\delta'_0 - \theta_0) - E'_{d0}]}{T'_{do} D} \quad (4.72)$$

$$J_{\dot{E}'_q Q_e} = \frac{(x_d - x'_d) E'_{q0}}{T'_{do} D} \quad (4.73)$$

$$J_{\dot{E}'_d P_e} = \frac{(x_q - x'_d)[E'_{q0} - 2V_0 \cos(\delta'_0 - \theta_0)]}{T'_{qo} D} \quad (4.74)$$

$$J_{\dot{E}'_d Q_e} = \frac{(x_q - x'_d) E'_{d0}}{T'_{qo} D} \quad (4.75)$$

The state space system for the linearized two-axis model can be formed by using (4.45) (where (4.67) is plugged in), linearizing (4.33), and adding (4.67) to form the states equations. (4.53) forms the observation equation. The resulting state space system is:

$$\begin{bmatrix} \Delta\dot{\delta} \\ \Delta\dot{\omega} \\ \Delta\dot{E}'_q \\ \Delta\dot{E}'_d \end{bmatrix} = \begin{bmatrix} 0 & 1 & J_{\dot{\delta}E'_q} & J_{\dot{\delta}E'_d} \\ 0 & 0 & 0 & 0 \\ 0 & 0 & J_{\dot{E}'_q E'_q} & J_{\dot{E}'_q E'_d} \\ 0 & 0 & J_{\dot{E}'_d E'_q} & J_{\dot{E}'_d E'_d} \end{bmatrix} \begin{bmatrix} \Delta\delta \\ \Delta\omega \\ \Delta E'_q \\ \Delta E'_d \end{bmatrix} + \begin{bmatrix} J_{\dot{\delta}P_e} & J_{\dot{\delta}Q_e} \\ -\omega_0/2H & 0 \\ J_{\dot{E}'_q P_e} & J_{\dot{E}'_q Q_e} \\ J_{\dot{E}'_d P_e} & J_{\dot{E}'_d Q_e} \end{bmatrix} \begin{bmatrix} \Delta P_e \\ \Delta Q_e \end{bmatrix} + \begin{bmatrix} J_{\dot{\delta}E_{fd}} \\ 0 \\ 1/T'_{do} \\ 0 \end{bmatrix} \Delta E_{fd} \quad (4.76)$$

$$\begin{bmatrix} \Delta\theta \\ \Delta V \end{bmatrix} = \begin{bmatrix} 1 & 0 & J_{\theta E'_q} & J_{\theta E'_d} \\ 0 & 0 & J_{VE'_q} & J_{VE'_d} \end{bmatrix} \begin{bmatrix} \Delta\delta \\ \Delta\omega \\ \Delta E'_q \\ \Delta E'_d \end{bmatrix} + \begin{bmatrix} J_{\theta P_e} & J_{\theta Q_e} \\ J_{VP} & J_{VQ_e} \end{bmatrix} \begin{bmatrix} \Delta P_e \\ \Delta Q_e \end{bmatrix} \tag{4.77}$$

where:

$$J_{\dot{\delta}E'_q} = \frac{E'_{d0} J_{\dot{E}'_q E'_q} - E'_{q0} J_{\dot{E}'_d E'_q}}{{E'_0}^2} \tag{4.78}$$

$$J_{\dot{\delta}E'_d} = \frac{E'_{d0} J_{\dot{E}'_q E'_d} - E'_{q0} J_{\dot{E}'_d E'_d}}{{E'_0}^2} \tag{4.79}$$

$$J_{\dot{\delta}P_e} = \frac{E'_{d0} J_{\dot{E}'_q P_e} - E'_{q0} J_{\dot{E}'_d P_e}}{{E'_0}^2} \tag{4.80}$$

$$J_{\dot{\delta}Q_e} = \frac{E'_{d0} J_{\dot{E}'_q Q_e} - E'_{q0} J_{\dot{E}'_d Q_e}}{{E'_0}^2} \tag{4.81}$$

$$J_{\dot{\delta}E_{fd}} = \frac{E'_{d0}}{T'_{do} {E'_0}^2} \tag{4.82}$$

4.4.1.2 Sub-set Selection and System Downsizing

The system (4.76)-(4.77) includes many parameters which can be estimated but with different degrees of success. [39] proposes to use sensitivity matrix to select a sub-set of parameters to be estimated. Sensitivity matrix is used to study the impact of the various parameters on the output of a system, in other words, it tries to find the most influential and the least influential parameter on the output.

Mathematically speaking, the sensitivity matrix of the system (4.76)-(4.77) is the Jacobian matrix χ of the output $\mathbf{Y}$ wrt. $\mathbf{M}= \left\{x'_d, H, x_q, x_d, T'_{do}, T'_{qo}\right\}$.

$$\chi_{ij} = \frac{\partial Y_i}{\partial M_j} \tag{4.83}$$

Accordingly, χ for the system (4.76)-(4.77) will be $N \times 6$ where N is the total number of samples.

The importance of the sensitivity matrix in least squares based estimations (like system identification) comes from the objective of the least squares estimation of minimizing the output error by manipulating $\mathbf{M}$ around a value M_0 [39] to find its estimate $\hat{M}$:

$$\hat{\mathbf{M}} = \arg\min_{\mathbf{M}} \sum_{i=1}^{N} (Y(i) - \hat{Y}(i|M))^2 \tag{4.84}$$

$$\hat{\mathbf{M}} = M_0 + (\chi^T \chi)^{-1} \chi^T \zeta \tag{4.85}$$

ζ is the $1 \times N$ error (noise) matrix associated with the output equation. A good estimation of $\mathbf{M}$ will reduce the impact of ζ by having $(\chi^T \chi)$ far from singularity. Should $(\chi^T \chi)$ be close to singular, then $(\chi^T \chi)^{-1}$ will amplify the impact of ζ and distorts the estimation of $\mathbf{M}$.

Singular value decomposition (SVD) of χ provides an insightful relation between each parameter singular value and the possibility of the least squares estimation to find a good value of the parameter. The singular value decomposition of of χ is:

$$[\Upsilon, \mathbf{S}, \Omega] = \text{SVD}(\chi) \tag{4.86}$$

$$\chi = \Upsilon \mathbf{S} \Omega^T \tag{4.87}$$

Υ is $N \times N$ orthonormal matrix, Ω is 6×6 orthonormal matrix, and $\mathbf{S}$ is the singular value matrix and is Υ is $N \times 6$ matrix. The first 6 diagonal elements of S are the singular values of χ and the rest of the matrix equals to 0.

The estimation of $\mathbf{M}$ around M_0 can now be written as [39]:

$$\hat{\mathbf{M}} = M_0 + \sum_{i=1}^{6} \frac{o_i u_i^T}{s_i} \zeta \tag{4.88}$$

where o_i, u_i are the ith columns of Ω and Υ. s_i is the ith diagonal value of $\mathbf{S}$.

Equation (4.88) shows the inverse proportional impact of the singular value s_i associated with a parameter M_i. As s_i decreases the error ζ introduces more distortion on the estimated parameter and leads to a larger deviation from the correct value. Accordingly, it is better to estimate the parameters with high singular values which also have the highest impact on the output. In order to find the singular values, the matrix χ needs to be calculated.

χ can be calculated analytically sometimes [85] in case the the associated differential equations are simple enough and clear. In the case of (4.76)-(4.77) the input function U is not defined analytically which makes better to find χ numerically. The sensitivity matrix χ was calculated numerically [86] using finite differences by perturbating each parameter M aside by a value h and then recording the output of the system Y_h. The recorded output before (Y) and after (Y_h) perturbation are used for the Jacobian calculation:

$$\chi = \frac{Y_h - Y}{h} \tag{4.89}$$

Following the calculation of the χ, SVD wass performed in order to extract $\mathbf{S}$:

$$\mathbf{S} = \begin{bmatrix} 3.9 & 0 & 0 & 0 & 0 & 0 \\ 0 & 0.2 & 0 & 0 & 0 & 0 \\ 0 & 0 & 0.12 & 0 & 0 & 0 \\ 0 & 0 & 0 & 0.08 & 0 & 0 \\ 0 & 0 & 0 & 0 & 0.04 & 0 \\ 0 & 0 & 0 & 0 & 0 & 0.03 \end{bmatrix} \tag{4.90}$$

It was found that x'_d is associated with 3.9, H with 0.2, x_q with 0.12, x_d with 0.08, T'_{qo} with 0.04, $T'_D do$ with 0.03. In order to to test the estimation system, it was decided to estimate the parameters associated with the highest singular values (which they have the most impact on the output) and consider the rest of the parameters (which they have the

least impact on the output) to be known. Accordingly, the set of unknown parameters M to be estimated $\mathbf{M}= \{x'_d, H, x_q, x_d\}$.

The state space system (4.76)-(4.77) can be downsized into a system with two states only δ and ω with an additive error $Err1$ and $Err2$, since the equations of these two states include all the parameters in $\mathbf{M}$.

$$\begin{bmatrix} \dot{\Delta\delta} \\ \dot{\Delta\omega} \end{bmatrix} = \begin{bmatrix} 0 & 1 \\ 0 & 0 \end{bmatrix} \begin{bmatrix} \Delta\delta \\ \Delta\omega \end{bmatrix} + \begin{bmatrix} J_{\dot{\delta}P_e} & J_{\dot{\delta}Q_e} \\ -\omega_0/2H & 0 \end{bmatrix} \begin{bmatrix} \Delta P_e \\ \Delta Q_e \end{bmatrix} + Err1 \tag{4.91}$$

$$\begin{bmatrix} \Delta\theta \\ \Delta V \end{bmatrix} = \begin{bmatrix} 1 & 0 \\ 0 & 0 \end{bmatrix} \begin{bmatrix} \Delta\delta \\ \Delta\omega \end{bmatrix} + \begin{bmatrix} J_{\theta P_e} & J_{\theta Q_e} \\ J_{VP} & J_{VQ_e} \end{bmatrix} \begin{bmatrix} \Delta P_e \\ \Delta Q_e \end{bmatrix} + Err2 \tag{4.92}$$

The system (4.96)-(4.97) is state space model written as:

$$\begin{aligned} \dot{X} &= [A]X + [B]U + Err1 \\ Y &= [C]X + [D]U + Err2 \end{aligned} \tag{4.93}$$

with the state vector $X = [\Delta\delta \ \Delta\omega]^T$, the observation (or measurement) vector $Y = [\Delta\theta \ \Delta V]^T$, the input vector $U = [\Delta P_e \ \Delta Q_e]^T$, and the error vectors $Err1$ and $Err2$.

4.4.1.3 System Stabilization

The Eigenvalues of $[A]$ as shown in 4.91 are zeros which risks instability. $[A]$ will be slightly modified to ensure stability. $[A]$ as a general (2×2) matrix has the following form:

$$\begin{bmatrix} A \end{bmatrix} = \begin{bmatrix} \text{a} & \text{b} \\ \text{c} & \text{d} \end{bmatrix} \tag{4.94}$$

Taking $b = 1$ and $(a\ c\ d \to 0)$ then $[A]$ has the following two Eigenvalues:

$$\lambda_{1,2} \approx \frac{a+d}{2} \pm \sqrt{c}(1 + \frac{a^2 + d^2 - 2ad}{8c}) \tag{4.95}$$

A simple solution to stabilize $[A]$ by making the real parts of $\lambda_{1,2} < 0$ and maintaining $(a\ c\ d \to 0)$ is to take $(a = 0,\ c = d = \epsilon < 0,\ \ \epsilon \to 0)$. The simulation part will show the effects of various values of ϵ.

Accordingly, the proposed model state space system to be estimated is written as:

$$\begin{bmatrix} \dot{\Delta\delta} \\ \dot{\Delta\omega} \end{bmatrix} = \begin{bmatrix} 0 & 1 \\ \epsilon & \epsilon \end{bmatrix} \begin{bmatrix} \Delta\delta \\ \Delta\omega \end{bmatrix} + \begin{bmatrix} J_{\dot{\delta}P_e} & J_{\dot{\delta}Q_e} \\ -\omega_0/2H & 0 \end{bmatrix} \begin{bmatrix} \Delta P_e \\ \Delta Q_e \end{bmatrix} + Err1 \tag{4.96}$$

$$\begin{bmatrix} \Delta\theta \\ \Delta V \end{bmatrix} = \begin{bmatrix} 1 & 0 \\ 0 & 0 \end{bmatrix} \begin{bmatrix} \Delta\delta \\ \Delta\omega \end{bmatrix} + \begin{bmatrix} J_{\theta P_e} & J_{\theta Q_e} \\ J_{VP} & J_{VQ_e} \end{bmatrix} \begin{bmatrix} \Delta P_e \\ \Delta Q_e \end{bmatrix} + Err2 \tag{4.97}$$

$$Err1 = \begin{bmatrix} J_{\dot{\delta}E'_q} & J_{\dot{\delta}E'_d} \\ \epsilon\Delta\delta/\Delta E'_q & \epsilon\Delta\omega/\Delta E'_d \end{bmatrix} \begin{bmatrix} \Delta E'_q \\ \Delta E'_d \end{bmatrix} + \begin{bmatrix} J_{\dot{\delta}E_{fd}} \\ 0 \end{bmatrix} \Delta E_{fd} \tag{4.98}$$

$$Err2 = \begin{bmatrix} J_{\theta E'_q} & J_{\theta E'_d} \\ J_{VE'_q} & J_{VE'_d} \end{bmatrix} \begin{bmatrix} \Delta E'_q \\ \Delta E'_d \end{bmatrix} \tag{4.99}$$

The model in (4.101) and(4.97) will be referred to as 'model 2' whereas the the model without the terms $J_{\dot{\delta}P_e}$ and $J_{\dot{\delta}Q_e}$ will be referred to as 'model 1'. 'Model 1' is more similar to classical model than 'model 2'.

The set of unknown parameters M to be estimated is:

$$M = (x'_d,\ H,\ x_d,\ x_q). \tag{4.100}$$

The unknown parameters are observed in the state space system as follows: x'_d in $(J_{\theta P_e}, J_{\theta Q_e}, J_{VP_e}, J_{VQ_e})$, H in $^{-\omega_0}/_{2H}$, and $(x_d,\ x_q)$ in $(J_{\delta P_e}, J_{\delta Q_e})^3$. Knowing $J_{\delta P_e}$ and $J_{\delta Q_e}$ is not enough to estimate the rest of parameters $\delta_0,\ E'_{d0},\ E'_{q0}$.

The system (4.96)-(4.97) is considered as grey box model [12] where the parameters of the box take physical characteristics (e.g. H). The parameters of the system can be estimated by a system identification software such as MATLAB System Identification Toolbox.

4.4.2 Gray Box Model and Error Quantification

The grey box (4.96)-(4.97) subject to system identification is modeled as:

$$\dot{X} = [A]X + [B]U + [K]e \tag{4.101}$$

$$Y = [C]X + [D]U + e \tag{4.102}$$

$[A], [B], [C], [D]$ are parametrized matrices, $[e]$ is a noise formed by formulation errors and $[K]$ is used to fine tune the estimation by varying the impact of the noise e in the state space system.

The system identification algorithm for a grey box does iterative search to minimize an error function. The general iterative search is a prediction-error identification method (PEM)which minimizes a function of the error between the real output Y and the predicted output $\hat{Y}(M)$ [12].

$$\hat{M} = \arg\min_{M}\ V_N(M, U, Y) \tag{4.103}$$

where " arg min " stands for minimizer of the error function V_N by modifying M, and having U as input, Y as output, and N as the number of outputs.

A basic choice for V_N is the quadratic function:

$$V_N = \frac{1}{N}\sum_{n=1}^{N}(Y(n) - \hat{Y}(n|M))^2 \tag{4.104}$$

The outcome of the system identification of (4.96)-(4.97) is different solutions for M, i.e. $M_k = H_k, x'_{dk}$ pending on the value of $[k]$. The optimum set of M and value of $[K]$ will be chosen by the validation process. The values associated with $[K]$ are very influential and in the case of (4.96)-(4.97) can be shown to be:

$$[K] = Err1/Err2 \tag{4.105}$$

One solution for (4.105) is:

$$[K] = \begin{bmatrix} \frac{J_{\delta E'_q}\Delta E'_q + J_{\delta E'_d}\Delta E'_d}{J_{\theta E'_q}\Delta E'_q + J_{\theta E'_d}\Delta E'_d} & 0 \\ 0 & 0 \end{bmatrix} \tag{4.106}$$

Equation (4.106) shows that $[K]$ depends on the machine and system operating conditions (due to $J_{\delta E'_q}, \Delta E'_q, J_{\delta E'_d}, \Delta E'_d, J_{\theta E'_q}, \Delta E'_q, J_{\theta E'_d}, \Delta E'_d$) and varies with time (due to $\Delta E'_q, \Delta E'_d$). A detailed quantification of K under various four various operating conditions combining high and low active and reactive power output of the machine is provided under 4.4.3. An average $[K_0]$ of [K] will be calculated and various estimations resulting by varying $[K]$ around $[K_0]$ will be validated.

4.4.3 Simulation and Validation

Two cases will be studied, the first one is single machine infinity bus (case 1) and the second one is four-machine two-area system (case 2). Four sets of measurements for $P_e,\ Q_e,\ V,$ andθ will be taken following a three phase line to ground fault at a point right outside the machine or the power sub-system (case 2).

Small signal quantities $\Delta P_e, \Delta Q_e, \Delta V$ and $\Delta\theta$ were derived by removing the steady state value of the measurements. ΔP_e and ΔQ_e were considered as the input and ΔV and $\Delta\theta$ were considered as output. Both systems representing 'model 2' in (4.96)-(4.97) and 'model 1'were implemented with MATLAB System Identification Toolbox grey box. The input and output data sets were divided, time wise, to two subsets. The first subset of few

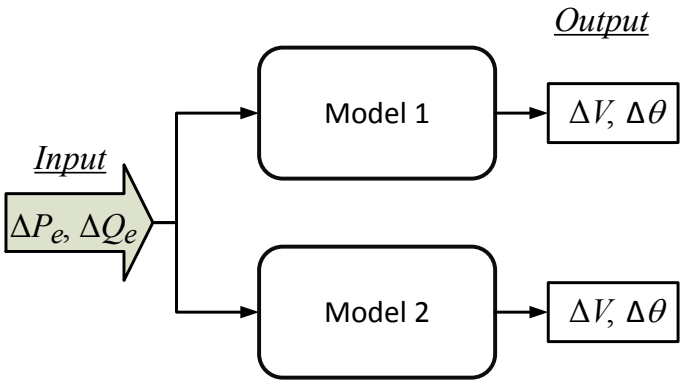

Figure 4.28. Validation process of proposed model

seconds was used in the estimation along with few values of K around $K0$. The second subset was used in the validation process along with specific values for K.

The simulation data is shown in Appendix B.

4.4.3.1 Validation

The purpose of the validation process is to test the output $(\Delta\theta, \Delta V)$ of 'model 2' and the output of 'model 1' against the output of the simulated machine. The comparison process between both models is shown in Fig 4.28.

Once the grey models are estimated, the models of Fig. 4.28 were implemented in Simulink and fed with the input $\Delta P_e, \Delta Q_e$ in addition to the estimated parameters. The output of the Simulink system and the states ($\Delta\delta$ and $\Delta\omega$) will be compared to the simulated output and mechanical states $\Delta\delta'$ and $\Delta\omega$.

4.4.3.2 Case 1: Single Machine Infinity Bus

A single machine infinity bus was built using MATLAB SimPowerSystems (Fig. 4.29) with G_1 representing the machine and the transmission network repressing the infinity bus. The model is a detailed 8^{th} order model, six for the electromagnetic subsystem and two for the mechanical subsystem.

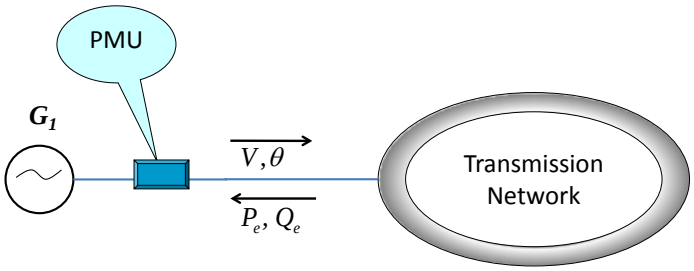

Figure 4.29. System configuration

The operating conditions for G_1 were set to deliver high active power (1 pu) and relatively high reactive power (0.25) with a power factor of 0.97. The data of case 1 are shown in Fig 4.30.

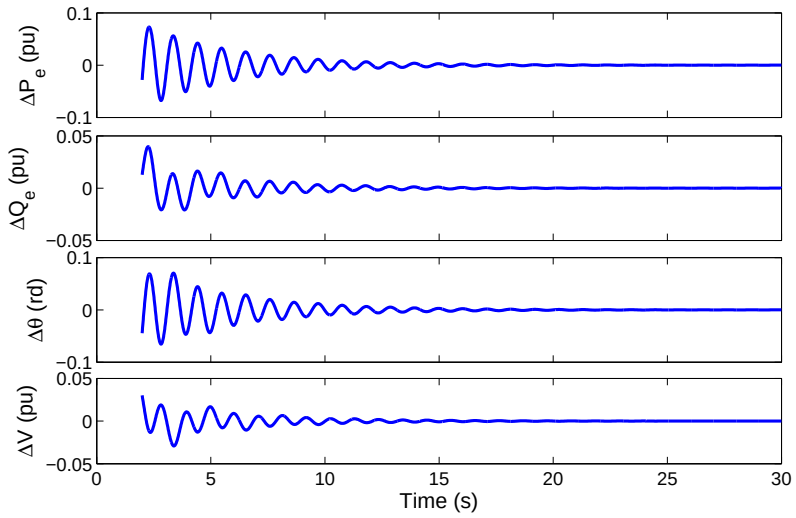

Figure 4.30. Case 1: Input and output of the system

The simplified case of $k = 0$ was used for the estimation process because it not possible to calculate a priori k for the machine subject to estimation. ϵ was set to -0.1 as per Section 4.91.

The initial estimated parameters using 'model 2' are $\{H,\ x'_d,\ J_{\dot{\delta}P_e},\ J_{\dot{\delta}Q_e}\}$. Should $T'_{do},\ T'_{qo},\ \delta'$ be known, then $\{x_q,\ x_d\}$ can be extracted from $\{J_{\dot{\delta}P_e},\ J_{\dot{\delta}Q_e}\}$. For 'model 1', the estimated parameters are $\{H,\ x'_d\}$. The results of the estimation for both 'model 1' and 'model 2' in addition to the cost function are displayed in Table 4.5 where It is assumed that the simulated machine, being the base model, has a cost of 0.

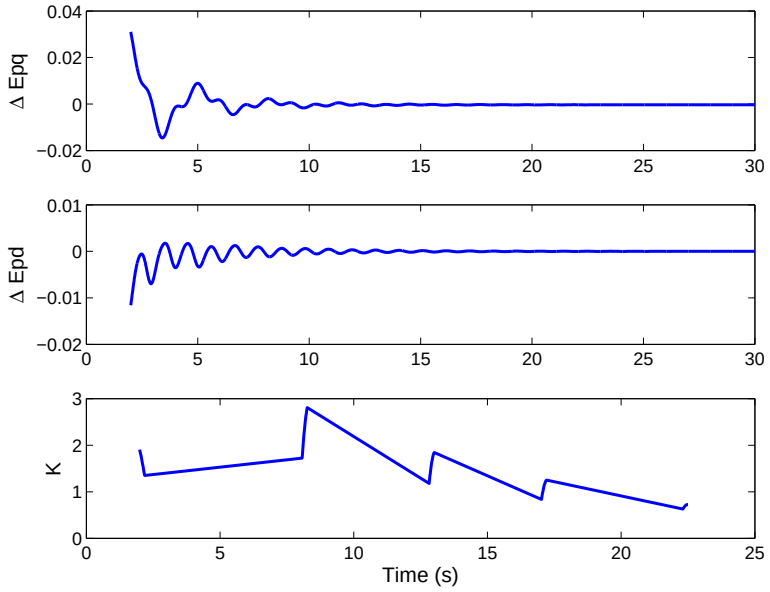

Figure 4.31. Case 1: k progress with time

Table 4.5. Case 1: Estimated parameters for 'model 2' and 'model 1'

Parameter	H	x'_d	$J_{\dot{\delta}P_e}$	$J_{\dot{\delta}P_e}$	x_q	x_d	cost
Simulated machine	3.7	0.4	-0.43	0.45	1.81	1.81	0
model 2 ($k=0$)	3.68	0.37	-0.43	0.32	1.52	2.65	$2.5e^{-11}$
model 1 ($k=0$)	3.66	0.37	-	-	-	-	$2.6e^{-10}$

The estimated systems (matrices $[A], [B], [C], [D]$) for both 'model 2' and 'model 1' along with the input data were fed to the validation systems (part of MATLAB System Identification) as shown in Fig. 4.28. The output $\{\Delta\theta,\ \Delta V\}$ of the validation system compared with the simulated one is shown in 4.32. The model was built with MATLAB Simulink ($\epsilon = -0.5$ was needed) in order to show a comparison of the states ($\Delta\delta$ and $\Delta\omega$) (Fig. 4.33).

The following *remarks* can be made:

1. The common estimated parameters ($H,\ x'_d$) of both 'model 2' and 'model 1' are close to the simulated ones.

2. 'model 2' provides a good estimation for x_q provided some additional information are available. 'model 1' which is closer the the classical machine model cannot give any indication on x_q.

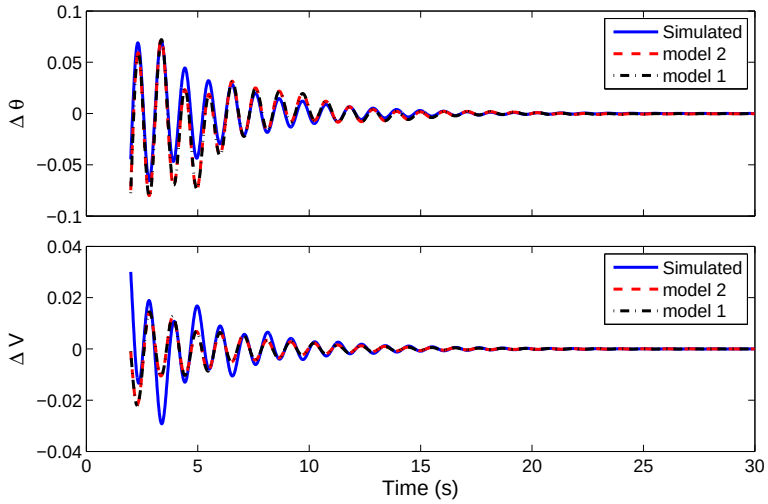

Figure 4.32. Case 1: Validation of the output

3. The validated output $\Delta\theta$ of 'model 2' is closer to the simulated one than the output $\Delta\theta$ of 'model 1' as displayed in Fig. 4.32.

4. 'model 2' catches the mechanical dynamics of the simulated machine batter than 'model 1' as evidenced by Fig. 4.33.

4.4.3.3 Case 2: Subsystem Identification

The purpose of this case is to represent Area 1 machines (Fig. 4.34) by one single machine and run the estimation algorithm to find the equivalent machine parameters. Validation of the estimated machine will show if the equivalent machine truly represents Area 1. A similar approach can be used to represent Area 2 then the whole system can be scaled down to two equivalent machines connected by a radial transmission line.

The simulation was carried out in Power System Toolbox (PST) [77]. The simulated machines are similar and were built around sub-transient model and equipped with dc exciters and governors. The simulation details are shown in the appendix. Input and Output data were extracted in bus 20 were a PMU is supposed to be installed. The primary angle data (θ) suffers from trending as shown in Fig. 4.35, hence a preprocessing

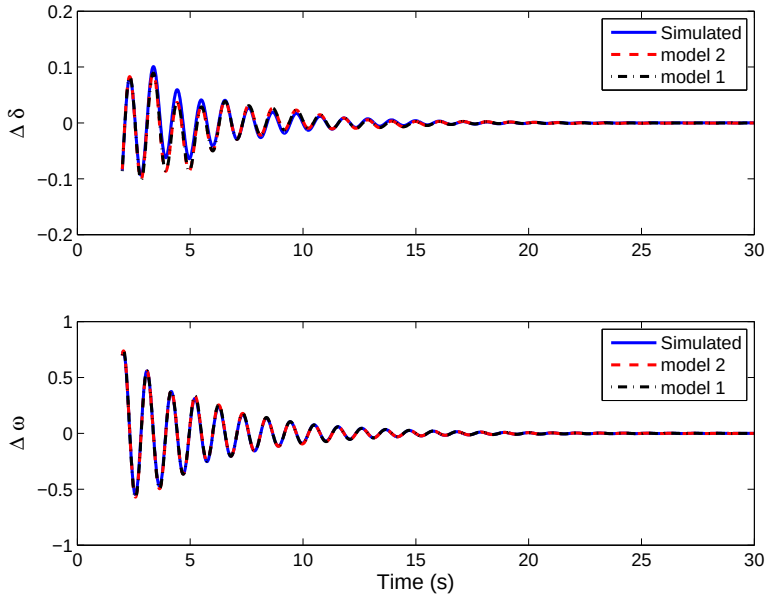

Figure 4.33. Case 1: Simulated and validated mechanical states

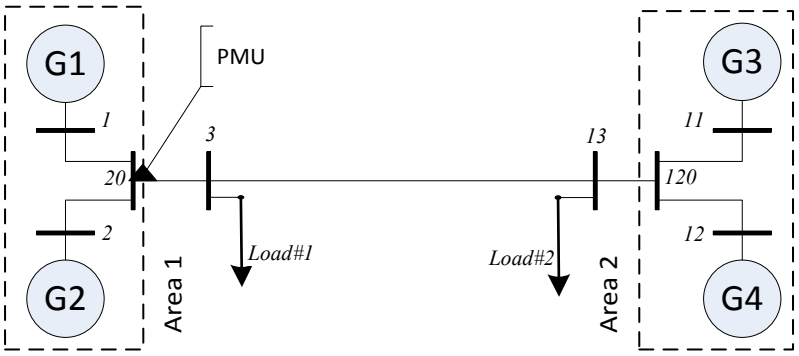

Figure 4.34. Case 2: Four-machine two-Area System

of input and output was done by removing the first five seconds and by removing the linear trend in θ. The resulting input and output data are shown in Fig. 4.36

The estimation algorithm was run on the first few seconds of the data (Fig. 4.36)in order to extract the equivalent machine based on both 'model 2' and 'model 1'.

The stabilizing term ϵ formulated in Section 4.91 is set to -0.9 which is higher than -0.1 used in case 1 (Section 4.4.3.2). The value -0.9 for ϵ is still small compared to the other factor $(-\omega_0/2H)$ affecting $\Delta\dot{\omega}$ which is around -15. The reason for higher negative feedback in matrix **A** is:

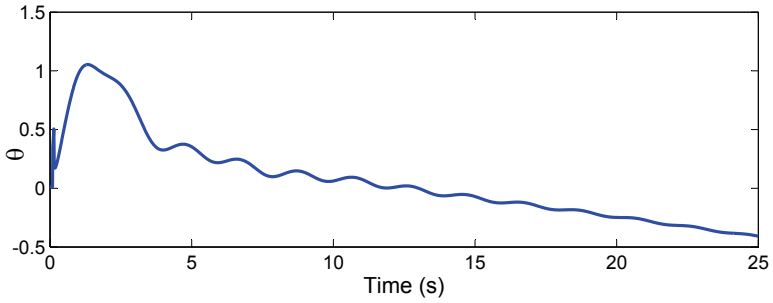

Figure 4.35. Case 2: Trend in angle output θ

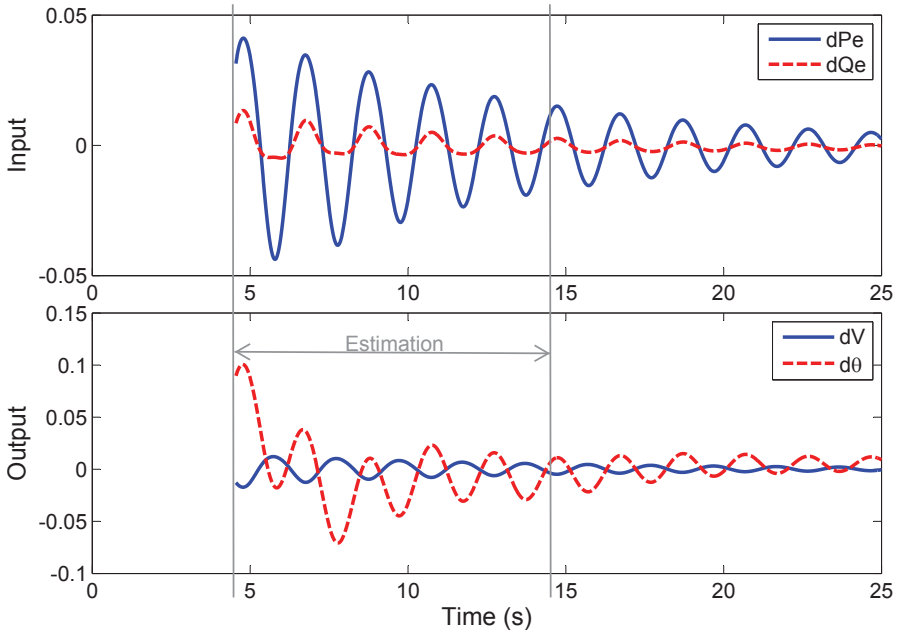

Figure 4.36. Case 2: De-trended input and output

1. The losses on the transmission lines inside the power subsystem: As δ gets bigger, Pe from every machine gets bigger while the mechanical input is considered constant, which means ω will get smaller. This causes the negative impact of δ on $\dot{\omega}$.

2. The presence of local damping within the power subsystem. The two machines in the subsystem are never completely synchronized which creates a mutual damping effect (albeit small) between them. Damping is modeled usually as a negative impact of ω on $\dot{\omega}$

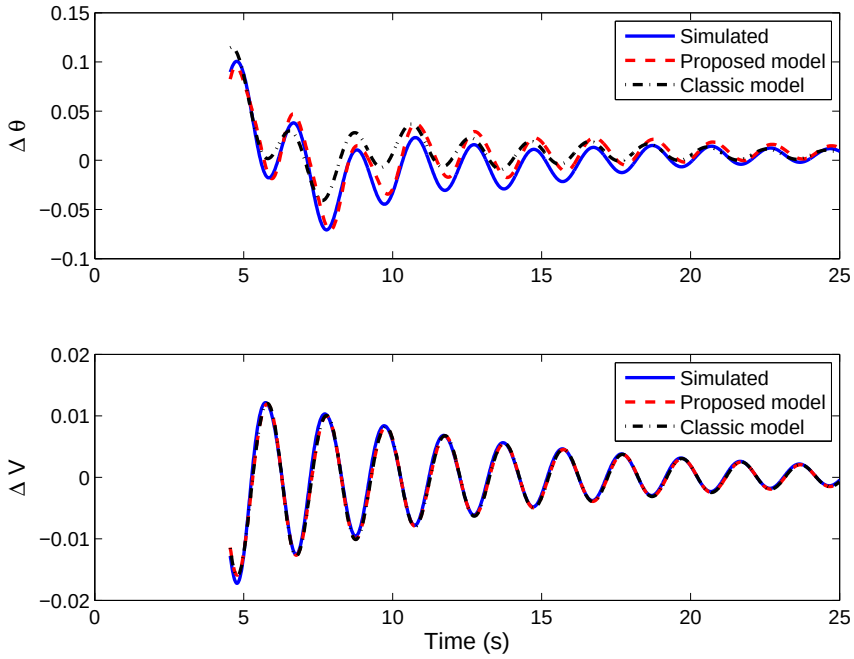

Figure 4.37. Case 2: Validated output of 'model 2' and 'model 1'

Table 4.6. Case 2: Estimated parameters of 'model 2' and 'model 1'

Parameter	H	x'_d	cost function
Simulated equivalent machine	13	0.27	0
'model 2' ($k = 0$)	12.3	0.31	$2.5e_{-11}$
'model 1' ($k = 0$)	16	0.31	$4.4e_{-10}$

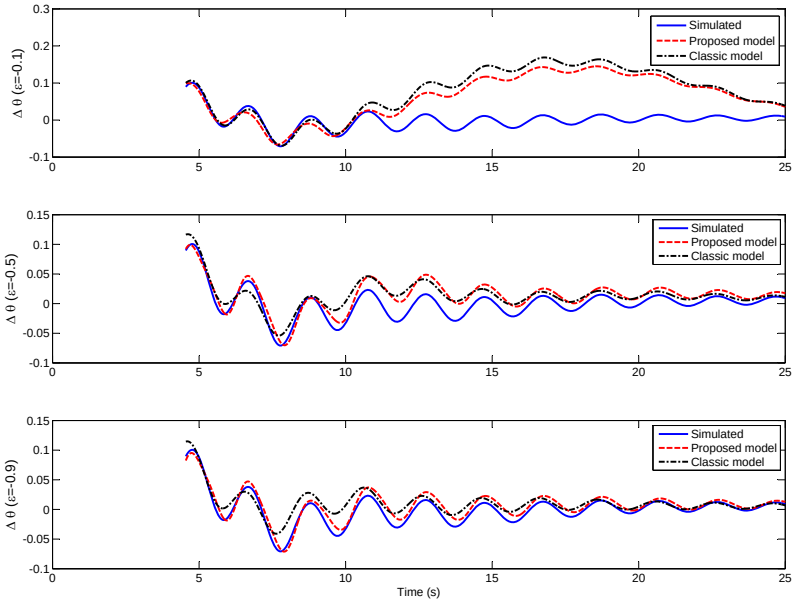

Figure 4.38. Case 2: The impact of varying ϵ on the angle output of 'model 2' and 'model 1'

Similar to case 1 in Section 4.4.3.2, the simplified case of $k = 0$ was used. The estimated parameters along with the cost function provided by the system identification algorithm are shown in Table 4.6. It is assumed that the simulated machine, being the base model, has a cost of 0. The simulated equivalent machine of the power subsystem has theoretically a total inertia equals the sum of the inertias of its individual machines (when perfectly coherent) and a transient reactance equals the Thevenin equivalent of the reactances seen from bus 20 (i.e. $H = 13$ and $x'_d = 0.27$).

The validated output of 'model 2' and 'model 1' are shown in 4.37. The impact of various values for ϵ on angle validation is shown in Fig. 4.38, which clearly shows the the proposed model is better in every case. The impact on ΔV was insignificant.

CHAPTER 5: CONCLUSION AND FUTURE WORK

The dissertation conducted research in the model estimation of power systems based on PMU data due to its importance as shown in Section 1.3. The studied power systems are either a single synchronous machine or power generating are formed of multiple synchronous machines (in Section 4.4.3.3 for example). The dissertation brings incremental knowledge to the power systems and smart grid research area. Such incremental benefit is evidenced by the peer reviewed papers from this dissertation ([78, 60] are published,[61, 79] are in 2nd round review).

In particular, the dissertation research benefits are summarized in the following conclusions:

5.1 Source of Data

The research explored the use of PMU data in model and parameter estimation. The results prove that one PMU can be the sole provider of data in order to estimate the parameters of synchronous classic and flux decay models and power systems all subject to electro-mechanical dynamics. Such outcome is shown in Chapter 3 and in Chapter 4 and in [78, 60, 61, 79]. When PMU data is supplemented by additional data then more parameters can be estimated (Section 4.4.3.2 for example).

5.2 Estimation Techniques Algorithms

The research examined two approaches for the estimation and validation problem i) LSE based on the time window of data coupled with FN or as System Identification and ii) non-linear Kalman Filter extensions namely EKF and UKF.

The research showed that EKF coupled with new decoupling technique can be used to estimate four parameters and two states of the classical machine model (Section 3.3 and [61]). UKF method was also shown to be effective in estimating parameters and states of the flux decay model (Section 3.4 and [60]). The UKF implementation as dual filter with colored noise solved the problem of rotor angle and x_q simultaneous estimation.

Using LSE for parameters estimation required either the use of finite differences or System Identification. Finite differences technique estimated some states and their derivatives wrt. time numerically and transformed the problem into a linear overestimated problem which was solved with LSE (Section 4.3 and [78]). The System Identification approach estimated the parameters of a linearized model of the synchronous machine using a grey box (Section 4.4.3.2) and of a power subsystem (Section 4.4.3.3). The sub-set selection analysis provided good insight to the precision to which the parameters can be estimated (Section 4.4.2 and Table 4.5). The validation of the developed model output was closer to the simulated output compared with the classical machine model (Fig. 4.37).

5.3 Impact of Machine Model Differences and Controls on the Estimation Quality

The developed algorithms (Section 5.2) provided a precise estimate when the machine estimated model and the simulated model have the same complexity or state space system (Set 1 and Set 2 in Section 3.3.4, and Section 3.4.5).

The developed algorithms provided a good estimate when the machine simulated model is more complex (higher order) than the estimated model (Set 3 in Section 3.3.4, Sections 3.4.6 and 4.3.2.1).

The machines controls (AVR and governor) were found to induce deviations in the estimated values of the parameters and the research explained the cause of such deviations (Set 4 in Section 3.3.4, and Section 4.3.2.2). In the case of System Identification, the use of exciter (with AVR) did not affect all estimated parameters (Section 4.4.3.2).

In the case of model estimation of a power subsystem formed of multiple machines, System Identification algorithm with the developed linearized machine model provided better output than the classical machine model (Section 4.4.3.3).

Estimation of real power subsystems in the electric grid in the United States carried out in Section 4.3.3 showed the need for low pass filter in order to eliminate the impact of white noise.

5.4 Further Research

Further research can be extended from the research in this dissertation to cover:

1. How the developed model and parameter estimations can be applied on other types of power systems. The reliance on the one single PMU at the output of the power subsystem to provide the input and the measurement data makes this approach independent from the rest power system. Such independence makes it suitable to use it in parallel across a transmission network at the output of synchronous machines powerplant, or wind farm built around induction generators not synchronous generators.

2. How sampling rate affect parameter estimation. In Section 4.4, it was shown that some parameters estimated parameters were far from the simulated parameters. The sampling rate affect the precision of sensitivity matrix which in turn affects the quality of the estimation.

3. How to improve a poor estimation model for some parameters as shown in Section 4.4.1.2 due to poor observation function.

REFERENCES

[1] J. Machowski, *Power system dynamics stability and control*. Chichester, U.K: Wiley, 2008.

[2] A. Phadke and J. Thorpe, *Synchronized Phasor measurements and Their Applications*. Springer, 2008.

[3] A. Phadke and J. Thorp, "History and applications of phasor measurements," in *Power Systems Conference and Exposition, 2006. PSCE '06. 2006 IEEE PES*, 29 2006-nov. 1 2006, pp. 331 –335.

[4] A. Monticelli, *State estimation in electric power systems : a generalized approach*. Boston: Kluwer Academic Publishers, 1999.

[5] A. Phadke and R. de Moraes, "The wide world of wide-area measurement," *Power and Energy Magazine, IEEE*, vol. 6, no. 5, pp. 52 –65, september-october 2008.

[6] E. Schweitzer, D. Whitehead, G. Zweigle, K. Ravikumar, and G. Rzepka, "Synchrophasor-based power system protection and control applications," in *Modern Electric Power Systems (MEPS), 2010 Proceedings of the International Symposium*, sept. 2010, pp. 1 –10.

[7] "Test guidelines for synchronous unit dynamic testing and model validation," Western Systems Coordinating Council, Tech. Rep., 1997. [Online]. Available: "http://www.wecc.biz/library/rro/Shared\%20Documents/synctest.pdf"

[8] "Generating unit model validation policy," Western Electricity Coordinating Council, Tech. Rep., 2006. [Online]. Available: http://www.nerc.com/docs/pc/tis/04_Generating_Unit_Model_Validation.pdf

[9] U. C. P. S. O. T. Force. (2004, april) Final report on the august 14, 2003 blackout in the united states and canada: Causes and recommendations. [Online]. Available: https://reports.energy.gov/BlackoutFinal-Web.pdf

[10] "standard mod-013-1 RRO dynamics data requirements and reporting procedures". [Online]. Available: "http://www.nerc.com/files/MOD-013-1.pdf"

[11] R. Aster, *Parameter estimation and inverse problems*. Amsterdam Boston: Elsevier Academic Press, 2005.

[12] L. Ljung, *System identification : theory for the user*. Upper Saddle River, NJ: Prentice Hall PTR, 1999.

[13] T. Cutsem and C. Vournas, *Voltage stability of electric power systems.* Boston: Kluwer Academic Publishers, 1998.

[14] G. Gross, "Analysis techniques for large scale electrical systems 1. introduction and overview," Online: http://courses.engr.illinois.edu/ece530/Lectures/Lecture%201-%20Introduction%20and%20Overview%202012.pdf, 2012.

[15] M. Klein, G. Rogers, and P. Kundur, "A fundamental study of inter-area oscillations in power systems," *Power Systems, IEEE Transactions on*, vol. 6, no. 3, pp. 914 –921, aug 1991.

[16] "Ieee guide for synchronous generator modeling practices and applications in power system stability analyses," *IEEE Std 1110-2002 (Revision of IEEE Std 1110-1991)*, pp. 1–72, 2003.

[17] P. Sauer and M. Pai, *Power System Dynamics and Stability.* Prentice Hall, 1998.

[18] K. Morison, L. Wang, F. Howell, J. Viikinsalo, and A. Martin", *Real-time Stability Assessment in Modern power System control Centers.* New Jersey, USA: Wiley, 2009, ch. Implementation of Online Dynamic Security Assessment at Southern Company.

[19] H. Yin and L. Fan, "Pmu data-based fault location techniques," in *North American Power Symposium (NAPS), 2010*, sept. 2010, pp. 1 –7.

[20] E. Kyriakides, G. T. Heydt, and V. Vittal, "Online parameter estimation of round rotor syncronous generators including saturation," *IEEE Trans. Energy Conversion*, vol. 20, no. 3, pp. 529–537, September 2005.

[21] J. Melgoza, G. Heydt, A. Keyhani, B. Agrawal, and D. Selin, "Synchronous machine parameter estimation using the hartley series," *Energy Conversion, IEEE Transactions on*, vol. 16, no. 1, pp. 49 –54, mar 2001.

[22] G. Valverde, E. Kyriakides, G. Heydt, and V. Terzija, "Nonlinear estimation of synchronous machine parameters using operating data," *Energy Conversion, IEEE Transactions on*, vol. 26, no. 3, pp. 831 –839, sept. 2011.

[23] J. H. Chow, A. C. Chakrabortty, L. Vanfretti, and M. Arcak, "Estimation of radial power system transfer path dynamic parameters using synchronized phasor data," *IEEE Trans. Power Syst.*, vol. 23, no. 2, pp. 564–571, May 2008.

[24] Z. Huang, K. Schneider, and J. Nieplocha, "Feasibility studies of applying kalman filter techniques to power system dynamic state estimation," in *Power Engineering Conference, 2007. IPEC 2007. International*, dec. 2007, pp. 376 –382.

[25] Y. Wehbe and L. Fan, "Estimation of a shunted radial transfer path dynamics using pmus," in *Power and Energy Society General Meeting, 2011 IEEE*, july 2011.

[26] M. Humer and S. Kulig, "Measurement and assessment of torsion oscillations in turbogenerators by using a torque sensor and robust observer," in *Industrial Electronics Society, 2003. IECON '03. The 29th Annual Conference of the IEEE*, vol. 2, nov. 2003, pp. 1369 – 1377 Vol.2.

[27] Z. Huang, P. Du, D. Kosterev, and B. Yang, "Application of extended kalman filter techniques for dynamic model parameter calibration," in *Power Energy Society General Meeting, 2009. PES '09. IEEE*, july 2009, pp. 1 –8.

[28] E. Ghahremani and I. Kamwa, "Dynamic state estimation in power system by applying the extended kalman filter with unknown inputs to phasor measurements," *Power Systems, IEEE Transactions on*, vol. 26, no. 4, pp. 2556 –2566, nov. 2011.

[29] ——, "Online state estimation of a synchronous generator using unscented kalman filter from phasor measurements units," *Energy Conversion, IEEE Transactions on*, vol. 26, no. 4, pp. 1099 –1108, dec. 2011.

[30] E. Eitelberg and R. G. Harley, "Estimating synchronous machine electrical parameters from frequency response tests," *IEEE Transactions on Energy Conversion*, vol. 2, no. 1, pp. 132–136, 1987.

[31] R. Escarela-Perez, T. Niewierowicz, and E. Campero-Littlewood, "Synchronous machine parameters from frequency-response finite-element simulations and genetic algorithms," *IEEE Transactions on Energy Conversion*, vol. 16, no. 2, pp. 198–203, 2001.

[32] I. Kamwa and R. Grondin, "Fast adaptive schemes for tracking voltage phasor and local frequency in power transmission and distribution systems," *Power Delivery, IEEE Transactions on*, vol. 7, no. 2, pp. 789 –795, apr 1992.

[33] J.-Y. Choi, B. Cho, H. VanLandingham, H. soo Mok, and J.-H. Song, "System identification of power converters based on a black-box approach," *Circuits and Systems I: Fundamental Theory and Applications, IEEE Transactions on*, vol. 45, no. 11, pp. 1148 –1158, nov 1998.

[34] B. Miao, R. Zane, and D. Maksimovic, "System identification of power converters with digital control through cross-correlation methods," *Power Electronics, IEEE Transactions on*, vol. 20, no. 5, pp. 1093 – 1099, sept. 2005.

[35] K. Chau and C. Chan, "Nonlinear identification of power electronic systems," in *Power Electronics and Drive Systems, 1995., Proceedings of 1995 International Conference on*, feb 1995, pp. 329 –334 vol.1.

[36] L. Xu and L. Fan, "System identification based vsc-hvdc dc voltage controller design," in *North American Power Symposium (NAPS), 2012*, sep. 2012.

[37] J. Pierre, N. Zhou, F. Tuffner, J. Hauer, D. Trudnowski, and W. Mittelstadt, "Probing signal design for power system identification," *Power Systems, IEEE Transactions on*, vol. 25, no. 2, pp. 835 –843, may 2010.

[38] I. Kamwa and L. Gerin-Lajoie, "State-space system identification-toward mimo models for modal analysis and optimization of bulk power systems," *Power Systems, IEEE Transactions on*, vol. 15, no. 1, pp. 326 –335, feb 2000.

[39] A. Cintron-Arias, H. T. Banks, A. Capaldi, and A. L. Lloyd, "A sensitivity matrix based methodology for inverse problem formulation." *Journal of Inverse & Ill-Posed Problems*, vol. 17, no. 6, pp. 545 – 564, 2009.

[40] M. Burth, G. Verghese, and M. Velez-Reyes, "Subset selection for improved parameter estimation in on-line identification of a synchronous generator," *Power Systems, IEEE Transactions on*, vol. 14, no. 1, pp. 218 –225, feb 1999.

[41] P. S. Maybeck, *Stochastic models, estimation, and control*, ser. Mathematics in Science and Engineering, 1979, vol. 141.

[42] D. Simon, *Optimal state estimation : Kalman, H [infinity] and nonlinear approaches.* Hoboken, N.J: Wiley-Interscience, 2006.

[43] R. van der Merwe, "Sigma-point kalman filters for probabilistic inference in dynamic state-space models," Ph.D. dissertation.

[44] J. Grainger and W. D. Stevenson, *Power System Analysis.* New York, USA: McGraw-Hill, 1994.

[45] S. Azad and J. Tate, "Parameter estimation of doubly fed induction generator driven by wind turbine," in *Power Systems Conference and Exposition (PSCE), 2011 IEEE/PES*, march 2011, pp. 1 –8.

[46] K. Kalsi, Y. Sun, Z. Huang, P. Du, R. Diao, K. Anderson, Y. Li, and B. Lee, "Calibrating multi-machine power system parameters with the extended kalman filter," in *Power and Energy Society General Meeting, 2011 IEEE*, july 2011.

[47] J. J. Sanches-Gasca, C. Bridenbaugh, C. Bowler, and J. Edmonds, "Trajectory sensitivity based identification of synchronous generator and excitation system parameters," *IEEE Transactions on Power Systems*, vol. 3, no. 4, pp. 1814–1821, 1988.

[48] M. Karrati and O. Malik, "Identification of physical parameters of a synchronous generator from online measurements," *IEEE Transactions on Energy Conversion*, vol. 19, no. 2, pp. 407–415, 2004.

[49] C. C. Lee and O. Tan, "A weighted-least-squares parameter estimator for synchronous machines," *IEEE Transactions on Power Apparatus and Systems*, vol. 96, no. 1, pp. 97–101, Jan./Feb. 1977.

[50] M. Namba, T. Nishiwaki, S. Yokokawa, K. Ohtsuka, and Y. Ueki, "Identification of parameters for power system stability analysis using kalman filter," *IEEE Transactions on Power Apparatus and Systems*, vol. 100, no. 7, pp. 3304–3310, Jul. 1981.

[51] J. Ma, B. W. Hogg, N. Zhiyuan, and Y. Yihan, "Online decoupled identification of transient and subtransient generator parameters," *IEEE Transactions on Power Systems*, vol. 9, no. 4, pp. 1908–1914, 1994.

[52] Z. Zhao, F. Zheng, J. Gao, and L. Xu, "A dynamic online parameter identification and full-scale system experimental verification for large synchronous machines," *IEEE Transactions on Energy Conversion*, vol. 10, no. 3, pp. 392–398, 1995.

[53] R. Wamkeue, C. Jolette, A. Mabwe, and I. Kamwa, "Cross-identification of synchronous generator parameters from rtdr test time-domain analytical responses," *IEEE Transactions on Energy Conversion*, vol. 26, no. 3, pp. 776–786, 2011.

[54] S. M. Benchluch and J. Chow, "A trajectory sensitivity method for the identification of nonlinear excitation system models," *IEEE Transactions on Energy Conversion*, vol. 8, no. 2, pp. 159–164, 1993.

[55] E. Kyriakides, G. Heydt, and V. Vittal, "Online parameter estimation of round rotor synchronous generators including magnetic saturation," *IEEE Transactions on Energy Conversion*, vol. 20, no. 3, pp. 529–537, sep 2005.

[56] J. Melgoza, G. Heydt, A. Keyhani, B. Agrawal, and D. Selin, "An algebraic approach for identifying operating point dependent parameters of synchronous machines using orthogonal series expansions," *IEEE Transactions on Energy Conversion*, vol. 16, no. 1, pp. 92–98, mar 2001.

[57] E. Kyriakides, G. Heydt, and V. Vittal, "On-line estimation of synchronous generator parameters using a damper current observer and a graphic user interface," *IEEE Transactions on Energy Conversion*, vol. 19, no. 3, pp. 499–507, sep 2004.

[58] A. Keyhani, S. Hao, and R. P. Schulz, "Maximum likelihood estimation of generator stability constants using SSFR test data," *IEEE Transactions on Energy Conversion*, vol. 16, no. 1, pp. 140–154, 1991.

[59] I. Kamwa, P. Viarouge, H. Le-Huy, and J. Dickinson, "A frequency domain maximum likelihood estimation of synchronous machine high order models using SSFR test data," *IEEE Transactions on Energy Conversion*, vol. 7, no. 3, pp. 525–536, 1992.

[60] Y. Wehbe and L. Fan, "UKF based estimation of synchronous generator electromechanical parameters from phasor measurements," in *North American Power Symposium (NAPS), 2012*, sep. 2012.

[61] L. Fan and Y. Wehbe", ""ekf-based real-time dynamic state and parameter estimation using pmu data"."

[62] A. Phadke, J. Thorp, and K. Karimi, "State estimation with phasor measurements," *IEEE Transactions on Power Systems*, vol. 1, no. 1.

[63] L. Vanfretti, J. Chow, D. E. S. Sarawgi, and B. Fardanesh", ""a framework for estimation of power systems based on synchronized phasor measurement data"," in *"Proc. IEEE Power and Energy General Meeting"*, "Calgary, CA", jul.

[64] L. Zhao and A. Abur, "Multiarea state estimation using state estimation with phasor measurements," *IEEE Transactions on Power Systems*, vol. 20, no. 2, may "2005".

[65] A. Agarwal, J. Ballance, B. Bhargava, J. Dyer, K. Martin, and J. Mo, "Real time dynamics monitoring system (rtdms) for use with synchrophasor technology in power systems," *Proc. of IEEE Power & Energy General Meeting*, July 2011.

[66] E. Ghahremani and I. Kamwa", ""dynamic state estimation in power system by applying the extended kalman filter with unknown inputs to phasor measurements"," *IEEE Transactions on Power Systems*.

[67] ——, ""online state estimation of a synchronous generator using unscented kalman filter from phasor measurements units"," *IEEE Transactions on Energy Conversion*.

[68] Z. Huang, D. Kosterev, R. Guttronmson, and T. nguyen", ""model validation with hybrid dynamic simulation"," *"in Proc. of IEEE Power Engineering Society General Meeting"*, 2006.

[69] P. Du, Z. Huang, R. Diao, B. Lee, and K. Anderson", ""application of kalman filter to improve model integrity for securing electricity delivery"," *"IEEE/PES Power Systems Conference and Exposition (PSCE)"*, 2001.

[70] F. Okou, L.-A. Dessaint, and O. Akhrif", ""power systems stability enhancement using a wide-area signals based hierarchical controller"," *IEEE Transactions on Power Systems*, vol. 20, no. 3, aug 2005.

[71] J. Chapman, M. Ilic, C. K. nd L. Eng, and H. Kaufman", ""stabilizing a multimachine power system via decentralized feedback linearizing excitation control"," *IEEE Transactions on Power Systems*, vol. 8, no. 3, aug 1993.

[72] M. Grewal and A. Andrews, *Kalman filtering : theory and practice using MATLAB*. Hoboken, N.J: Wiley, 2008.

[73] D. Simon, *Optimal State Estimation*. Wiley-Interscience, A John Wiley & Sons, Inc., 2006.

[74] J. H. Chow and K. W. Cheung, "A toolbox for power system dynamics and control engineering education and research," *IEEE Transactions on Power Systems*, vol. 7, no. 4, pp. 1559–1564, nov 1992.

[75] G. Welch and G. Bishop". "an introduction to the kalman filter". [Online]. Available: "http://www.cs.unc.edu/\~welch/media/pdf/kalman_intro.pdf"

[76] P. Kundur, *Power System Stability and Control*. New York, USA: McGraw-Hill, 1994.

[77] J. Chow, G. Rogers, and K. Cheung, "Power System Toolbox," Tech. Rep.

[78] Y. Wehbe, L. Fan, and Z. Miao, "Least squares based estimation of synchronous generator states and parameters with phasor measurement units," in *North American Power Symposium (NAPS), 2012*, sep. 2012.

[79] L. Fan, Z. Miao, and Y. Wehbe", ""application of dynamic state and parameter estimation techniques on in real-world data"."

[80] B. Gibbs, *Advanced kalman filtering, least-squares and modeling a practical handbook*. Hoboken, N.J: Wiley, 2011.

[81] L. Ljung, ser. The Control Handbook. CRC Press IEEE Press, 1996, ch. 58, pp. 1033–1054.

[82] R. Isermann, U. Baur, W. Bamberger, P. Kneppo, and H. Siebert, "Comparison of six on-line identification and parameter estimation methods," *Automatica*, vol. 10, no. 1, pp. 81–103, jan 1974.

[83] P. Anderson and A. Fouad, *Power System Control and Stability.* Wiley-IEEE Press, 2007.

[84] B. Fornberg, *A Practical Guide to Pseudospectral Methods.* Cambridge University Press, 1998.

[85] Y. Bard, *Nonlinear parameter estimation.* New York: Academic Press, 1974.

[86] J. R. S. H. Thomas Banks, Marie Davidian and K. L. Sutton, *MATHEMATICAL AND STATISTICAL ESTIMATION APPROACHES IN EPIDEMIOLOGY.* Springer, 2009, ch. An Inverse Problem Statistical Methodology Summary, pp. 249–302.

APPENDICES

Appendix A: Nomenclature

Synchronous Machine Parameters

x_d, x_q	: d, q axis reactance
x'_d, x'_q	: d, q axis transient reactance
x''_d, x''_q	: d, q axis sub-transient reactance
r_s	: Stator resistance
E_{fd}	: Field voltage
E'_d, E'_q	: d, q axis transient voltage
T'_{do}, T'_{qo}	: d, q axis transient open circuit time constant
T''_{do}, T''_{qo}	: d, q axis sub-transient open circuit time constant
I_d, I_q	: d, q axis current
P_e, Q_e	: Active, reactive electrical power :
V, θ	: Magnitude and angle of output phasor voltage
H	: Machine inertia
δ', ω	: Rotor angle and speed
ω_0	: Rotor steady state angular speed≈ 376.99
P_m	: Mechanical power

Appendix B: Simulation Data

Chapter 3 cases

Simulations in Section 3.4.4 were carried out in Power System Toolbox [77] with the following machine details:
x_l=0.2, r_a=0.0, x_d=1.8, $x_d^{'}$=0.25, $x_d^{''}$=0.2, $T_{do}^{'}$=8, $T_{do}^{''}$=0.03, x_q=1.5, $x_q^{'}$=0.25, $x_q^{''}$=0.2, $T_{qo}^{'}$=0.4, $T_{qo}^{''}$=0.05, H=6.5 (G_1), D=3.

Data for Section 4.3 cases

Simulations in Section 4.3.2 were done using Power System Toolbox [77]. Machines details: G_1 and G_2: x_l=0.2, r_a=0.2, x_d=1.8, x_d'=0.25, $x"_d$=0.2, T_{do}'=8, $T"_{do}$=0.03, x_q=1.7, x_q'=0.55, $x"_q$=0.24, T_{qo}'=0.4, $T"_{qo}$=0.05, H=6.5 (G_1), H=16.5 (G_2). Exciter: Simple exciters with Tr=0, K_a=200, T_a=0.05, T_b=10, T_c=1, V_{rmax}=5, V_{rmin}=-5, the rest of the parameters are equal to zero. Governor: Simplified turbine governor with w_f=1, $1/R$=35, T_{max}=1, T_s=1, T_c=0.5, T_3=0, T_4=1.25, T_5=5.

Section 4.4 cases

Simulations in Section 4.4.3.2 were carried out in MATLAB SimPowerSystems with the following machine details:
$H = 3.7\ s,\ x_d' = 0.4\ pu,\ x_q' = 0.4\ pu,\ x_d = 1.81\ pu,\ x_q = 1.81\ pu,\ r_s = 0,\ x_d'' = 0.15\ pu,\ x_q'' = 0.15\ pu,\ T_{d0}' = 8\ s,\ T_{q0}' = 1\ s,\ T_{d0}'' = 0.03,\ T_{q0}'' = 0.07\ s.$ Exciter: $T_r = 0\ s,\ K_a = 200,\ T_a = 0.03\ s,\ K_e = 1,\ T_e = 0.1\ s,\ T_b = 5\ s,\ T_c = 0.3\ s,\ K_f = 2.5e^{-3},\ T_f = 0.21\ s,\ Ef_{min} = -11.5,\ Ef_{max} = 11.5,\ K_p = 0$
Simulations in Section 4.4.3.3 were carried out in Power System Toolbox [77] with the following details:
Machines: MVA base = 900, $H = 6.5\ s,\ D = 3,\ x_d' = 0.3\ pu,\ x_q' = 0.55\ pu,\ x_d = 1.8\ pu,\ x_q = 1.7\ pu,\ r_s = 0.0025,\ x_d'' = 0.25\ pu,\ x_q'' = 0.25\ pu,\ T_{d0}' = 8\ s,\ T_{q0}' =$

Appendix B (Continued)

0.4 s, $T''_{d0} = 0.03$, $T''_{q0} = 0.05$ s.

DC Exciters: $T_r = 0.01$ s, $K_a = 46$, $T_a = 0.06$ s, $K_e = 0$, $T_e = 0.46$ s, $T_b = 0$ s, $T_c = 0$ s, $K_f = 0.1$, $T_f = 1$ s, $Vr_{min} = -0.9$, $Vr_{max} = 1$, $E_1 = 3.1$, $Se(E_1) = 3.1$, $E_2 = 0.33$, $Se(E_2) = 2.3$

Governor: Simplified turbine governor with w_f=1, $1/R$=25, T_{max}=1, T_s=0.1, T_c=0.5, T_3=0, T_4=1.25, T_5=5.

Appendix C: Copyrights Permissions

IEEE Copyright Permission

Appendix C (Continued)

Power Information Technology Lab, University of Tennessee, Copyright Permission

Yasser Wehbe <ywehbe@gmail.com>

Use of FNET website material

Penn Markham <markham@utk.edu> Fri, Sep 7, 2012 at 8:15 PM
To: Yasser Wehbe <ywehbe@gmail.com>

Hello,
That's fine. All we ask is that you acknowledge the source (Power Information Technology Lab, University of Tennessee) in your work.

Thanks,
PENN

On 9/7/2012 1:37 PM, Yasser Wehbe wrote:

> Dear Sirs,
>
> I am contacting you to seek permission to use materials from your website in my dissertation.
>
> I am a PhD student at the University of South Florida working with Dr. Fan on parameters estimation using PMUs data. The work FNET has done is remarkable and I would like very much to include graphs obtained with PMU and published on your website. The graph I would like to use in my dissertation for now is angle contour map (http://fnetpublic.utk.edu/anglecontour.html).
>
> If you kindly agree on my use of the FNET materials then I would highly appreciate providing me with any statement or policy you would like me to insert in my dissertation.
>
> Looking forward to hearing from you.
>
> Yasser WEHBE

Appendix C (Continued)

NERC Copyright Permission

Appendix C (Continued)

Dr. George Gross Copyright Permission

Yasser Wehbe <ywehbe@gmail.com>

Chart use permission request

Gross, George <gross@illinois.edu> Sun, Sep 16, 2012 at 2:14 AM
To: Yasser Wehbe <ywehbe@gmail.com>

Yasser, Habibi

Go ahead and use the charts you need. Good Luck with your thesis!

On Sep 15, 2012, at 3:16 PM, Yasser Wehbe wrote:

> Dear Dr. Geroge Gross,
>
> I am contacting you with regards to permission to use one of your charts in my dissertation.
>
> I am a Ph.D. student at the University of South Florida researching power system models estimation under the supervision of Dr. Lingling Fan. While I was reading your course handouts (Analysis Techniques for Large Scale Electrical Systems) I came on a chart summarizing power system dynamics time scales. I am kindly requesting the permission to use this chart in my dissertation.
>
> The presentation web address is: http://courses.engr.illinois.edu/ece530/Lectures/Lecture%201-%20Introduction%20and%20Overview%202012.pdf
>
> Of course I will be more than happy to show your chart copyrights in the way you see appropriate.
>
> Thank you very much.
>
> Yasser WEHBE

George Gross
Professor of Electrical and Computer Engineering, and
Professor, Institute of Government and Public Affairs (IGPA)
University of Illinois at Urbana-Champaign
339 Everitt Laboratory
1406 W. Green Street
Urbana, IL 61801
Office : (217) 244-6346
Fax : (217) 333-1162
e-mail : gross@illinois.edu

Appendix D: List of Publications

1. Y. Wehbe and L. Fan, "Estimation of a Shunted Radial Transfer Path Dynamics Using PMUs", in the proceedings of the IEEE PES General Meeting 2011

2. L. Fan and Y. Wehbe, "RTDMS Data Analysis", technical report submitted to Midwest ISO, 2011

3. Y. Wehbe and L. Fan, "UKF Based Estimation of Synchronous Generator Electromechanical Parameters From Phasor Measurements", in the proceedings of the 44th North American Power Symposium, 2012

4. Y. Wehbe, L. Fan and Z. Miao, "Least Squares Based Estimation of Synchronous Generator States and Parameters with Phasor Measurement Units", in the proceedings of the 44th North American Power Symposium, 2012

5. L. Fan and Y. Wehbe, "EKF-Based Real-time Dynamic State and Parameter Estimation Using PMU Data", 2nd round review by IEEE Transactions on Smart Grid

6. L. Fan, Z. Miao, and Y. Wehbe, "Application of State and Parameter Estimation Techniques on Real-World Data", 2nd round review by IEEE Transactions on Smart Grid

7. Y. Wehbe and L. Fan, "Modified Classic Generator Model and Its Applications in PMU Data Based System Identification", to submit to IEEE Transactions on Smart Grid

8. L. Fan and Y. Wehbe, "Electromechanical Dynamic State and Parameter Estimation Using PMU Data", presented at the NASPI RITT workshop, Feb. 2012

ABOUT THE AUTHOR

Yasser Wehbe received his Master of Science in Electrical Engineering in Dec. 2009 from the University of South Florida in Tampa, FL. Before that, he received the Master of Aeronautical Science in July 2007 from Embry-Riddle Aeronautical University Worldwide Campus. He had obtained his Diploma in Electrical and Electronics Engineering in Oct. 1992 from the Lebanese University in Beirut, Lebanon.

Yasser's research focuses on power systems dynamics and modeling, wide area monitoring systems, system identification, and numeric techniques. He has worked on Eastern Interconnection real-time PMU data to estimate system parameters such as equivalent inertia and interned at the Pacific Northwest National Laboratory working on machines models simulation and estimation.